DESIGN OF AN EEG SYSTEM TO RECORD TMS EVOKED POTENTIALS

DESIGN OF AN ELECTROENCEPHALOGRAPHY SYSTEM TO RECORD TRANSCRANIAL MAGNETIC STIMULATION EVOKED POTENTIALS

By

MARK ARCHAMBEAULT, B.ENG.M.

A Thesis

Submitted to the School of Graduate Studies

in Partial Fulfillment of the Requirements

for the Degree

Master of Applied Science

McMaster University

Master of Applied Science (2007) McMaster University

(Electrical Engineering) Hamilton, Ontario

TITLE: Design of an Electroencephalography System to Record Transcranial Magnetic Stimulation Evoked Potentials

AUTHOR: Mark Archambeault, B.Eng.M. (McMaster University)

SUPERVISOR: Dr. H. de Bruin

NUMBER OF PAGES: xv, 106

Abstract

The purpose of this thesis was to design, build and test a prototype artifact suppressing electroencephalogram data acquisition system (AS-EEG-DAQ-S) to collect electroencephalogram (EEG) evoked potential (EP) data during repetitive transcranial magnetic stimulation (rTMS) without the EEG signal being masked by transcranial magnetic stimulation (TMS) artifact. A functional AS-EEG-DAQ-S capable of blocking TMS artifact would provide for the first time a quantitative measurement system to assist in optimal TMS coil positioning during the rTMS treatment of depression, an alternative to electroconvulsive therapy (ECT). This thesis provides the details for an AS-EEG-DAQ-S. Preliminary TMS EP results on a human subject were collected. Results showed transcallosal conduction times of 12ms to 31ms, which are consistent with those predicted and collected by other researchers in the TMS field.

The first portion of this work provides electrode heating data for modern rTMS paradigms for the recording of EEG during rTMS. The concern is that during rTMS EEG electrodes can heat to an unsafe temperature. Seven electrode types were tested: silver/silver chloride, silver cup, gold cup, notched gold cup, notched silver cup, notched gold-plated silver cup, and carbon. All electrodes tested are commercially available, including the carbon electrodes designed for MRI use. The three notched electrodes tested were standard electrodes notched using metal clippers to reduce induced currents. Induced currents are responsible for electrode heating during rTMS and can cause burns to the skin. The results of this study show that electrode heating is a concern when

collecting EEG during rTMS. However, a number of standard electrodes or slightly modified standard electrodes are suitable for recording EEG during rTMS if certain stimulating parameters are adhered to.

The second portion of this work provides the detailed development and design of the AS-EEG-DAQ-S. Four different approaches were tested and their ability to withstand a TMS pulse compared.

Short circuiting the input pins of a commercially available EEG amplifier was the first approach tried and yielded only marginal results due to the switches used being designed for digital logic, transistor built, and creating an undesirable offset between input pins.

The second approach tested involved continuing to work with a commercially available EEG amplifier and implementing a sample-and-hold circuit between the patient and the EEG machine inputs. This approach had the drawback of requiring that the EEG signal be attenuated back to EEG signal levels, which are near noise amplitude levels.

The third approach involved using a high bandwidth amplification circuit to recover quicker from the baseline voltage offset created by the TMS artifact. However, increasing the bandwidth also allows the artifact to saturate the input amplifiers, which then require on the order of 500ms to recover fully.

The fourth approach involved combining the second and third approaches to create a high bandwidth amplifier that incorporates a sample-and-hold circuit to prevent amplifier saturation when gain is increased. The fourth approach provided the high bandwidth and artifact blocking behavior desired.

Acknowledgements

I would like to thank Dr. Hubert de Bruin for the assistance, guidance and knowledge provided in my academic and professional career. In addition, I would like to acknowledge Dr. Gary Hasey and Dr. Duncan MacCrimmon for contributing their medical knowledge and expertise to advance my research.

Table of Contents

List of Figures

List of Tables

List of Abbreviations

A = amperes

A/μs = Amperes per microsecond

A/D = Analog to digital

ADC = Analog to digital converter

AS-EEG-DAQ-S = Artifact Suppressing Electroencephalogram Data Acquisition System

BPF = Band Pass Filter

BRF = Band Reject Filter

cm = centimeters

DC = direct current

EEG = Electroencephalography

ECT = Electro Convulsive Therapy

EP = Evoked Potential

Hz = Hertz

HPF = High Pass Filter

LPF = Low Pass Filter

m = meters

mm = millimeters

MOSFET = Metal Oxide Semiconductor Field Effect Transistor

ms = milliseconds

MT = Motor Threshold

rTMS = repetitive Transcranial Magnetic Stimulation

s = seconds

TMS = Transcranial Magnetic Stimulation

μs = microseconds

μV = microvolts

V = volts

Chapter 1: Introduction

Transcranial magnetic stimulation (TMS) was originally applied to the motor cortex to elicit muscle evoked potentials (EP's), usually from the thenar muscle, to study upper motor neuron disease or dysfunction in humans. Since this time the use of TMS has expanded to the field of neuropsychiatry and is now used as an experimental treatment for depression. Depression therapy is carried out through stimulation of the frontal lobe of the brain. Though standard clinical procedures exist for locating the frontal lobe, there is no quantitative measure to ensure the stimulation is optimal for the patient. This work aims to optimize rTMS depression therapy by designing a system to record TMS brain evoked potentials (EP's), which could be used to give an indication of TMS coil placement during frontal lobe stimulation.

Present TMS techniques involve finding thenar muscle upper motor neurons through muscle EP's, measuring 5cm anterior from this point along the sagittal (parallel to midline of the head) plane and stimulating there over the frontal lobe. The stimulus amplitude is preset and is a percentage of the amplitude required to elicit thenar muscle EP's. The frequency is fixed for a set number of stimulus pulses. Under current practice there is no immediate feedback to determine whether the position, amplitude or frequency is optimal for the treatment. Results using clinical outcome measures are not available for efficacy of treatment until several weeks of treatment have begun.

To optimize clinical efficacy for treatment and to gain further knowledge about the immediate neural effects of stimulating the frontal lobes and midline, it would be

advantageous to obtain short and long latency brain evoked potentials during stimulation. This has been attempted in the past using Electroencephalography (EEG), but with little success for short latency EP's.

Figure 1.1 shows how a TMS coil is placed over the frontal hemisphere. To record EP's during TMS, EEG electrodes are placed on the scalp in proximity to the coil. Collecting EEG data during TMS is complicated as it is affected by the large magnetic field created by the coil.

Figure 1.1: TMS coil placement. Source: Medtronic, 2004.

The very large magnetic fields induce current in the brain tissue. In addition the short-duration, high intensity magnetic pulses induce currents in the hardware components (EEG electrodes and EEG amplifiers). This results in very large voltage artifacts being presented to the amplifiers. The capacitances of both electrodes and electronics prolong the duration of the artifact. Even if the first amplifier stage is low gain and does not saturate, for example when using voltage clipping diodes, the subsequent high gain amplifiers will be saturated since the overall gain is typically at

least one thousand. This is the minimum gain required to present microvolt (μV) EEG signals to the analog to digital (A/D) converter. Sophisticated numerical artifact reduction techniques can only be applied once a highly amplified signal has been recorded.

Many researchers in the field have attempted to block the TMS artifact, usually using low slew rate amplifiers (band limited amplifiers), but to date, no one has published an artifact free plot of a TMS Evoked Potential (EP) recorded with EEG (Ilmoniemi, 1997, Fuggetta, 2005, Thut, 2005, Ives, 2006, Shutter, 2006). It is the goal of this research study to define an optimal system, given present day stimulating paradigms and present day technology, to collect TMS EPs using EEG.

An additional concern with EEG recording during repetitive TMS (rTMS) is patient safety. Due to the large induced electric field, any metal objects, especially recording electrodes in the vicinity of the TMS coil, will have an induced voltage across them which will result in significant current flow and heating. Before clinical studies could be proposed, this issue had to be considered. This thesis investigates the extent of this heating and determines the associated risk to the patient.

The chapters of the thesis are organized as follows: Chapter 2 provides additional background information covering EEG, TMS and artifact blocking. Chapter 3 discusses the issue of electrode heating when combining rTMS and EEG. Chapter 4 presents the artifact blocking approaches studied. Chapter 5 presents preliminary EP results recorded from one subject undergoing TMS. Chapter 6 discusses the conclusions and future work.

Chapter 2: Background

2.1 Electroencephalography

The EEG signals present after TMS are a result of volume conduction and neuronal pathway conduction within the brain. Signals are collected by extra-cellular recordings on the scalp, which means the potentials recorded are primarily generated in the cerebral cortex, the 2-5mm thick folded layer of neurons at the brains surface. Due to the impedance properties of the volume conductor, the signals collected are a summation of many individual sources within the brain (Nunez, 2006).

The origin of ambient EEG is the post-synaptic potentials from the cerebral cortex. Evoked Potentials (EP's) however, may be recorded from the cortex or much deeper structures, and may be largely a result of conducted action potentials.

The method of recording ambient EEG is shown in figure 2.1. This is the same method as used to record EP's using EEG, except that a much higher sampling rate must be used because the EP signals are much shorter in duration. Usually an EEG signal is around 100μV in amplitude. Ambient EEG bandwidth is usually 0.5 to 60Hz. EP EEG bandwidth is expected to far exceed the normal 100Hz range of commercial EEG machines and could be an order of magnitude greater, around 1000Hz.

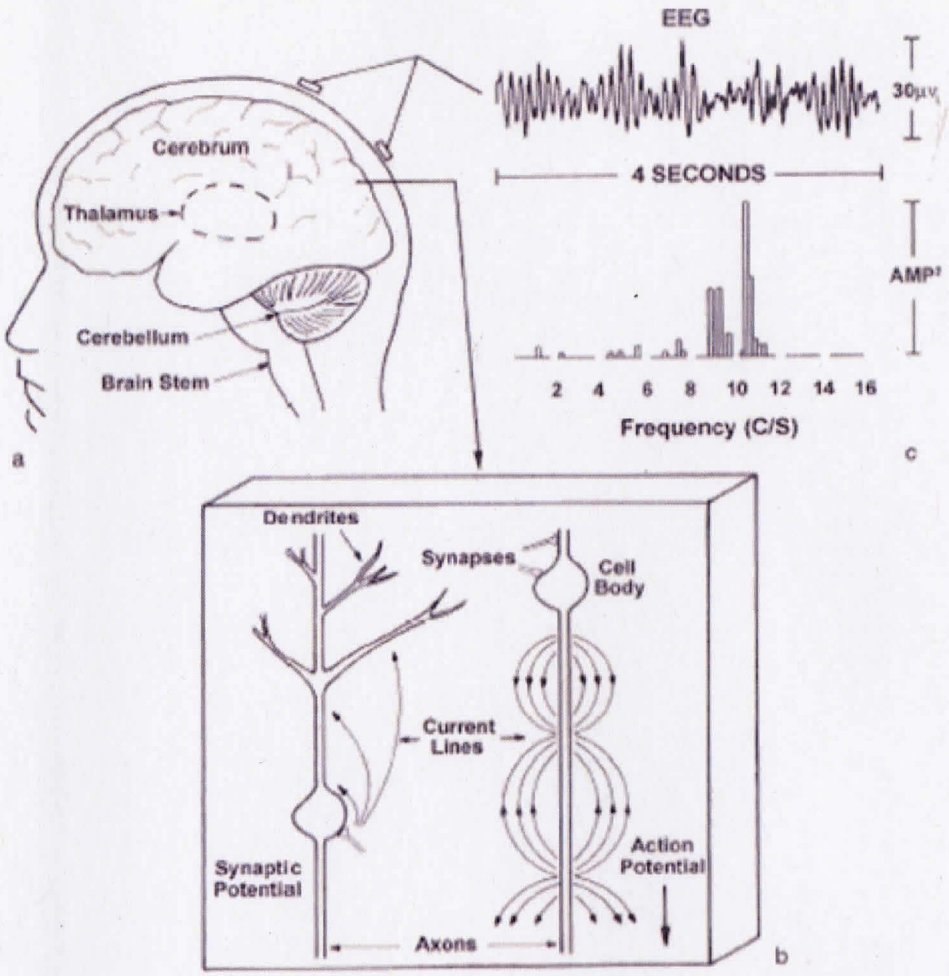

Figure 2.1: How EEG is recorded from the scalp. (a) Shows the human brain with EEG electrodes attached to the scalp. (b) Shows a section of the cerebral cortex and how the current sources are due to traveling action potentials and synaptic potentials. (c) Shows 4s of alpha rhythm EEG with the power spectrum shown below (Nunez, 2006). Source: Nunez (2006)

For EEG combined with TMS, electrodes that have been used include Ag/AgCl (Ilmoniemi, 1997, Iramina, 2004, Shutter, 2006), conductive plastic coated with Ag epoxy (Thut, 2005, Ives, 2006), and notched Ag/AgCl coated electrodes (Fuggetta, 2005). Standard electrode sizes used by other researchers have been 10mm because they are usually already available in most EEG laboratories. Some researchers have used smaller electrodes, as small as 4mm in diameter, to help reduce heating concerns.

The types of EEG recorders used in these studies have most commonly been standard EEG machines with varying filter settings to reduce the TMS artifact. The different settings have included: sampling at 3kHz with a 250Hz digital low pass filter (LPF) (Ilmoniemi, 1997), sampling at 200Hz with a 70Hz LPF low slew rate amplifier (Thut, 2005), sampling at 1024Hz with a 512Hz LPF (Fuggetta, 2005), and sampling at 250Hz with a 70Hz LPF low slew rate amplifier (Shutter, 2006).

To record EP's, or ambient EEG, surface electrodes are placed at standardized locations on the scalp, known as the 10-20 system. The 10-20 system is shown in figure 2.2. These standard positions are used to allow researchers at different institutions to compare results.

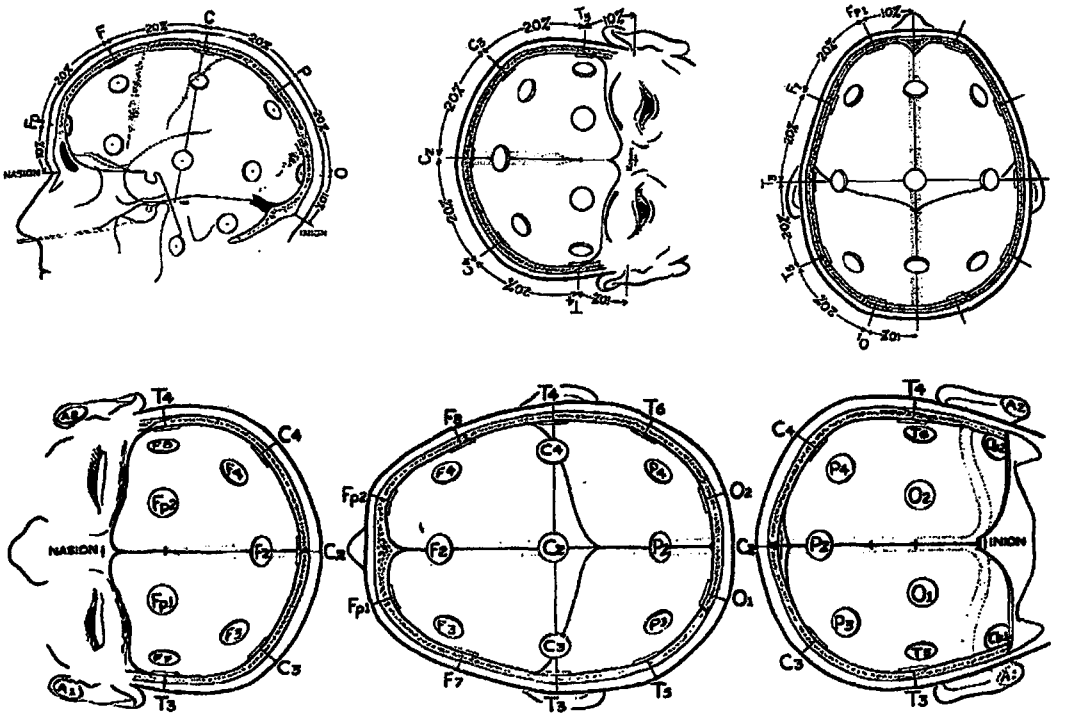

Figure 2.2: 10-20 EEG electrode system. Source: Webster (1998)

The brain, skull and cerebral spinal fluid (CSF) are volume conductors. Although EEG has very high temporal resolution, it has poor spatial resolution because all potentials can be volume conducted over large areas of the scalp when surface recording techniques are employed. Therefore, the measured signal is a combination of potentials generated immediately under the electrodes plus attenuated signals volume conducted from more distant sources, either through cortical or even deeper structures.

For this thesis, the concentration will be on the EEG's recorded from TMS and the instrumentation systems used.

2.2 Transcranial Magnetic Stimulation

TMS, introduced in 1985, involves placing a magnetic coil over the subject's head and sourcing a large electric current through the coil, which creates a brief 1-2 Tesla magnetic field near the coil. TMS was first proposed for studying upper motor neuron disease and was used to stimulate upper motor neurons directly by placing the coil over the motor cortex in the area where the upper motor neurons of a skeletal muscle are located. The amplitude of the TMS would then be increased until an electrical response from the thenar muscle, known as an M-wave, was recorded. The TMS stimulus amplitude from that initial M-wave is called the motor threshold (MT).

To delve more into the details of TMS, the magnetic field plot for a circular coil and a figure-of-eight coil are shown in figure 2.3. This changing magnetic field induces an electric field inside the brain, which stimulates the brain's neurons to fire. The electric fields induced by these changing magnetic fields are shown in figure 2.4.

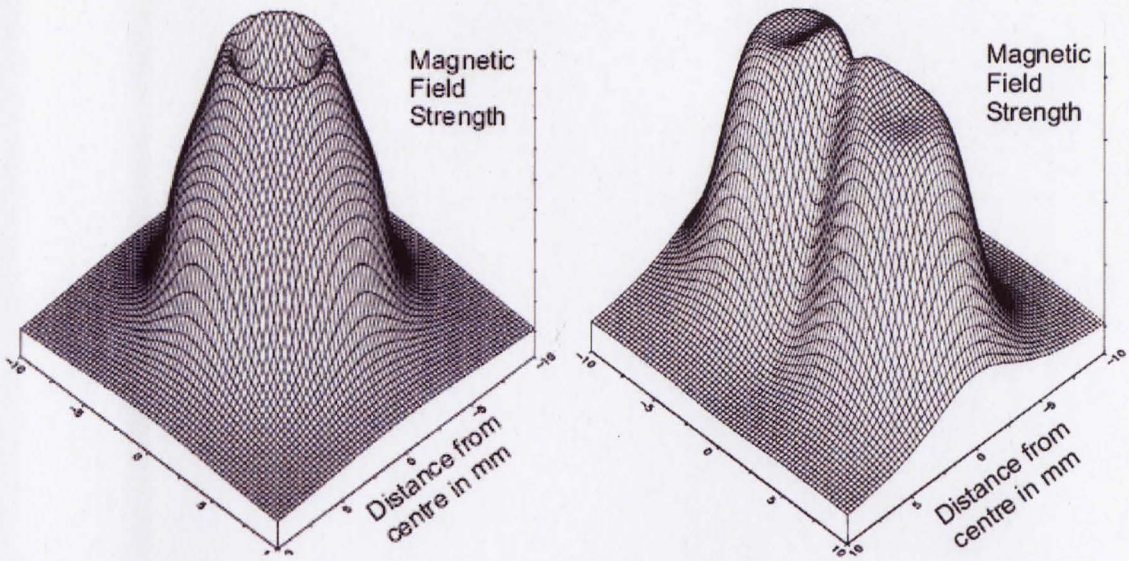

Figure 2.3: Left: Magnetic field plots for a 90mm diameter circular coil. Right: Magnetic field plot for a figure-of-8 coil with 70mm diameter coils. Source: Hovey, 2003.

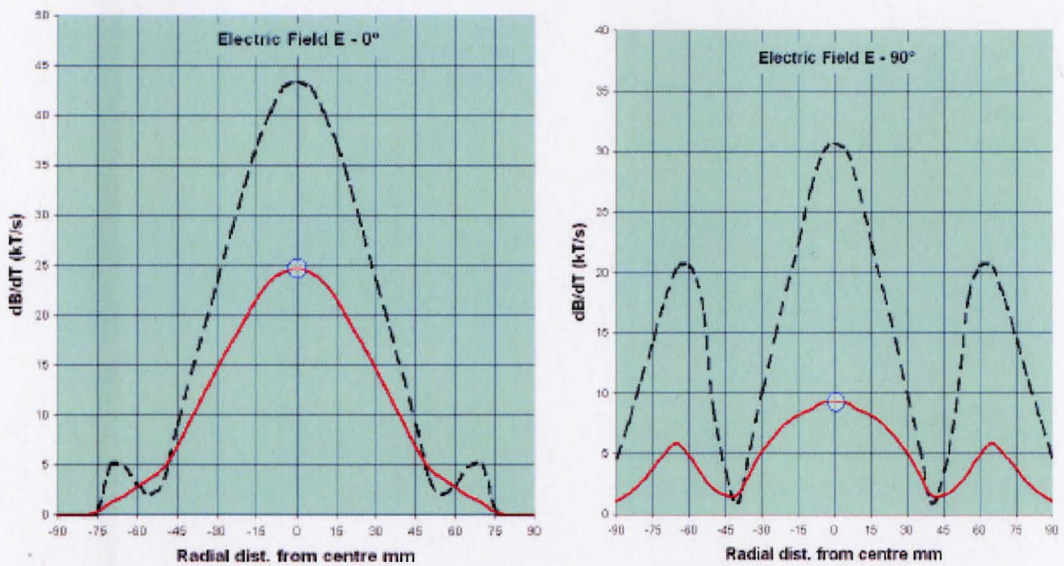

Figure 2.4: Left: Electrical field strength from a circular TMS coil. Right: Electrical field strength from a figure-of-eight TMS coil. The dotted line shows the Electric field strength at 2mm from the coil surface. The solid red line shows the Electric field strength at 20mm from the coil surface. Source: Medtronic, 2004.

Once neurons are stimulated to fire, the activation can spread through the cerebral cortex and other brain centers by neuronal pathways. TMS pulses are usually 200-400μs in duration and have a realized instantaneous initial current slope (di/dt) of up to 100 A/μs. Ives (2006) states that important information is found in EEG signal bandwidths up to and including 90Hz. Short latency brain evoked responses should have bandwidths even higher (e.g. auditory brain stem evoked potentials). TMS equipment used by other researchers (Ilmoniemi, Thut, Fuggetta, and Shutter) has used figure-of-eight coils with biphasic waveforms and stimulus intensities of 70% to 100% of MT. Stimulation rates of around 10Hz are most commonly used to treat depression (Ilmoniemi, 1997, Thut, 2005, Fuggetta, 2005, Shutter, 2006).

In 1995 TMS was demonstrated to have possible therapeutic effects on depression (Wassermann, 1998). rTMS is currently being used as an experimental treatment for depression and schizophrenia, as an alternative to Electro Convulsive Therapy (ECT), in experimental clinics around the world. Unfortunately in these applications, areas of the brain other than the motor cortex are stimulated, with no immediately measurable response from each stimulus. The current protocol is to find the cortical area and MT for the thenar muscle as described in the introduction chapter.

Safety is the primary concern when doing any type of biomedical research. A very notable paper was published in 1998 by Eric M. Wassermann that detailed the issues and suggested guidelines for rTMS treatment. It is believed that single pulse TMS is safe and useful for investigative purposes of human neurophysiology (Wassermann, 1998). Slow or Low Frequency TMS (that with stimulation rates of 1Hz or less) is currently

considered safe (Wassermann, 1998). Repetitive TMS (rTMS) is potentially dangerous. Risks include regional blocking or facilitating of cortical processes. Wassermann notes in his paper of seven known cases where patients had seizures induced by rTMS. Fast or high frequency TMS (with stimulation rates of greater than 1Hz) are considered by the U.S. Food and Drug Administration (FDA) to carry some risk (Wassermann, 1998).

Based on clinical rTMS using rates of 20Hz versus the recommended 1Hz, electrode heating must be considered, since using TMS simultaneously with EEG recordings is relatively new and no official protocol has been agreed upon by all researchers. Currently a myriad of different recording electrodes are being used for TMS-EEG combined studies. In this thesis, a system has been designed to record EEG during TMS. Obviously, the very strong fields generated during TMS induce a circular current in the EEG electrodes, especially when the coils are placed directly over the electrode. This presents no problem during low frequency TMS since the heat generated by this current flowing through the electrode material (I^2R) will continually dissipate by radiation to the surroundings whether air or through the paste. However, during moderate to high rate rTMS, 10Hz to 20Hz, this heat cannot dissipate fast enough and builds up.

The next question to consider is how many stimuli should be given to get a reliable average, free of background EEG, in the interest of keeping the total number of stimuli given per subject to a minimum. Previous studies have found that 50 stimuli are enough to generate a reliable average signal (Shutter, 2006). When recording from scalp electrodes during TMS, the resultant signal, despite good recording techniques and low

electrode impedance, will be composed of the brain response and residual 60Hz, environmental, instrumentation, and physiological noise. Since the signal-to-noise ratio (SNR) is usually less than 1, and in some cases less than 0.1, synchronous or ensemble averaging is employed to obtain the TMS brain EP. That is, the signal epochs, the one second recording period post TMS, for all stimuli are simply averaged.

2.3 Current Methods of Removing Artifact

The research in section 2.3 was presented and published in the proceedings of the *20th Canadian Conference on Electrical and Computer Engineering* (Apr. 22-26, 2007) Vancouver, BC, as a platform presentation and a four page paper (Archambeault[b] et al, 2007).

Multiple methods of artifact blocking have been attempted by other researchers in this field. One method that has been employed is a de-blocking function which switches off the EEG amplifiers during the TMS pulse but only allows viewing of the EEG 200ms post-stimulus (Shutter, 2006). Another approach used was slew rate limited amplifiers (Thut, 2005, Ives, 2006). Slew rate limiting amplifiers do not allow analysis of the evoked potential (EP) during the 30ms immediately following the TMS pulse and also reduce biological signal bandwidth, which is undesirable (Ives, 2006). Thus, 70Hz low-pass filtering used to give an amplifier or pre-amplifier a lower slew rate reduces the useful bandwidth of the EEG signal recorded, and certainly cannot be used to record short duration EPs.

High slew rate or high bandwidth amplifiers which allow viewing of the EP 15ms post-stimulus have also been used with a bandwidth of 500 Hz (Fuggetta, 2005). It is hypothesized that a higher bandwidth in the range of 1 kHz to 2 kHz would allow the early response EP to be seen much better.

One research group has also used sample-and-hold circuitry to hold the inputs to the EEG amplifiers constant until after the TMS pulse has finished (Ilmoniemi, 1997). However, they never released details on their circuit design, nor did they publish time plots of their recorded data. On the outset this approach appears to be both the most complicated to implement and should also provide the best results, allowing viewing of the EP within a few hundred microseconds of the magnetic stimulus.

In summary, there are many different recording systems being used by researchers in this field, ranging from standard EEG machines with low or high bandwidth filtering to custom built front end circuits implementing sample-and-hold circuitry. No standard currently exists and no one has yet published a working circuit design to implement sample-and-hold circuitry for the purpose of TMS artifact blocking.

Chapter 3: Electrode Heating

The research in chapter three was presented and published in the proceedings of the *30th Canadian Medical and Biological Engineering Conference* (June 16-19, 2007) Toronto, ON, as a poster and a four page paper (Archambeault[a] et al, 2007).

3.1 Introduction

The objective of this study was to determine experimentally whether modern standard or modified EEG electrodes are suitable for use in recording EEG during rTMS without the recording electrodes heating to a temperature that could cause thermal skin damage. This study builds on previous work by Pascual-Leone et al. in 1990 and Roth et al. in 1992 that helped clarify the heating of metal electrodes during rTMS. This study adds to their analysis the newly available carbon EEG electrodes available from Biopac Inc. and re-analyzes notching electrodes to reduce eddy currents (Pascual-Leone, 1990; Roth, 1992).

Many research groups currently use different electrodes to record EEG during rTMS and no standard choice has yet been determined. This study has been conducted to provide quantitative evidence for the safe use of intact or slightly modified commercially available EEG electrodes during rTMS.

The safe temperature an electrode can reach without causing cutaneous damage depends on the exposure time. To determine these thresholds a human study conducted in 1947 on healthy subjects that applied surface heating to the point of producing a first degree (1°) burn, i.e. a mild burn of the top layer of the skin characterized by pain and redness but without blistering, was reviewed. Condensing the results of this study a time-surface temperature table of thresholds for thermal injury of human skin relevant to the current experimentation was constructed. This compilation is shown in figure 3.1.

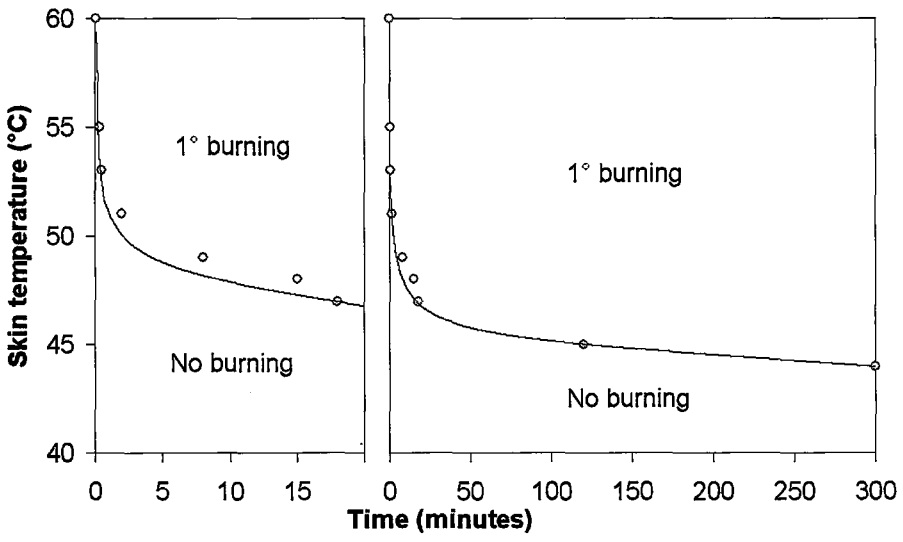

Figure 3.1: Time-temperature thresholds for burning of human skin. For points above the curve a first degree (1°) burn can result. For points below the curve no burning should occur. The left side plot is a close up view of the first 20 minutes of the right side plot. Source: Moritz et al., 1947.

Given that current rTMS treatment can include as many as 2,400 pulses at a frequency of 0.25Hz up to 20Hz, electrode heating is a concern for causing thermal skin damage. A typical rTMS treatment of 10Hz with train length of 80 pulses given once every minute would last 10 minutes for an 800 pulse treatment and 30 minutes for a

2,400 pulse treatment. From figure 3.1 it was determine that for a 30 minute study, 46°C is the hottest temperature any scalp EEG electrode should be allowed to heat to. This is not to say that at all temperatures below 46°C no thermal damage will occur, because subjects will vary in their skin's susceptibility to burning (Moritz, 1947). As well, any level of discomfort such as heat spots should be avoided. However, 46°C is a good estimate of an absolute upper limit.

The estimated range of normal body temperature in an adult is 36°C to 37.5°C (Guyton, 2000, pg. 823). Taking 37.5°C as the high-end skin temperature and use the previously determined skin temperature of 46°C as the temperature at which a 1° burn can occur during a combined TMS-EEG study, the maximum allowed temperature increase of electrodes attached to human skin should be less than 8.5°C for a rTMS session lasting no more than 30 minutes. To err on the safe side and ensure no 1° burns, the temperature increase of the electrode in the worst position possible (that with the largest perpendicular magnetic field creating the most substantial planar electric field and thus the greatest heating) should be chosen such that it is less than 8.5°C.

The temperature increase of an electrode per stimulus is directly related to the electrical conductivity of the electrode, the square of the radius of the electrode and the square of the stimulus strength (Roth, 1992). Looking at conductivities of different materials (Table 3.1) that could be used as electrode material hypotheses can be made about which electrodes will be suitable for rTMS-EEG studies.

Table 3.1: Electrode conductivities (σ)

Material	Conductivity (x 10^6 S/m)
Silver	62.9
Gold	41.0
Carbon	0.029

Source: Serway, 2000, pg. 847

3.2 Test Equipment

Temperature measuring equipment used was a thermistor temperature probe with 0.01°C accuracy (Digi-Sense LN5775, Cole-Parmer, Illinois) calibrated to +/- 0.2°C and read to 0.1°C. The TMS machine used was a Magstim Super Rapid (The Magstim Company Ltd., Whitland, Wales, U.K.). The TMS coil used was a Magstim figure-of-eight air-cooled coil P/N 1640 (Inner diameter 56mm, outer diameter 87mm, 9x2 turns, 16.4μH inductance, 0.93Tesla peak magnetic field). Four commercially available EEG electrode types were tested. They were: (i) reusable EEG/EP electrodes Part no. #101339 (silver cup, 10mm diameter, 2mm hole) (XLTEK, Oakville, Ontario, Canada); (ii) Standard gold cup electrodes (10mm diameter, 2mm hole) (Clevemed, Cleveland, Ohio, U.S.A.); (iii) Ag/AgCl surface electrodes model F-E5SCH-48 (10mm diameter, 2mm hole) (Grass Technologies, West Warwick, Rhode Island, U.S.A.); (iv) EL258RT reusable, general purpose, 8mm diameter, no hole, radiotranslucent carbon electrodes with carbon leads (Biopac Systems Inc., 42 Aero Camino, Goleta, CA 93117, USA). Additionally, the above mentioned gold cup and silver cup electrodes were pie notched to reduce induced currents and tested. Plus a fully notched gold-plated silver cup electrode (10mm diameter, 2mm hole) (Nicolet Biomedical) was tested.

3.3 Methodology

All testing was done on a ¼ inch sheet of plywood that was marked with a 1cm grid pattern to help ensure accurate coil placement. Electrodes were attached using EEG paste (Ten20 conductive EEG paste, D.O. Weaver and Co. Aurora, CO, U.S.A.). Testing parameters used in this study mirrored those used in standard rTMS treatments, which are 10Hz stimulation for up to 8s trains and 20Hz stimulation for up to 3s trains. It is known that temperature increase of electrodes varies approximately in proportion to the square of the stimulus strength (Roth, 1992), thus stimulator intensity is a very important factor in electrode heating. Stimulus intensity applied was set at 85% of the stimulating machine's maximum intensity to slightly exceed 110% of motor threshold (MT) of an average subject at our own and other rTMS laboratories (Thut, 2005).

Multiple electrode tests were conducted, plus the control case, where only the temperature probe was present with no electrodes. For TMS a figure-of-eight coil was selected since it heats electrodes significantly more than a circular coil (Roth, 1992). Figure 3.2 shows how electrodes were positioned in relation to the stimulating coil.

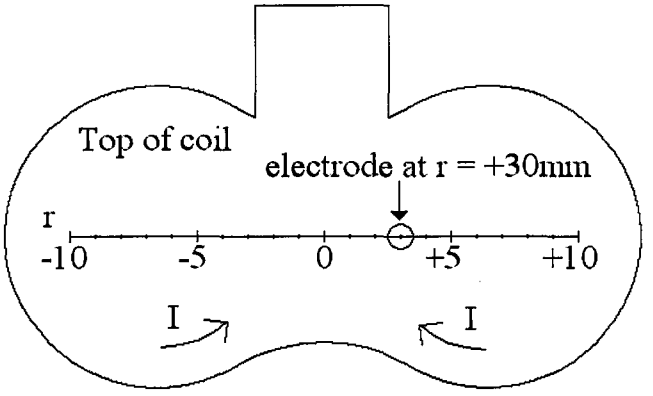

Figure 3.2: Stimulating coil showing how electrodes were positioned underneath with respect to the r-axis, labeled in cm.

Variable values were selected to provide the maximum heating while minimizing the number of experimental trials needed by using the work of Roth et al. (1992) to help determine optimal heating parameters. Looking at figure 2, and applying a standard x-axis and y-axis, electrode position was not varied along the y-axis because electrode heating under a symmetrical coil is largest along the x-axis at y=0 (Roth, 1992). A mechanical arm was used to position the coil and hold it in place during testing.

Room temperature during testing was 23°C. Coil temperature during testing was between 24°C and 26°C, held within that range by an air cooling system attached to the coil. Electrode heating was due to induced currents created within the electrodes by the large varying magnetic field and to a lesser extent by conduction of heat from the coil itself.

Looking at the thermal conductivity differences of the human skin versus the test case of plywood, wood has a thermal conductivity of 0.08W/m·°C, while a human, composed largely of water, would have a thermal conductivity closer to that of water which is 0.6W/m·°C (Serway, 2000). In comparing the wood used to skin on the human head, heat would be better conducted away by the human head, meaning that temperature results obtained on wood should be slightly higher than expected on the scalp.

All testing used the magnetic stimulator at 85% maximum intensity, except two tests: one with no electrode present and one with the carbon electrodes. Between every test the electrodes were allowed to cool to room temperature before the next test was started. For all tests the coil was placed directly against the electrode, with a distance of 10mm from the plane of the coil to the center of the electrode, accounting for the thickness of the plastic encasing the actual metal coils.

3.4 Results

The first test was conducted on a silver electrode, varying the distance from the center of the figure-of-eight coil (This distance will be referred to as r), to find the value for r where heating was a maximum. The results of this test are given in figure 3.3.

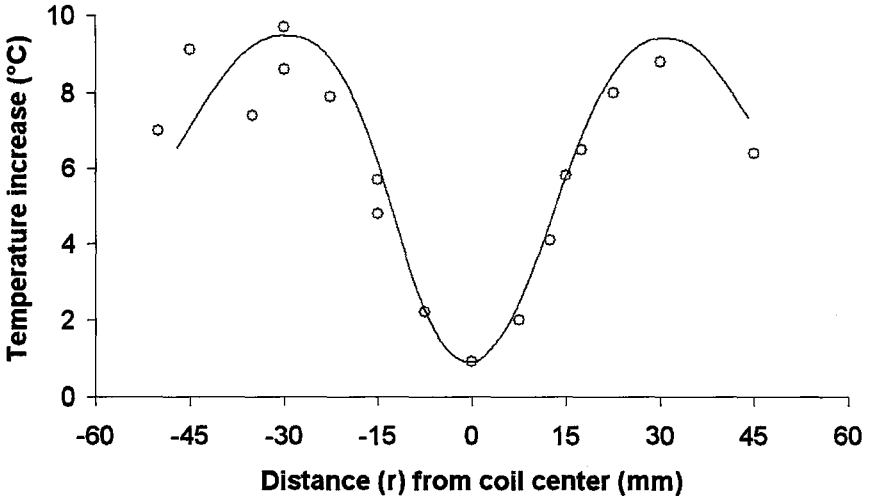

Figure 3.3: Temperature increase of a silver cup electrode from 3s at 20Hz at 85% intensity vs. the distance from the center of the figure-of-eight coil.

This agrees with the results presented by Roth et al. (1992) who showed that the maximum heating occurs at two locations, each half way between the center of one coil and the midpoint of a line drawn between the two centers of the two coils.

The same 3s 20Hz test was then conducted at the maximum heating location, determined to be r = 30mm, for 6 different electrodes. Figure 3.4 shows the heating and cooling curves for these tests.

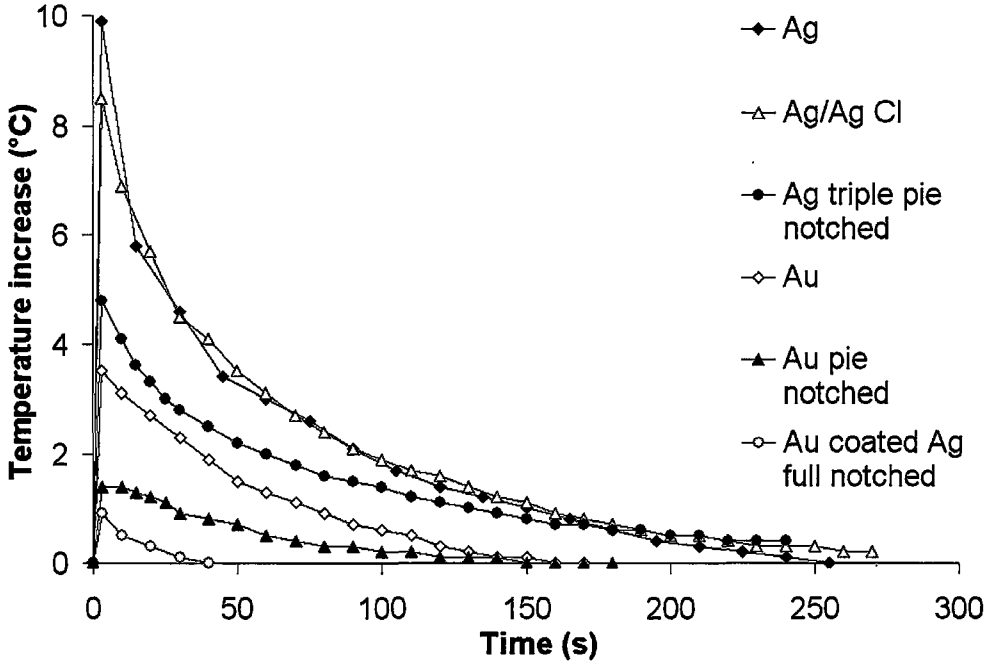

Figure 3.4: Temperature effects on 6 different electrodes from a single train of 3s at 20Hz at 85% intensity, r = -30mm.

Figure 3.5 shows three types of notching used. The pie notched electrodes did not eliminate the circular current path around the center hole and therefore did not result in as significant a heating reduction as the full notched electrode.

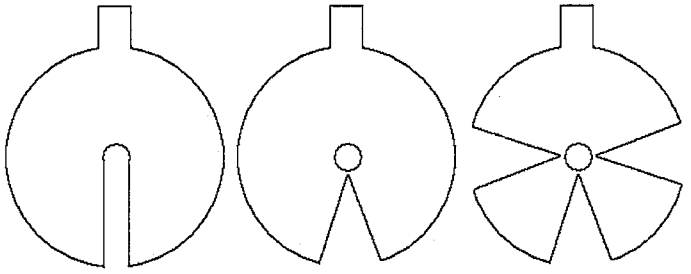

Figure 3.5: Differences in notching. From left to right: full notched, pie notched, triple pie notched.

The heating results of varying the distance from the center of the coil (r) for the gold-plated silver cup full notched electrode are shown in figure 3.6.

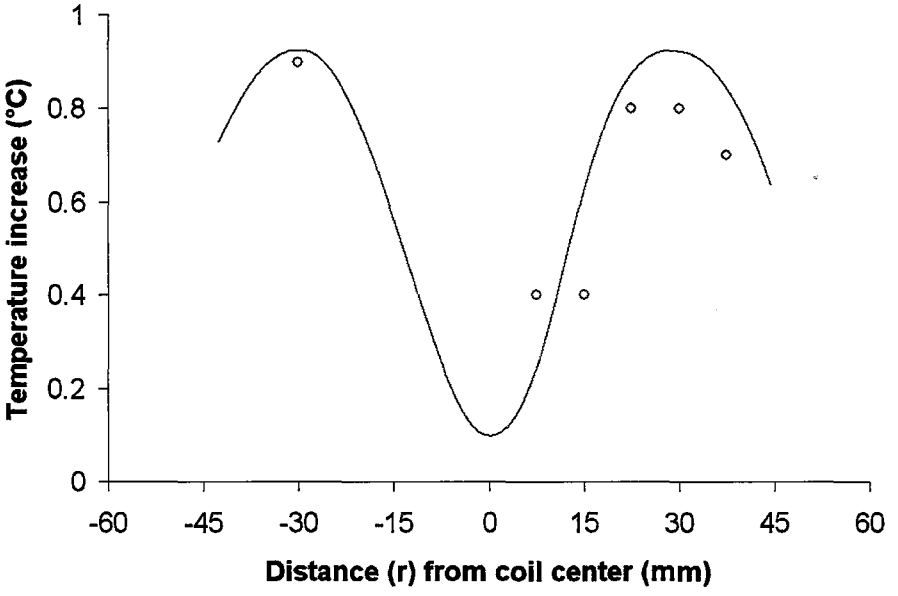

Figure 3.6: Temperature increase of a gold-plated silver cup electrode from 3s at 20Hz at 85% intensity vs. the distance from the center of the figure-of-eight coil.

When carbon electrodes were stimulated at 20Hz for 3s at 85% maximum intensity, r = -30mm, the temperature rose 0.0°C. When stimulated at 20Hz for 10s, r = -30mm, at 100% maximum intensity, the temperature rose 0.8°C. However, when the carbon electrode was removed from the stimulating environment leaving only the temperature probe and the EEG paste and stimulated at 20Hz for 10s at 100% intensity, the temperature rose 0.3°C. This showed that the temperature probe, the radiant heating from the coil and the induced currents in the paste accounted for some of the increase in temperature when 200 pulses were given. Clearly, the carbon electrodes do not pose a

heating risk under normal stimulating conditions. However, they are about three times the cost of Ag/Ag Cl electrodes.

Next, the gold cup electrodes were stimulated at 10Hz for 8s at 85% maximum intensity to simulate a standard rTMS treatment session. The results of this test are shown in figure 3.7.

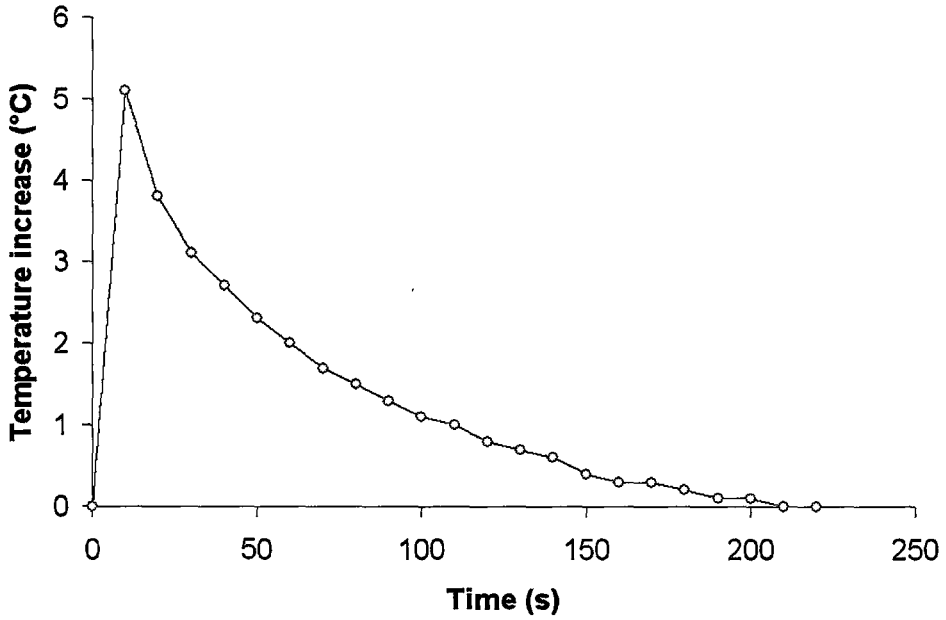

Figure 3.7: Temperature effects on gold cup electrodes from a single train of 8s at 10Hz at 85% intensity, r = -30mm.

Next, the same gold cup electrode was stimulated with 3 trains, starting times spaced 60s apart, of 3s at 20Hz, 85% intensity. Due to the fact that the next stimulus train started before the electrodes had a chance to completely cool, the next peak temperature reached for every pulse train after the first was significantly higher than the one before it. A plot showing the results of this test is given in figure 3.8.

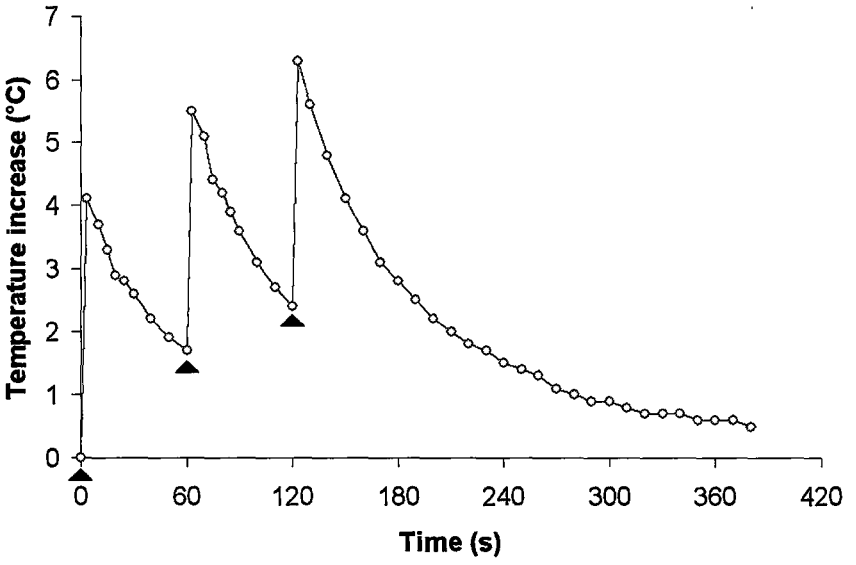

Figure 3.8: Temperature effects on gold cup electrodes from 3 trains of 3s at 20Hz at 85% intensity, r = -30mm. Trains were given at 0s, 60s, and 120s.

3.5 Conclusion

Unmodified silver and silver/silver chloride electrodes appear unsuitable for standard rTMS-EEG studies when high stimulus intensities are necessary due to the high conductivity of silver. If used at all, pulse trains should not exceed 30 pulses and electrodes should be allowed 290s to cool between trains, given the current TMS and coil parameters tested. Gold cup electrodes are suitable for rTMS-EEG studies for a Magstim cooled coil if stimulus intensity is kept below 85%, trains do not exceed 80 pulses, and electrodes are allowed to cool for 220s between stimulus trains. However, notching does work, and when notched properly (a full notch) electrode heating is reduced enough to make silver and gold-plated silver electrodes suitable for a standard rTMS-EEG study. The newly available carbon electrodes should be suitable for any rTMS-EEG patient study and their heating would not be the limiting factor in selecting stimulating parameters.

Chapter 4: Artifact Blocking Approaches

4.1 Introduction

The research presented in section 4.4 was presented and published in the proceedings of the *20th Canadian Conference on Electrical and Computer Engineering* (Apr. 22-26, 2007) Vancouver, BC, as a platform presentation and a four page paper (Archambeault[b] et al, 2007).

It is necessary to block the TMS artifact to analyze the short latency (sub 50ms) EP's. The simplest solution to avoid excessive artifact from damaging the input amplifiers would be to use back-to-back diodes between the signal leads and ground. However, that would just clip the artifact signal to a fraction of a volt. Since the recorded high gain EEG is in the μV range, the amplifier would be saturated by this clipping artifact. Without proper artifact blocking the TMS pulse can contaminate the EEG recorded and even saturate the signal leaving no useful information to signal process. Four different approaches to artifact blocking were tested before the best one was chosen.

Approach one short circuits standard EEG machine inputs together to prevent the artifact from getting through. Approach two pre-amplifies the signal, then uses sample-and-hold circuitry to block the artifact, then attenuates the signal back down to EEG voltage levels and feeds it into a standard EEG machine. Approach three uses a high bandwidth amplifier to allow fast recovery from the artifact, and a high sampling rate ADC board to collect the EEG. Approach four involves pre-amplifying the signal, using

sample-and-hold circuitry to block the artifact and then using a high sampling rate ADC board to acquire the EEG data, after additional post-sample-and-hold HPF, gain, and LPF.

4.2 Equipment

To test the circuits using TMS a Dantec MagPro magnetic stimulator model #05-1300 was used with a Dantec figure-of-eight coil MCB70 (Dantec, Skovlunde, Denmark). When a commercial EEG machine was needed a XLTEK 32 Channel EEG Headbox (500Hz sampling rate, 22bit A/D, 0.3μV resolution, 32 channels, +/-10mV maximum input range, input impedance 47 MOhms, CMRR 100dB from 0.1 to 100Hz, bandwidth 0.1 to 100Hz) with XLTEK Kortex EEG NeuroWorks 5.0 Software operating on a Pentium 4 computer was used (Xltek, Oakville, Ontario, Canada). For an ADC board a National Instruments PCI-6024E data acquisition card was used, capable of 200 kHz combined sampling, with an 8 channel breakout box, BNC-2110 (National Instruments, Austin, Texas). The LabVIEW board has 12 bit A/D converters. When using a voltage range of +/- 5V, this yields a post-amplifier voltage resolution of 2.5mV. When using a 1000 times gain amplifier this yields a pre-amplifier voltage resolution of 2.5μV.

All circuit testing was done using 10mm silver electrodes with a 2mm hole (XLTEK) with conductive paste, affixed with tape. Silver electrodes were suitable and

not considered a heating risk during these tests because very few stimuli were given with large delay times between stimuli to allow electrodes to cool down.

A trigger line split off box, for use with the Mag Pro stimulator external trigger input/output, was constructed to be able to gain access to the precise triggering needed to switch on and off an artifact blocking circuit for 400μs, timed to the TMS pulse. The trigger line split off box is shown in figures 4.1 and 4.2.

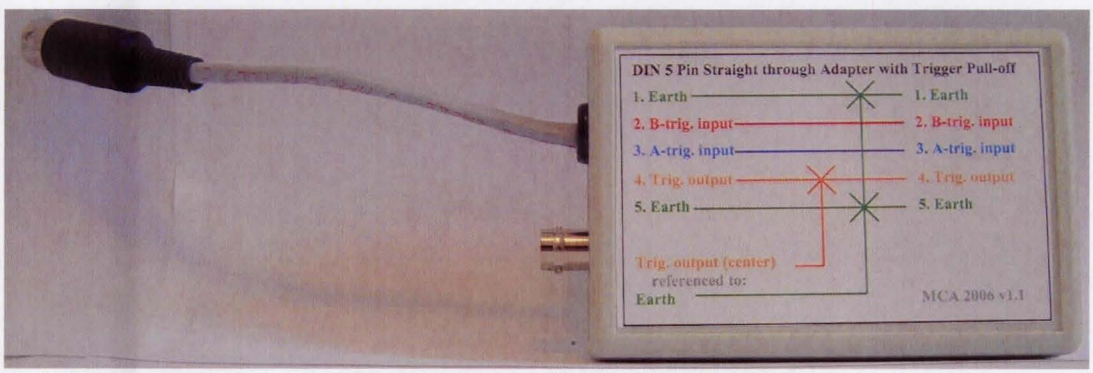

Figure 4.1: Trigger line split off box. Front side showing circuit connection.

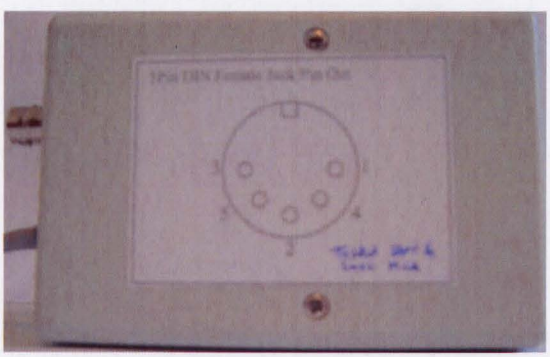

Figure 4.2: Trigger line split off box. Back side showing PIN out diagram.

4.3 Approach One

The first approach tested was to short circuit the inputs of a standard EEG machine (A blocking approach).

4.3.1 Design parameters

Short circuiting the input terminals of the EEG amplifier was tested using integrated circuit analog switches with low on-resistance (Texas Instruments TS3A4741DGKR and Analog Devices ADG512).

4.3.2 Circuit Tests

Initially, shorting the input pins of the input channels together to the reference using a 25ohm on-resistance analog switch (Analog Devices ADG512), was used. Two EEG electrodes were attached to a subject's arm and the stimulating coil placed over one of the electrodes. A commercial Dantec EMG system, triggered by the Mag Pro stimulator, was used to record the resulting artifacts. This 25ohm on-resistance resulted in a short-circuit condition offset of 15mV using the standard Dantec EMG recording system.

4.3.3 Discussion

There was a problem with using these integrated circuit analog switches because they are constructed of transistor networks; when the switch is activated the output pins short through the network and a small offset voltage exists. In general purpose, or higher voltage applications, this offset voltage is negligible. However, when dealing with EEG signals in the μV range, with EEG amplifiers having input ranges of +/-10mV, an offset voltage between the input terminals of the EEG amplifier can charge the input capacitance and result in an undesirable settling time, after the inputs are un-shorted, before the EEG signal can be recorded cleanly. It was this offset, as high as 15mV for the Analog Device's ADG512, which resulted in this approach being inadequate.

4.4 Approach Two

The second approach tested was to pre-amplify the EEG signal, use a sample-and-hold circuit, attenuate the signal back to EEG voltage levels, and then use a standard EEG machine (A blocking approach).

4.4.1 Design parameters

The first sample-and-hold circuit tested is shown in appendix 1. It is a microcontroller based circuit, designed to fit inline between the patient and a standard EEG amplifier. Appendix 1 shows the circuit diagram and appendix 2 shows the C code used to program the microcontroller in charge of the sample-and-hold circuit, which takes a digital trigger from the magnetic stimulator to synchronize timing.

Multiple sample-and-hold integrated circuits were tested to determine which ones met the required specifications to hold a μV amplitude signal. These specifications included a low hold-step, with a small hold mode offset (as tested). Table 4.1 shows the different sample-and-hold integrated circuits compared.

Table 4.1: Sample and Hold Integrated Circuits Evaluated (Worst case values)

	National Semiconductor LF398	Analog Devices SMP08	Analog Devices SMP04	Analog Devices AD783	Linear Technology LF398S8
Part description:	Monolithic Sample-and-hold circuit	Octal sample-and-hold with multiplexed input	Sample-and-hold amplifier	Complete very high speed sample-and-hold amplifier	Precision sample-and-hold amplifier
Input Impedance:	10^10Ω	N/A	N/A	10^7Ω	10^10Ω
Output Impedance:	4Ω	N/A	1Ω	0.6Ω	4Ω
"Hold Step":	2.5mV	4mV	4mV	85μV	2.5mV
Hold mode offset:	7mV	10mV	10mV	5mV	7mV
Sample mode offset:	7mV	10mV	10mV	200mV	7mV
Acquisition Time for 0.1% accuracy with 1000pF hold capacitor:	4μs	7μs	11μs	350ns	4μs
Droop Rate:	Depends on external capacitor selected	20mV/s	25mV/s	0.02μV/μs (20mV/s)	Depends on external capacitor selected
Pre-buffer needed:	No	Yes	Yes	No	No
Pre-amplifier needed:	Yes	Yes	Yes	Yes	Yes
Testing results:	Low offset ≤2mV	-	Low offset ≤2mV	Up to 200mV DC offset at output	Up to 100mV DC offset at output
Sample-and-hold IC passed testing criteria?	Yes	No	Yes	No	No
Reasoning:	Adequate, but expensive due to only one channel per chip. Will minimize noise, because channels can be kept separate.	Cheap, but due to multiplexed input design, you need an encoder, so 8 channels are not truly accessible.	Preferred chip. Cheap, with 4 independent channels. May not be used if noise is a big concern.	Very low noise, but offset way too big, plus it is very expensive.	Huge offset voltage during hold function.

The high level module diagram of the system is shown in figure 4.3. The stand-alone component is battery powered and uses one control line from the magnetic stimulator, through optical isolation, to trigger on and off the sample-and-hold circuitry timed to the TMS pulses. The detailed system design of a single channel is shown in figure 4.4. The sample-and-hold circuitry also contains a preamplifier and attenuator as shown in figure 4.5.

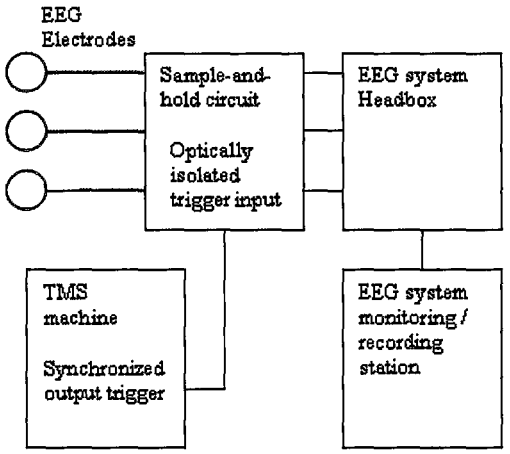

Figure 4.3: High level module diagram of artifact blocking system.

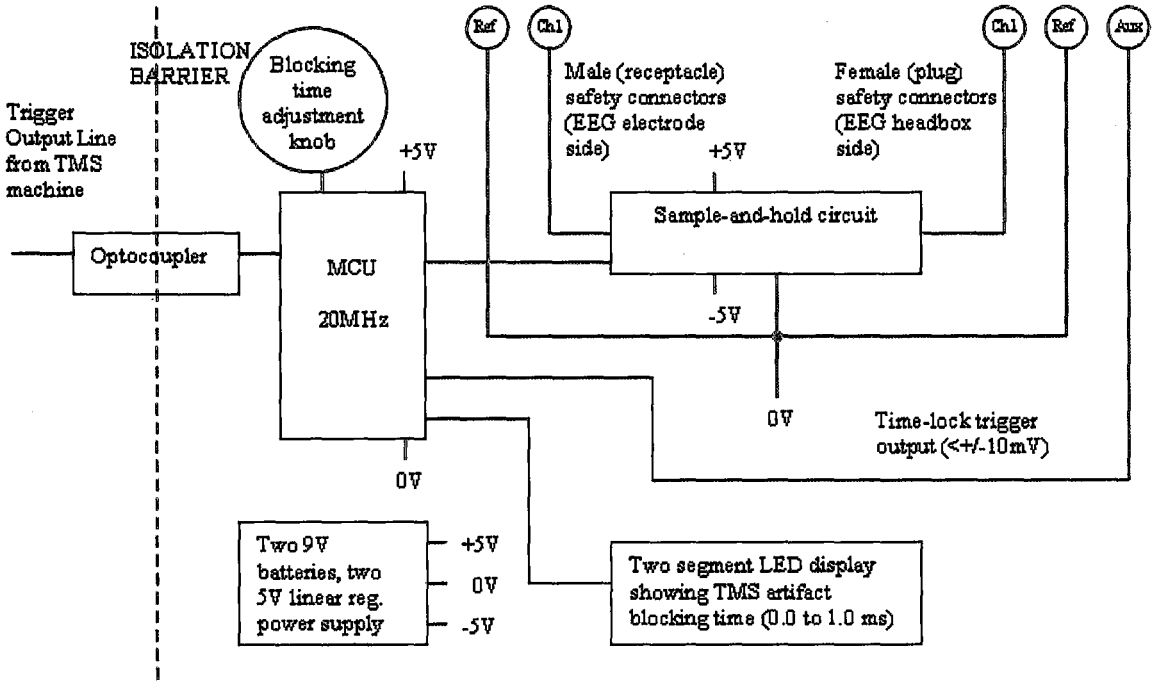

Figure 4.4: Detailed design of sample-and-hold circuitry for a single EEG channel with reference channel included. Every channel requires its own sample-and-hold circuit block.

The circuit for one channel, shown in figure 4.5, was built to be compatible with any commercially available EEG machine. It is designed to take an input signal with peak-to-peak amplitude of up to 5.4mV with a DC offset of up to +/- 270mV. If it is found that the input signal has a DC offset exceeding +/- 270mV this circuit should be modified by adjusting the gain on the first stage amplifier lower than 11. This will allow larger DC offset voltages without saturating the first stage amplifier. A suggested value for R6 of 3kΩ would reduce the gain to 4 and allow input signals with a DC offset of up to +/-750mV with peak-to-peak amplitude of up to 14.9mV. Another method to increase the range of both the DC offset and peak-to-peak amplitude would be to increase the voltage rails used to power the operational amplifiers from +/-5V to +/-15V. However, 5V is easily attained using 9V batteries with 5V linear regulators; whereas to attain +/-15V, DC-DC boost converters would need to be used. The operational amplifiers used were Texas Instruments OPA4277. The MOSFETs used were Fairchild Semiconductor N-channel logic level digital FETs (FDV301N).

Figure 4.6 shows the LTspice simulation when the input signal has no DC offset. The same plot is obtained for the V[vout] variable when the DC offset is within the allowable range. All simulated TMS pulses are 400μs in duration and biphasic. The 5 TMS pulses seen occur with respect to the "hold" function (i.e. the artifact blocking function) as follows: TMS pulse 1 starts 100μs after its hold function has ended and thus the entire TMS artifact is transmitted to the EEG machine; TMS pulse 2 starts 100μs before its hold function and thus a significant portion of the artifact is transmitted; TMS pulse 3 starts 100μs after the start of its hold function and thus a significant portion of the

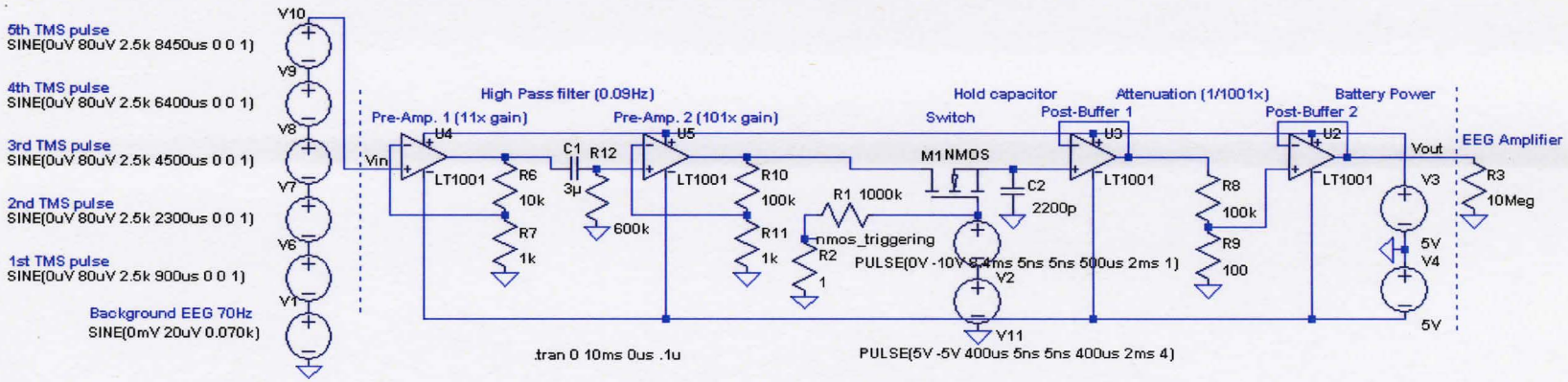

Figure 4.5: Sample-and-hold circuit designed in LTspice.

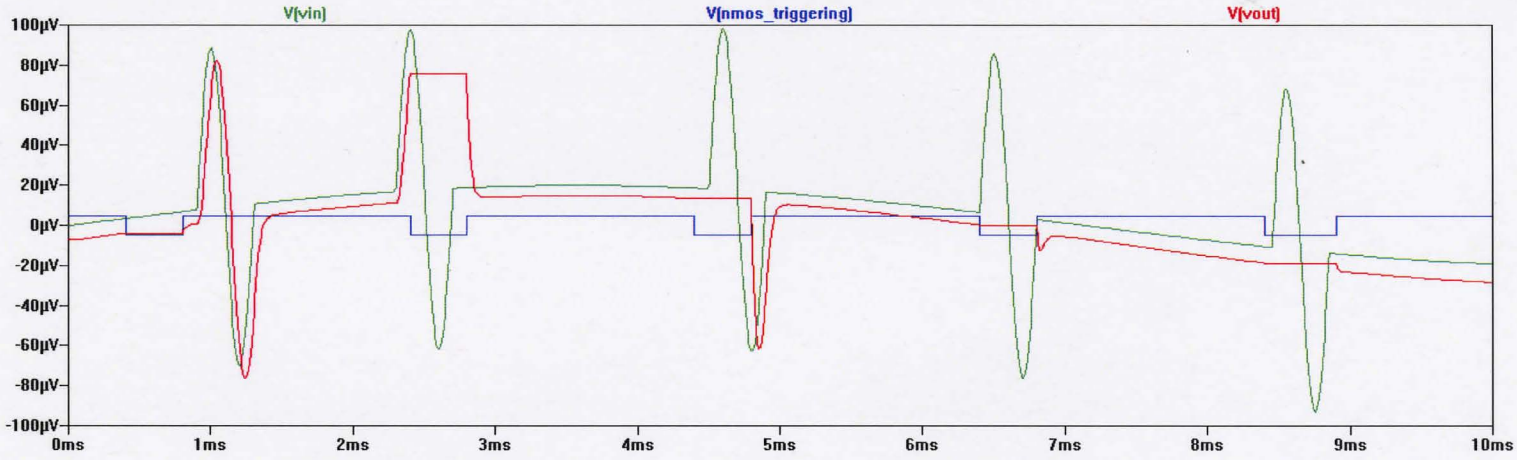

Figure 4.6: Simulation showing sample-and-hold circuit operation during 5 TMS pulses variously timed. The voltage signals are as defined in figure 4.5 above.

artifact is again transmitted since the pulse has not finished when the hold function stops; TMS pulse 4 is exactly timed with its hold function, which lasts exactly 400μs and thus blocks the artifact 95%, however, a small spike gets through, and when the start/stop times of the hold function were off by only a few μs a much larger portion of the artifact would be transmitted; TMS pulse 5 occurs 50μs after blocking has started and ends 50μs before blocking stops, resulting in the entire artifact being blocked. Given normal triggering circumstances, if the trigger line is read from the TMS machine, the initial 50μs delay between starting the hold function and the TMS pulse starting is not always possible to achieve, nor is it always necessary. It is sufficient for the blocking function to start a short time (<50μs) before the TMS pulse presents at the electrodes. However, the hold function should be kept on for a few μs post-stimulus to allow the input signal to stabilize before passing it through to the EEG machine.

4.4.2 Circuit Tests

Shown in figure 4.7 are preliminary results for the modular sample-and-hold artifact blocking circuitry. The top waveform in figure 4.7 shows the simulated input EEG signal created using a function generator, with a low-pass filter and attenuation stage to achieve a sufficiently small amplitude signal. The bottom waveform is the output from the sample-and-hold circuit, as triggered once every second. The large spikes show when the hold function is activated. It is hypothesized that these spikes are a result of the MOSFET switching on and off. The switching spike associated with turning the

MOSFET on and off is thought to be associated with the long wires used in creating the soldered breadboard which have inductances much greater than would be present in a final 32 channel milled circuit board version. This results in larger than expected inductive kickback when the MOSFET is switched on and off. When compared to results testing less robust circuit designs using MOSFETs or analog switches, the size of the switching spike has been greatly reduced in the current design. The spike is also an order of magnitude (ten times) shorter in duration than the TMS artifact it replaces, and should not adversely affect the collection of the EP a few milliseconds following the TMS pulse.

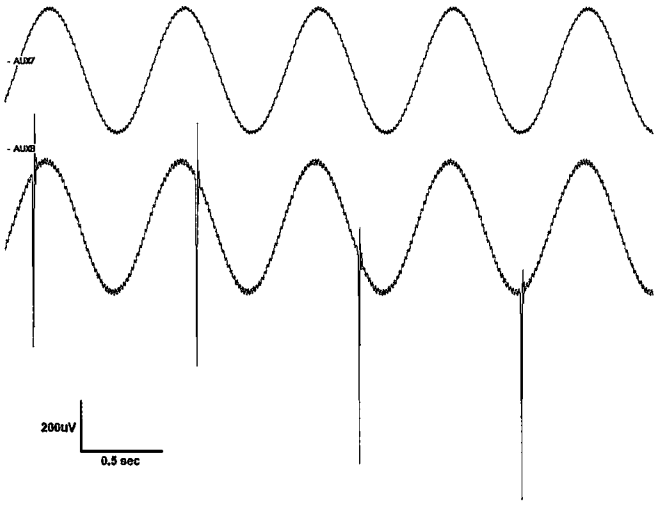

Figure 4.7: Actual testing results of the sample-and-hold circuit on a XLTEK 32 channel EEG machine.

4.4.3 Discussion

The sample and hold circuits present some transient voltage spiking when switching between sample and hold and vice versa. For example, of the best available monolithic sample-and-hold circuits, the LF398 from National has a switching transient of 0.7 V when switching to sample mode appearing at the output. Although this transient is very short in duration (< 2 μs) it still throws the baseline of the EEG amplifier away from equilibrium, which then takes longer to recover because it is a bandwidth-limited system. The transients that can be seen at the output of the LF398 are shown in figure 4.8.

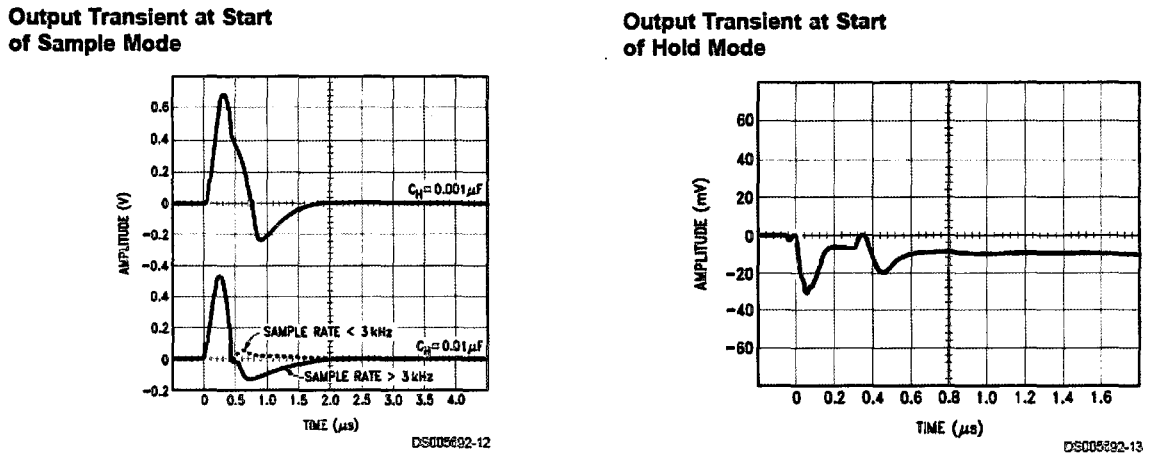

Figure 4.8: Output transients seen when the National LF398 switches from hold mode to sample mode (left) and from sample mode to hold mode (right).
Source: National Instruments data sheet: http://www.national.com/pf/LF/LF398.html#Datasheet

Building an EEG amplifier that has a much higher bandwidth, the switching transient should not upset the baseline longer than the 2μs specified in the sample-and-hold integrated circuit's data sheet. This would allow recording the first 30ms of post-stimulus EEG EP data switching transient and artifact free.

Figure 4.9 shows the feed through rejection ratio of the sample-and-hold circuit (LF398) with respect to input frequency. Using a hold capacitor of 2200pF the feed through rejection ratio is around -80dB. The LF398 sample-and-hold circuit selected has an excellent rejection ratio throughout the range of frequencies that make up the TMS artifact, which should have a fundamental frequency of approximately 2.5kHz, based on it being biphasic and having a duration of 400μs.

This approach would work for collecting long latency or low bandwidth EP's, however, to collect short latency EP's, a higher bandwidth EEG amplifier is required.

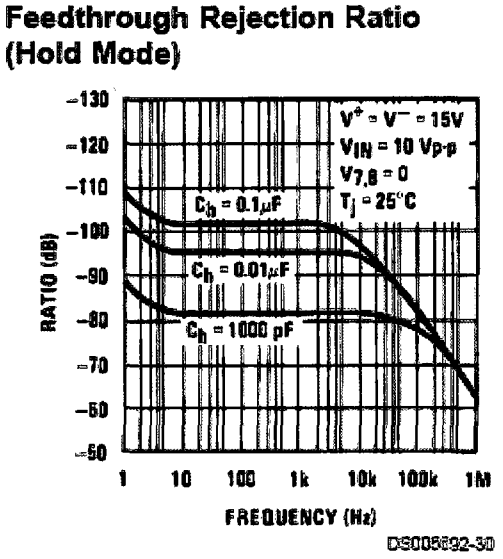

Figure 4.9: Feed through rejection ratio (during hold mode) of the LF398.
Source: National Instruments data sheet
http://www.national.com/pf/LF/LF398.html#Datasheet

4.5 Approach Three

Since commercial EEG systems have limited bandwidth and sampling rates, it was decided to design and build a system using a single stage high-bandwidth amplifier and a National Instruments PCI-6024E data acquisition board. A LabVIEW based software system had to be developed to control the hardware and display the recorded signals.

4.5.1 Design parameters

The high bandwidth design is shown in figure 4.10. A Texas Instruments INA126 instrumentation amplifier was used, with a typical common mode rejection ratio (CMRR) of 94dB, 83dB minimum.

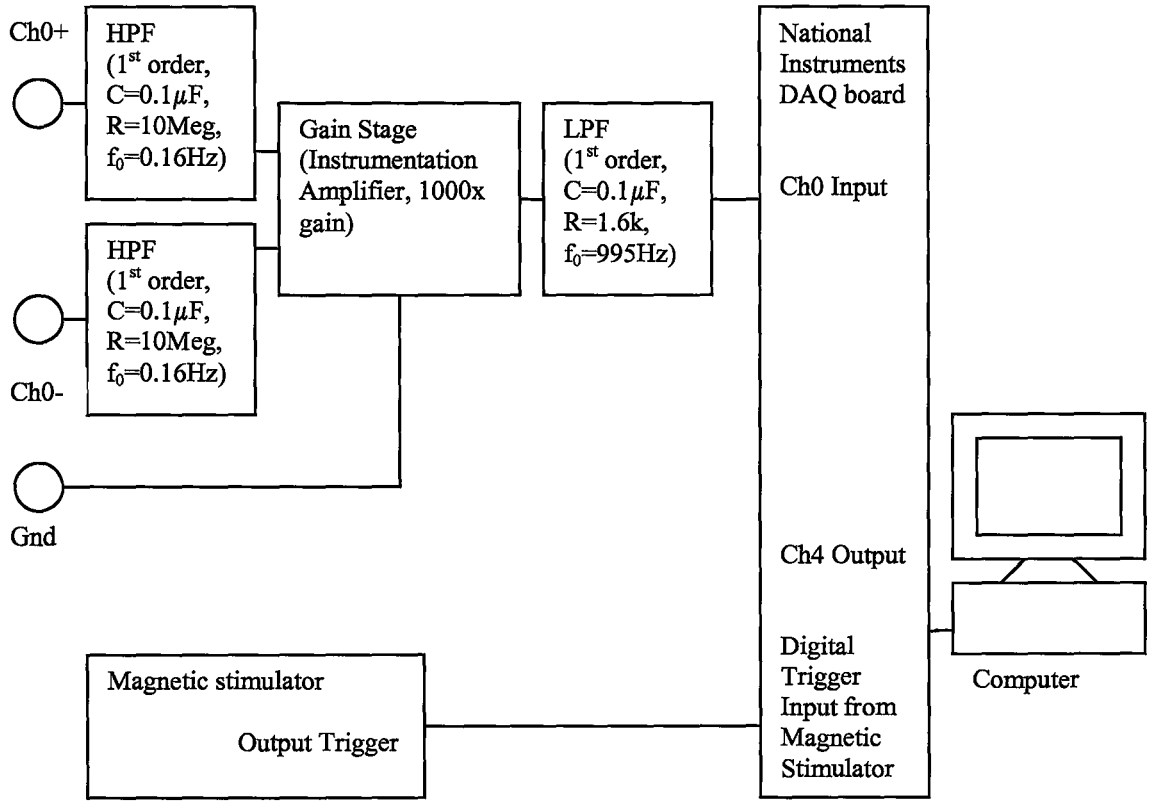

Figure 4.10: Artifact blocking EEG machine design using the high bandwidth (fast recovery) approach.

4.5.2 Circuit Tests

Using the high bandwidth amplifier, the biphasic TMS artifact is recorded, as shown in figures 4.11 and 4.12, for the first 10 ms and 1000 ms post TMS, respectively. The TMS artifact causes amplifier saturation, which requires 150 ms to settle below the op-amp supply voltage, and an additional 250 ms to return to an equilibrium state.

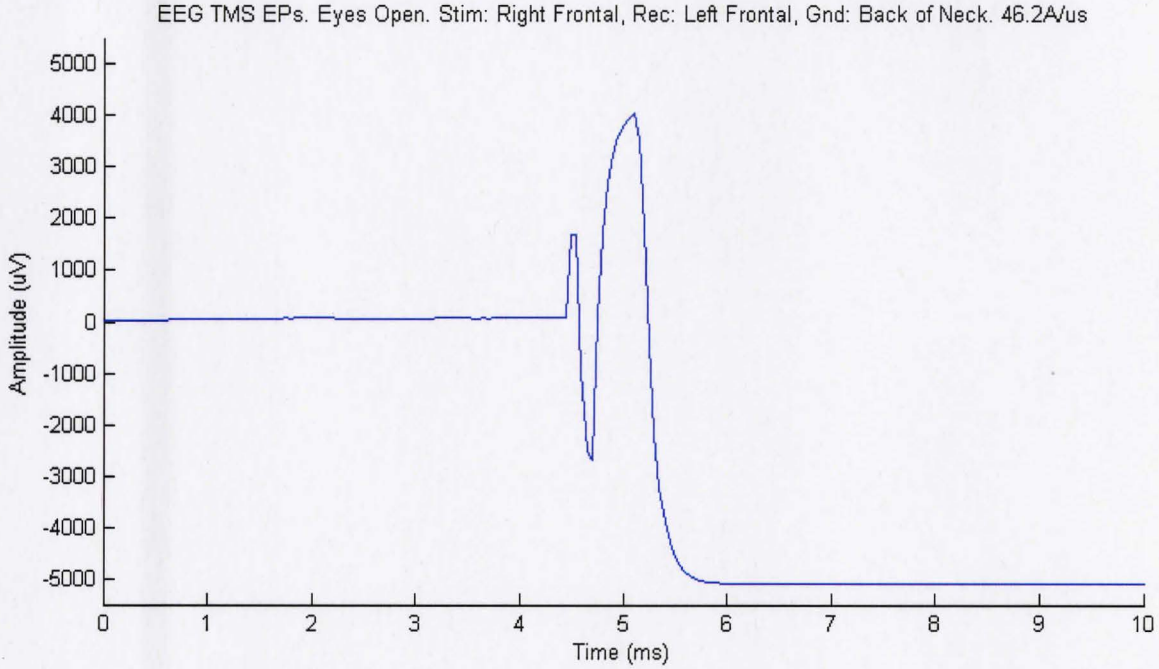

Figure 4.11: TMS pulse recorded with a 1000x gain high bandwidth amplifier, looking at the first 10ms of recording to show clearly the TMS pulse artifact.

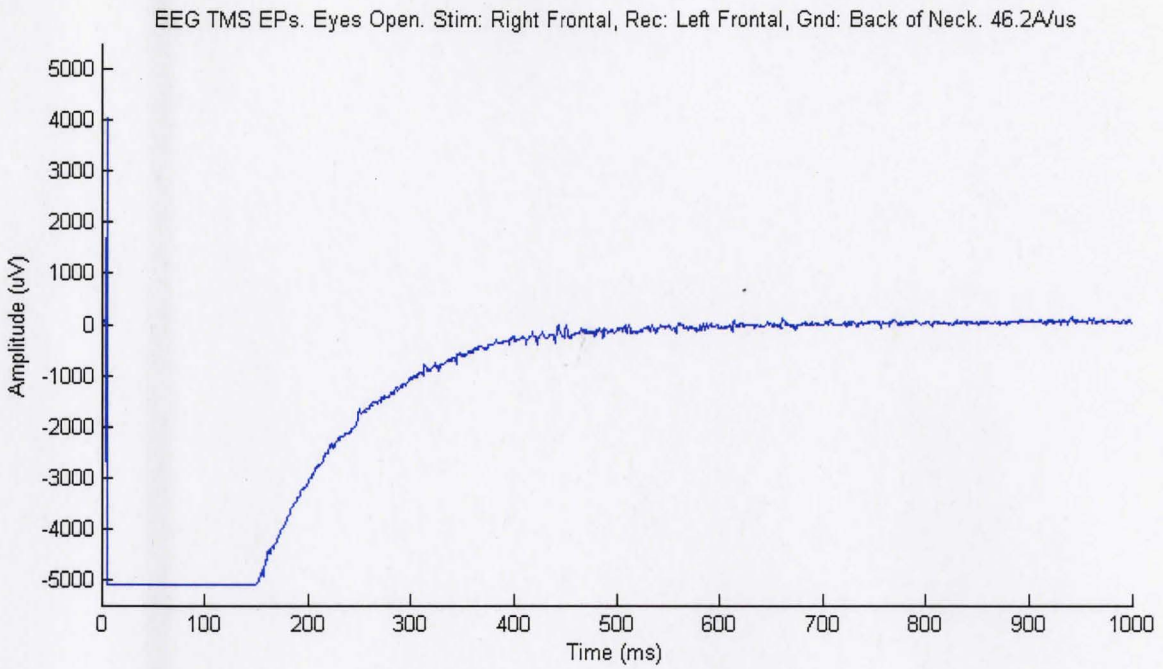

Figure 4.12: TMS pulse recorded with a 1000x gain high bandwidth amplifier, looking at the first 1000ms of recording to show how long the amplifier circuit saturates.

4.5.3 Discussion

The high bandwidth approach had the problem of easily being saturated by the TMS artifact due to its high gain, which is required for EEG acquisition. With the 1000 times gain high bandwidth amplifier, with a 46.2 A/μs pulse, the amplifier took 400 ms to recover after saturating, and no EP signal could be recovered for the first 150 ms regardless of the processing technique used. This is a problem since the short latency TMS EP's start appearing during the first 30ms post-TMS.

4.6 Approach Four

Approach four is a modification of approach three and involves pre-amplifying the signal, employing a sample-and-hold circuit, a buffer, a HPF, additional gain, a LPF, and an ADC board (A blocking approach).

4.6.1 Design parameters

This final design (one that does not require the use of a commercially available EEG machine) is given in figure 4.13. As for approach three, the artifact blocking circuit was designed without the constraints of including the use of a traditional EEG machine, thus eliminating the concern of attenuating the amplified EEG signal back to near noise levels. However, rather than a single gain stage, the collection circuit in approach four utilizes a 10x gain instrumentation amplifier (INA126), a sample-and-hold circuit (LF398), a 1.6Hz HPF (0.1μF, 1Meg), 100x gain stage differential amplifier (OPA277), and a 1600Hz LPF (1k, 0.1μF). This increases the total signal gain and removes larger DC offsets from mismatched half cell potentials or other sources, prior to the main amplifier stage. As before, analog filtering was limited to passive first order filters since the processing software used high order digital filters to more precisely limit the bandwidth.

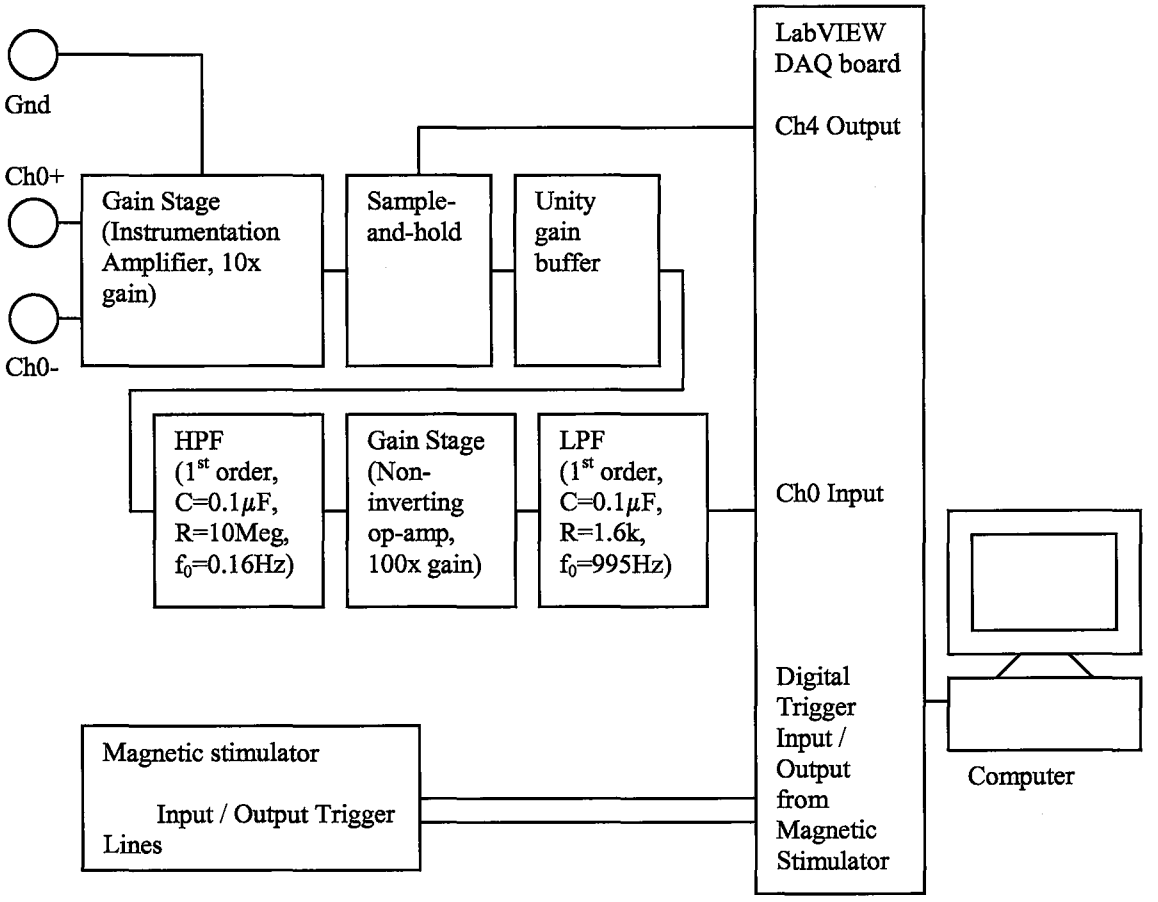

Figure 4.13: Artifact blocking EEG machine design using the sample-and-hold (blocking) approach.

For a component level schematic of this approach see figure 4.14, which was created using LTspice. The Instrumentation amplifier actually used was monolithic (INA126). The sample-and-hold circuit used was also monolithic (LF398).

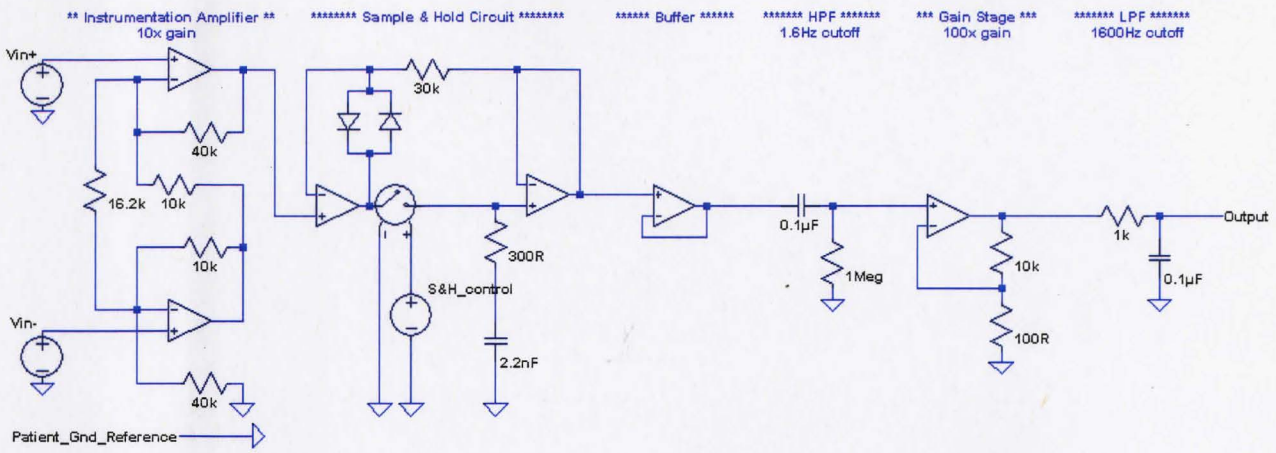

Figure 4.14: Approach four component level circuit in LTspice.

4.6.2 Circuit Tests

The LabVIEW design of the graphical user interface (GUI) is shown in figure 4.15. The LabVIEW program is in charge of controlling the sample-and-hold function, triggering the TMS machine, and collecting EEG data. The following parameters are user selectable within the control program created: sample-and-hold start and stop time, TMS triggering time, EEG sampling rate (up to 20kHz), EEG collection time), EEG channels to use (up to eight), filtering parameters (HPF,BRF,LPF), output generation rate for sample-and-hold function and TMS triggering (10kHz recommended, which yields 100μs accuracy). Digital filtering is fully implemented and allows the user to adjust three third order filters simultaneously, implementing a HPF, BRF, and LPF. To stimulate a patient the user executes the program, which then automates all activities, starting data collection on up to eight input channels, synchronized with two output channels, one controlling the "hold" function and one controlling the TMS machine using 0-5V logic.

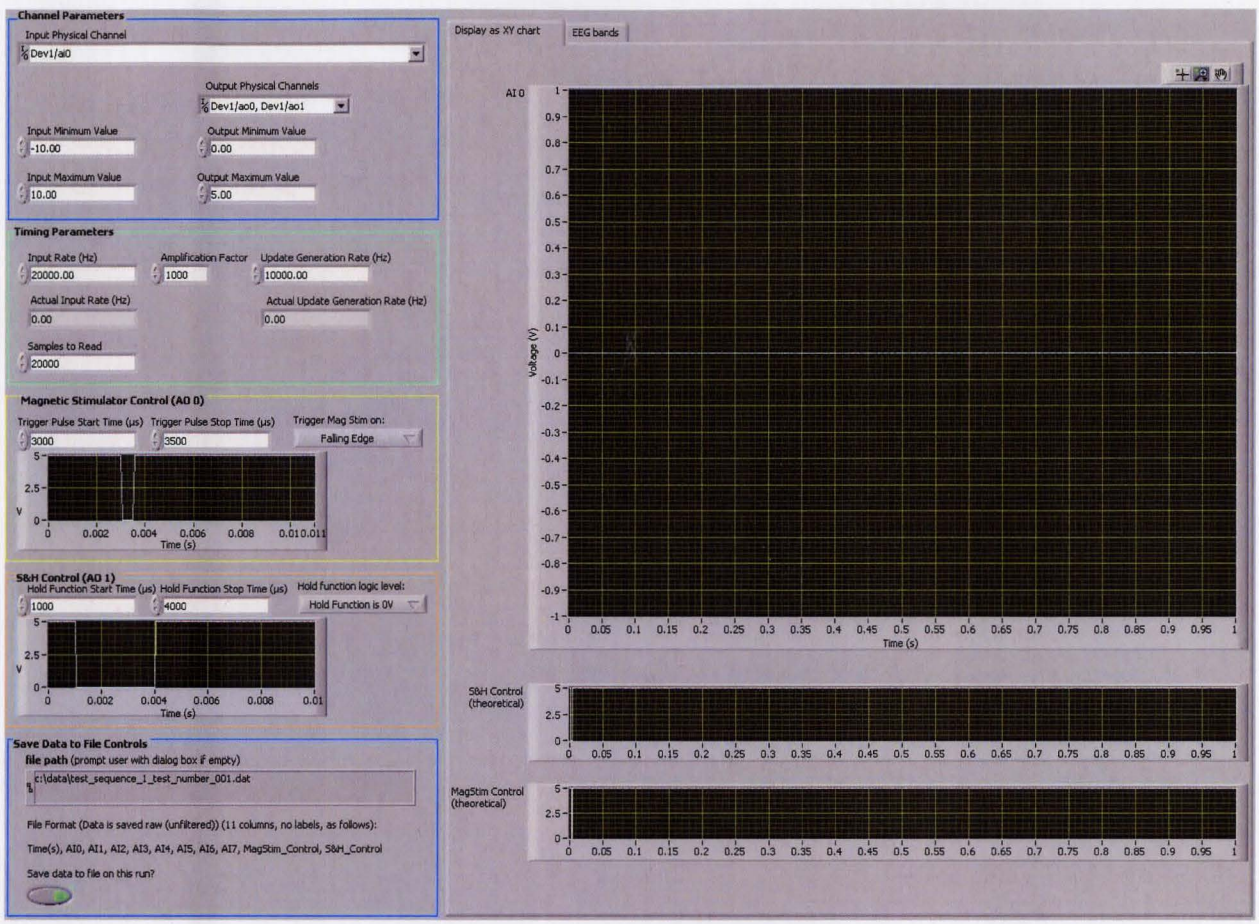

Figure 4.15: LabVIEW 8.0 front panel for approach four.

Once data collection is started, the "hold" function is activated, and then 1-2ms later the TMS machine is triggered. Soon after (0.5ms to 2ms) the TMS pulse finishes (400μs) the "sample" function is reactivated. As soon as the EEG data from one trial has been collected it is saved to a file in spreadsheet format to allow easy post-processing using Matlab or Excel. The wiring diagrams for the LabVIEW GUI shown in figure 4.15 are given in appendix 3.

Testing the sample-and-hold function, without the TMS pulse being administered, provided the results shown in figures 4.16 and 4.17, showing the first 50ms and first 1000ms post-TMS, respectively. These tests were performed by applying electrodes to a subject as indicated in the figures. These results show successful holding of the EEG signal level and also show that the sample-and-hold hold function does not result in large unwanted transients in the EEG signal that might invalidate collected data later on. The offset seen during the "hold" period is due to the finite hold-step of the LF398 sample-and-hold circuit used.

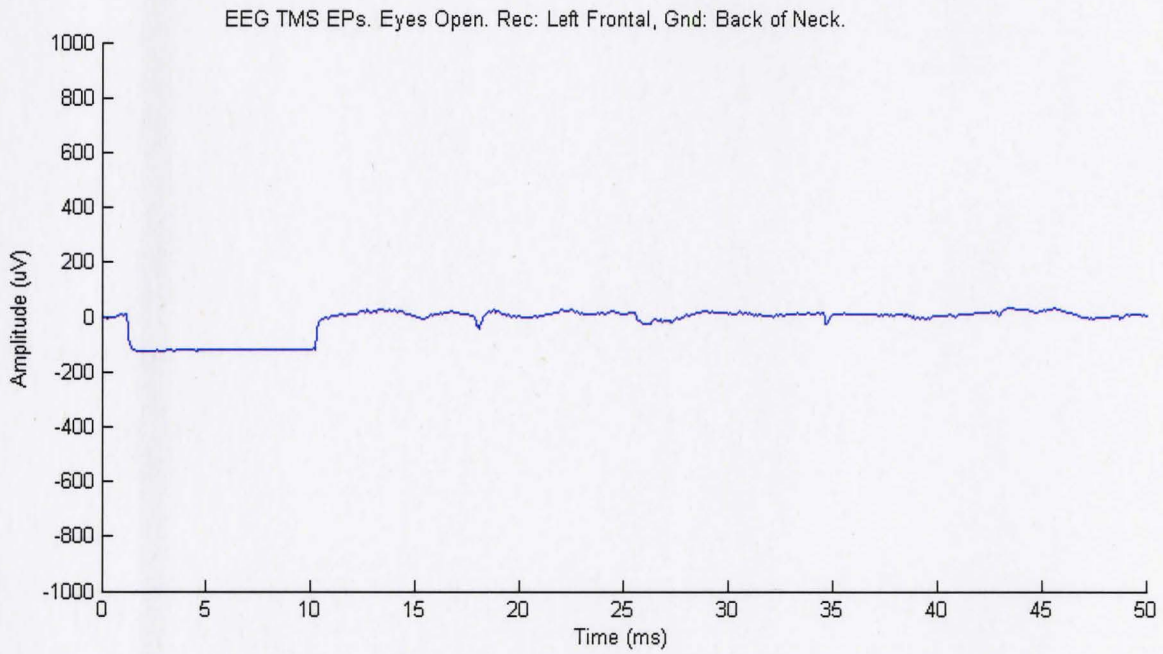

Figure 4.16: Sample-and-hold function activated without TMS pulse, with 50ms time axis. Reference electrode: Left Mastoid (A1). Recording electrode: left frontal (F3).

Figure 4.17, the 1000ms time axis, of the sample-and-hold function being activated without the TMS pulse, shows significant Electromyographic (EMG) activity from the occipital frontalis muscle since the recording is at F3.

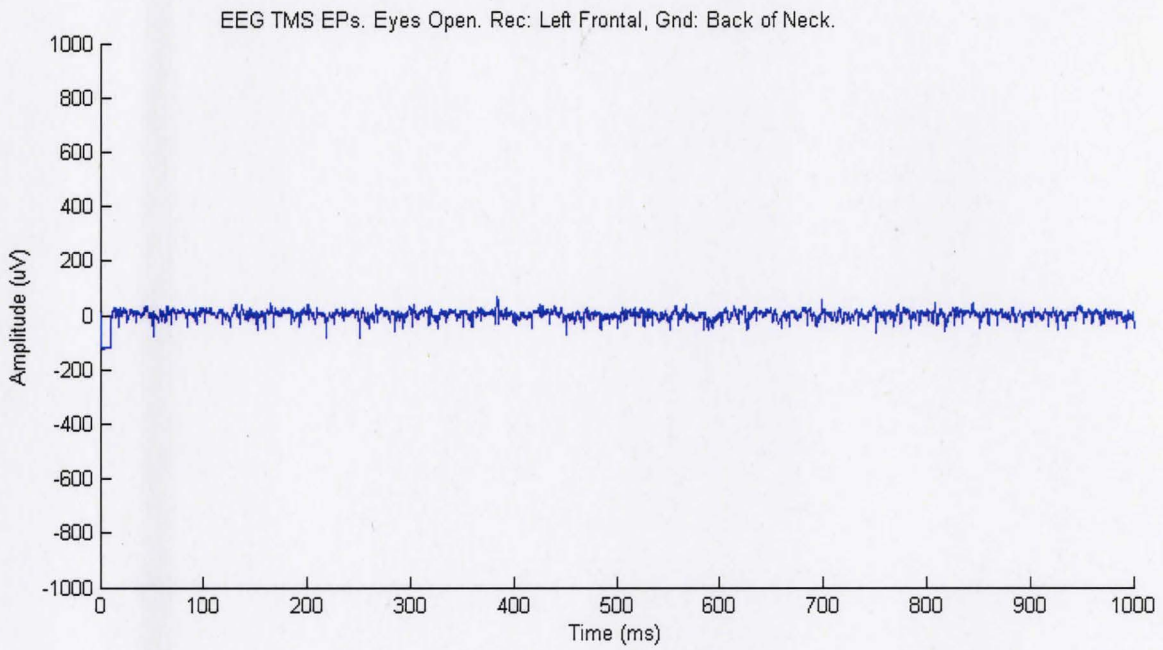

Figure 4.17: Sample-and-hold function activated without TMS pulse, with 1000ms time axis. Reference electrode: Left Mastoid (A1). Recording electrode: left frontal (F3).

Different hold function durations were tested to determine what hold time would provide the optimal signal collection. Based on these findings, the short hold time of only 1ms blocked the TMS artifact adequately. Hold time must be kept above 400μs to block the TMS pulse which affects the EEG for at least 400μs. In fact, the stimulus artifact will last longer than 400μs because it is being recorded by electrodes having a resistor-capacitor equivalent circuit (i.e. a filter). For large stimuli therefore, the hold

time may have to be increased because of the much longer duration of significant amplitude artifact.

4.6.3 Discussion

The fourth approach performed well during all functional and in vivo testing. The biggest difference between the fourth approach and the second approach is that the fourth approach does not require signal attenuation, which keeps the signal to noise ratio high. Additionally, the sample-and-hold circuit has been moved between the two gain stages instead of being placed after them. This prevents the second gain stage from being saturated by the TMS artifact while the hold function is activated. However, the broad band amplifier did record the magnetic stimulator charging pulses which seem to be coupled to the isolated recording system through the ground circuit. Low pass filtering the recorded signal to 70Hz, as is done in commercial EEG systems, would remove almost all of this artifact but then the anticipated short latency EP's could not be recorded. As well, neither the magnetic stimulator, nor the recording system can be allowed to float relative to ground because the chassis and the coil become antennas resulting in unacceptable 60Hz contamination of the recorded signals. A possible post-processing solution for this problem is suggested in chapter five, which gives more comprehensive test results.

4.7 Conclusion

After testing multiple circuit designs, the fourth approach was chosen, which utilized a multistage circuit with sample-and-hold function and a high bandwidth data acquisition system. This system provides the best trade off between blocking the artifact and seeing the EP very shortly after the TMS pulse finishes. The approach also maintains a high bandwidth, helping ensure EP data is not attenuated.

Chapter 5: Results

To treat depression using rTMS, the coil is usually placed near the F3 or F4 electrode position. It was decided that to test the new single channel EEG system the coil would be placed at either F3 or F4. However, if the coil is placed at F3 and the recording electrode is F3 as well, the stimulus artifact is very large and may still saturate the amplifier stage if a short blocking time is used. As well, short latency EP's will be masked by the very large M-wave elicited from the temporalis and/or occipital frontalis muscles underneath the coil. For that reason, stimulation and recording were conducted on opposite hemispheres.

The subject kept his eyes closed during all testing and relaxed the temporalis muscles as much as possible (by letting the mandible hang down) to eliminate as much EMG as possible from the recording.

For left frontal TMS the coil was positioned as shown in figure 5.1. For right frontal TMS the coil was positioned as shown in figure 5.2.

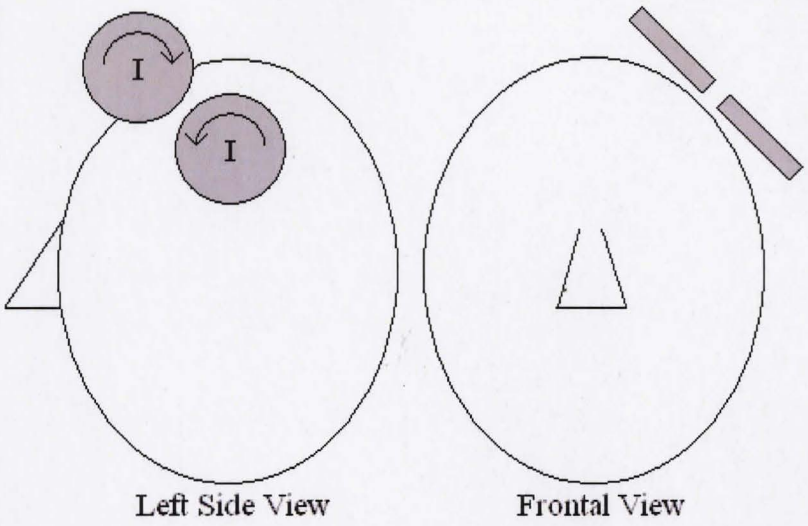

Figure 5.1: Left frontal TMS coil positioning diagram.

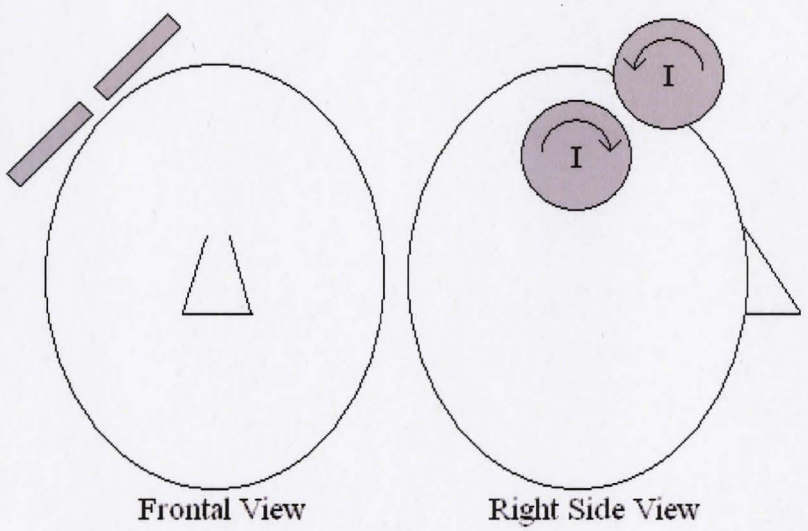

Figure 5.2: Right frontal TMS coil positioning diagram.

5.1 Commercial EEG machine Results

Preliminary testing involved determining how the TMS artifact presents during a single channel EEG recording without a blocking circuit on a commercially available 500Hz sampling rate EEG amplifier. This is similar to the limited slew-rate amplification employed by other researchers. Electrode placement was: right hemisphere frontal cortex (+ve electrode) F4, right ear (reference electrode) A2, back of neck (ground electrode). Peak stimulus amplitude (di/dt) through the coil was 80A/μs. EEG signals collected were band-pass filtered from 0.5Hz to 100Hz. Testing involved stimulation over the left hemisphere frontal cortex (F3). EEG signals were digitally notch filtered during post processing using a 58Hz to 62Hz third order digital Butterworth band-stop filter. Test data from six EPs were summed and averaged to create a synchronous average of the EP generated. The six EPs used to create the averaged EP are shown in figure 5.3. The averaged EP is shown in figure 5.4. The ringing seen following the stimulus artifact, an impulse input, is a result of the 60Hz notch filter used. As can be seen, the portion of the EP signal immediately following the stimulus artifact is masked. To be able to see more of the EP, artifact blocking is required. However, there seem to be long latency oscillations at approximately 4Hz frequency following the stimulus.

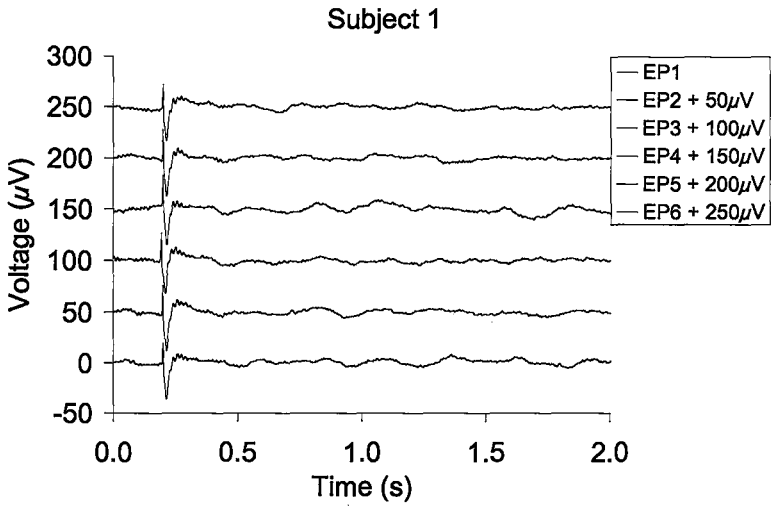

Figure 5.3: Six EPs recorded with XLTEK EEG machine. TMS over left hemisphere frontal cortex. EEG recorded from right hemisphere frontal cortex.

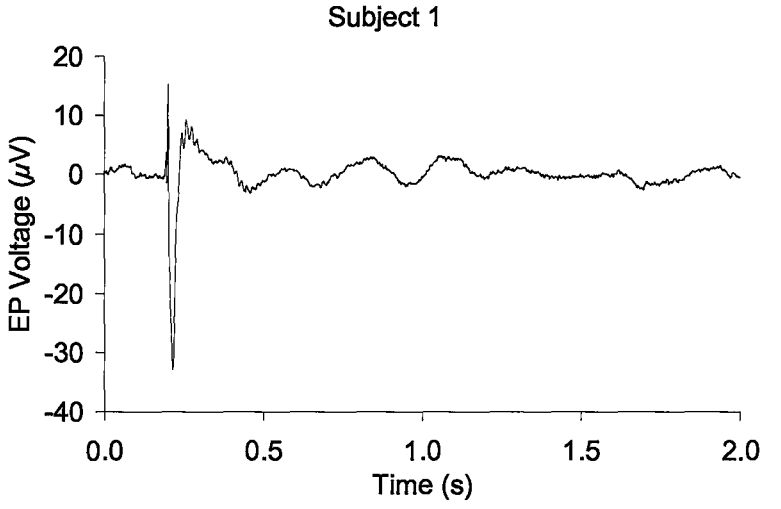

Figure 5.4: Averaged EP, created from six EPs recorded with XLTEK EEG machine. TMS over left hemisphere frontal cortex. EEG recorded from right hemisphere frontal cortex.

5.2 Approach 4 Results - Varied Amplitude

Once approach four was determined to provide the best short-latency results, preliminary testing was done at varying stimulus amplitudes. Stimulation for this testing was done over the left frontal area (F3), recording electrodes were placed at the right frontal area (F4) (+ve electrode), mastoid process behind the right ear (A2) (-ve electrode), and the base of the neck (GND electrode). The data were collected at a sampling rate of 20,000 samples per second. Hold function duration of 2ms was used after the TMS machine was triggered (total hold time was 7.5ms).

First, the TMS coil was placed on the floor four feet away from the subject to prevent stimulation or coupling from the TMS coil itself. These results, for a number of different amplitudes are shown in figures 5.5. There is a 100Hz waveform that presents in the first 45ms post TMS without the coil present. This signal is hypothesized to be from the TMS machine's switching power supply to the coil capacitor coupling through the grounding circuit. Obviously there is no stimulus artifact present since the coil was at least four feet away from the recording electrodes.

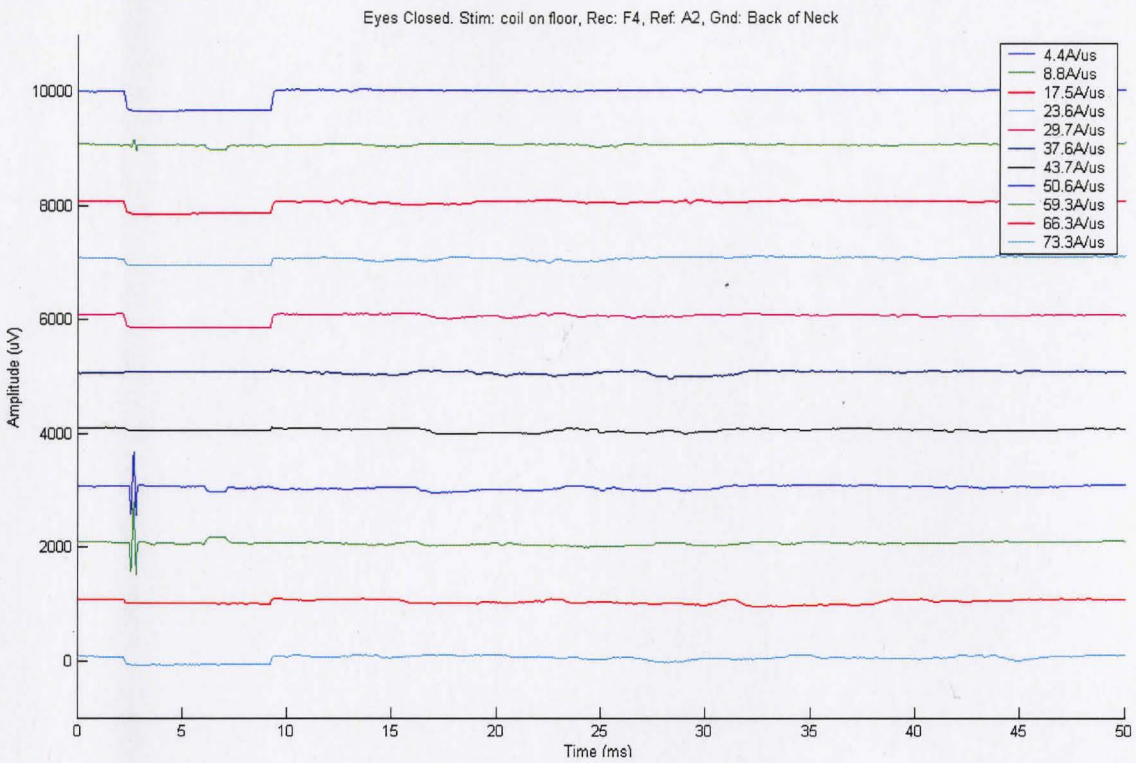

Figure 5.5: Control test with TMS coil on the floor, varied amplitudes. Channels have been offset from each other by 1mV for display purposes.

Figure 5.5 shows a total hold time of 7.5ms, with "hold" released at 9ms in the figure. For 50.6A/μs and 59.3A/μs the hold function did not activate properly, and thus the TMS pulse is recorded even though the coil is four feet away.

Next, the TMS coil was moved onto the head at F3. Results of F3 stimulation are shown in figure 5.6. At first, these 100Hz waveforms, also seen in the control case but at much lower amplitude, were hypothesized to be TMS EP's. However, upon further experimentation and upon closer inspection of the control case, it is now believed that they are mostly ground coupling and capacitive coupling through the TMS coil from the switching power supply of the TMS machine. This would make sense since the TMS

machine is capable of 20Hz stimulation, which means that it must fully recharge its capacitor bank before the next stimulus is due, 50ms later. At around 15ms the first peak of the charging waveform coupling through the grounding circuit is observed.

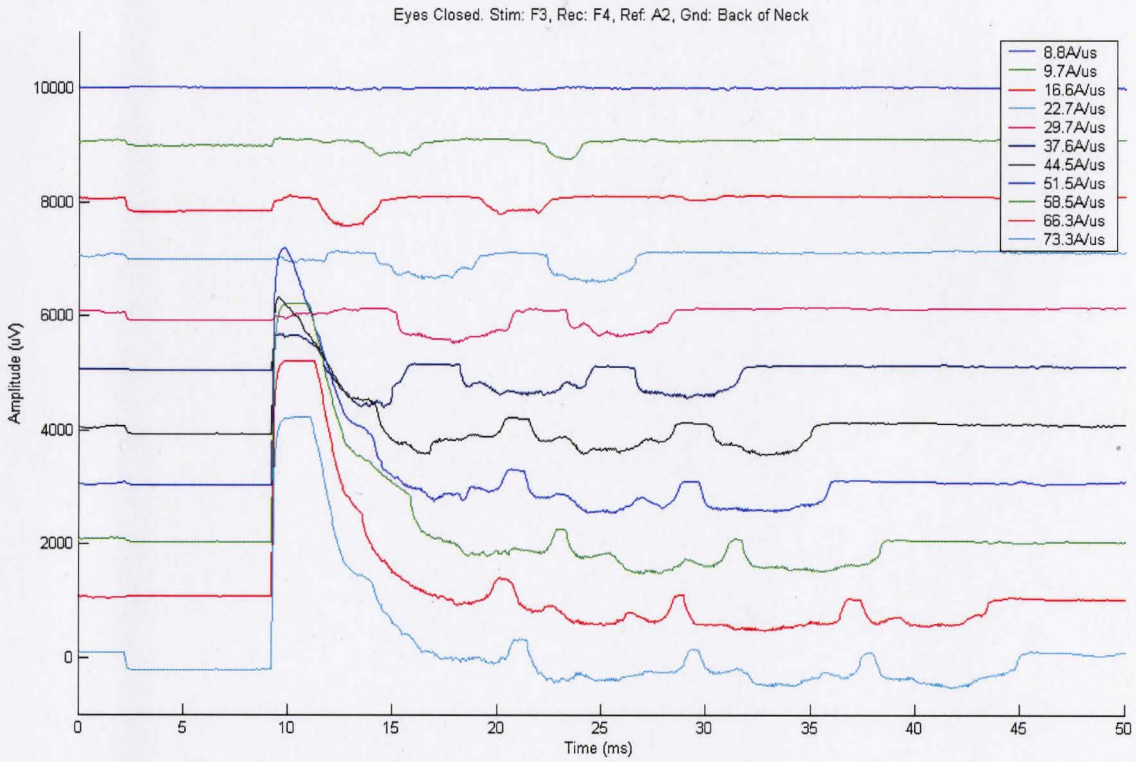

Figure 5.6: F3 stimulation, varied amplitudes.

The large spiking seen due to the TMS artifact can be reduced if a longer "blocking" time is selected. Some artifact will still be recorded due to the resistor-capacitor (RC) properties of the recording electrodes. When the sample-and-hold circuit is turned off, the signal remaining in the capacitive elements of the electrodes is presented directly to the amplifier inputs, which are very high impedance (10^9ohm). The

voltage created by the RC properties of the electrodes then takes about 10ms to settle back to baseline, thus creating a large input spike (mV range) that may exceed +/-5V post-amplification due to the 1000 times gain of the amplifier.

5.3 Approach 4 Results - 16 trials

Next, 16 trials of control (coil on floor) and 16 trials of F3 stimulation were repeated to get an average signal following TMS. The 16 control trials are shown in figure 5.7. As can be seen in the figure, significant coupling through the grounding circuit occurred as shown by the multiple negative peaks between 15ms and 38ms. This 100Hz waveform was also initially hypothesized to be an auditory EP, but upon inserting ear plugs, verifying that the subject could not hear the "click" of the coil, and seeing no difference in results between ear plugs in or out, that hypothesis was discounted.

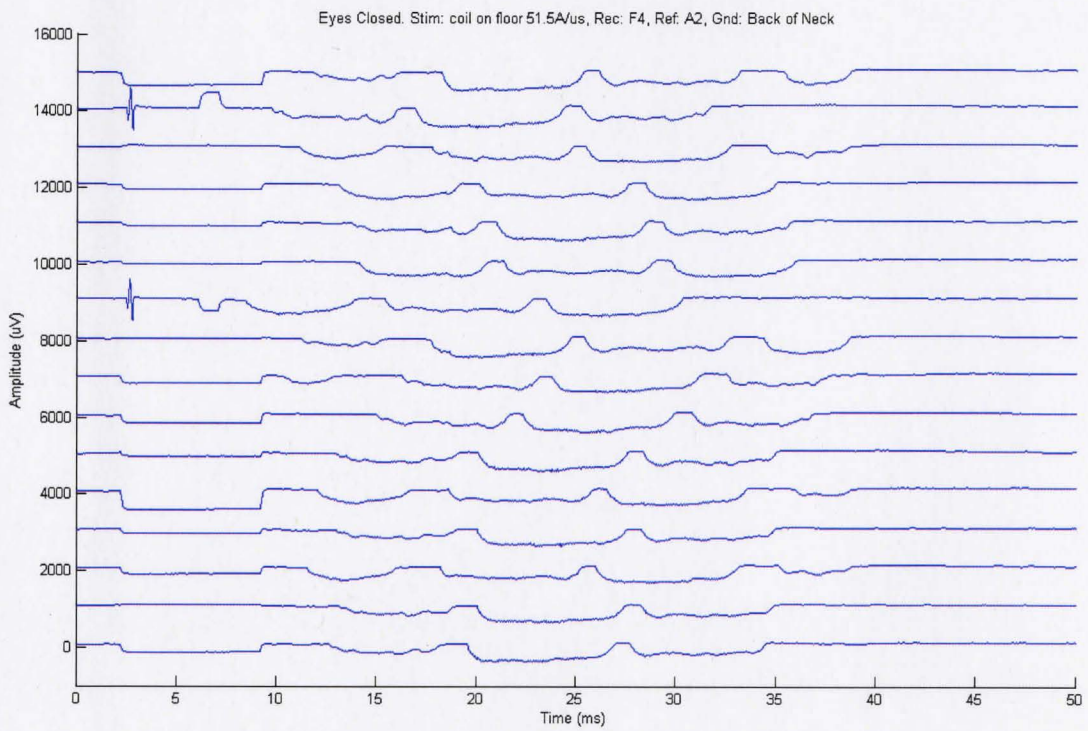

Figure 5.7: 16 control trials, 51.5A/μs.

From the figure of 16 control trials it is observed that the 100Hz coupled charging waveform has time jitter (varied timing of onset). With enough trials to create a synchronous average this should allow averaging out the details of the ground-coupled TMS charging artifact. However, since each pulse of the 100Hz signal is negative a large valley should be seen post-TMS in any synchronous average created. Figure 5.8 shows the synchronous average created from the 16 control trials.

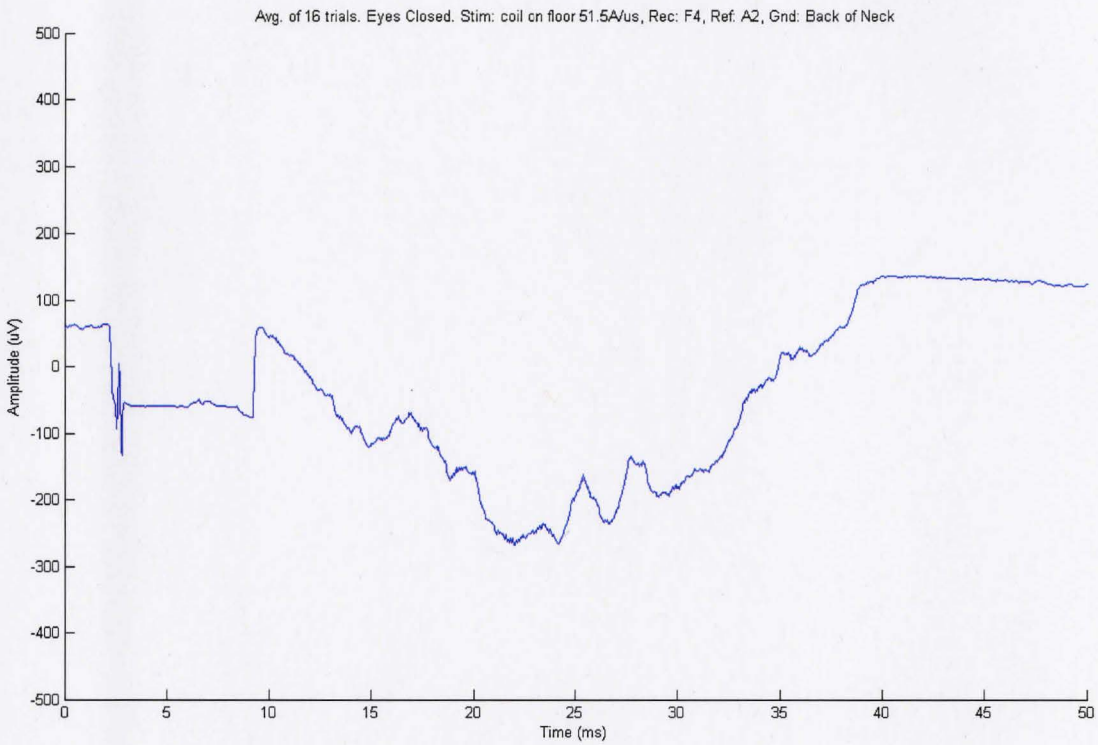

Figure 5.8: Synchronous average of 16 control trials, 51.5A/μs.

16 additional trials with the TMS coil moved to F3, at constant stimulus amplitude, were carried out. One trial was lost in data transfer. The 15 results are shown in figure 5.9.

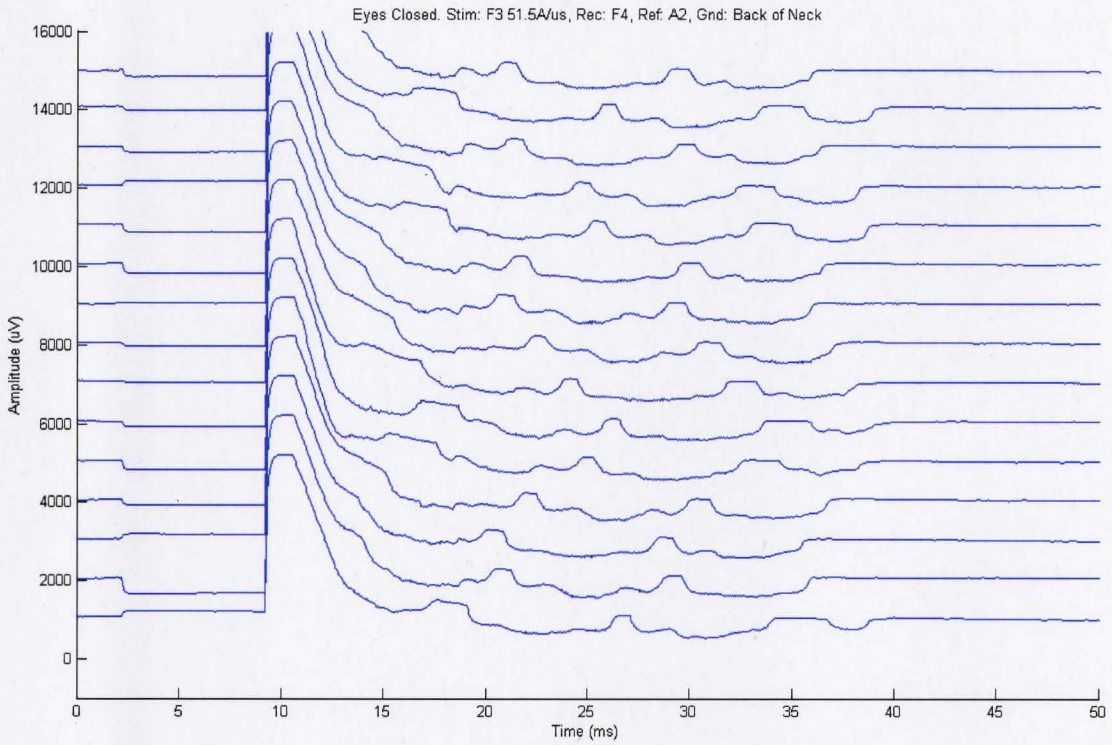

Figure 5.9: TMS at F3 results, 51.5A/μs.

From figure 5.9 of 15 F3 trials, similar to the control trials, the 100Hz ground-coupled charging waveform is seen. Again, using multiple trials to create a synchronous average, the 100Hz unwanted signal can be removed. However, since each pulse of the 100Hz signal is negative the large valley created post-TMS in the synchronous average is again seen. Figure 5.10 shows the synchronous average created from the 15 F3 trials.

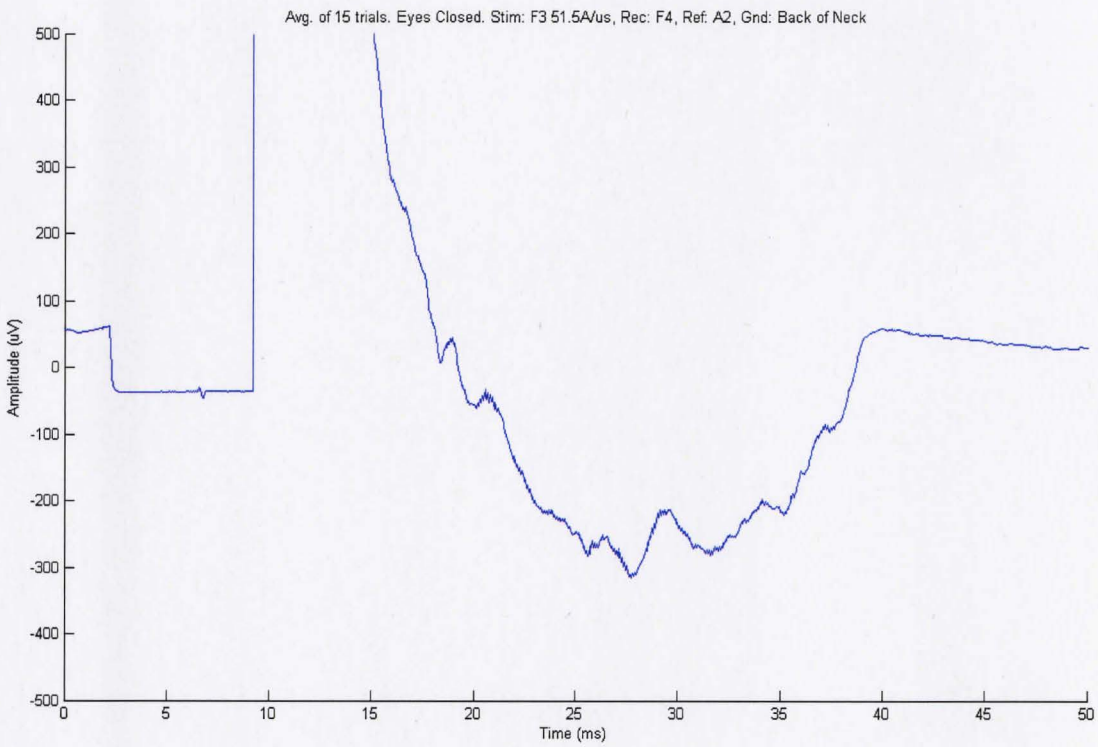

Figure 5.10: Synchronous average of 15 F3 trials, 51.5A/μs, 50ms time axis.

The many peaks throughout the valley may represent TMS EPs. The reasoning for more than one EP could be due to more than one path connecting the stimulation and recording area and different neuronal delays due to differences in path length.

The synchronous average is also plotted in figure 5.11 with a 1000ms time axis to see the longer-latency responses. This longer time axis was not plotted for the control case or the individual responses since the low frequency "alpha" waves seen following the TMS pulse were not observable.

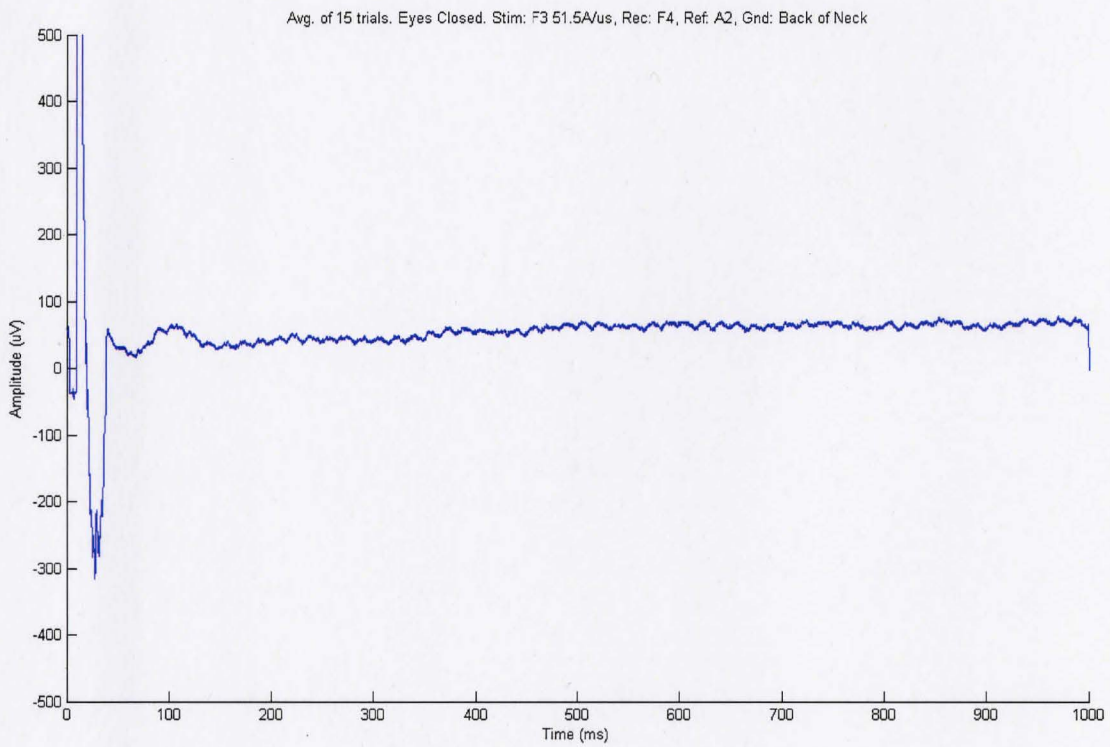

Figure 5.11: Synchronous average of 16 F3 trials, 51.5A/μs, 1000ms time axis.

As can be see in figure 5.11, between 50ms and 150ms post-TMS, a waveform with period of roughly 100ms is developed, which falls in the Alpha range. The synchronous average of the 16 control trials minus the synchronous average of the 15 F3 trials is plotted in figure 5.12. The valley created by the averaging of multiple coupled

negative charging waveforms has been largely eliminated by subtracting the synchronous average of the 16 control trials, essentially using it as an artifact template for the coupled switching noise. The stimulus artifact is constant for each stimulus and its exponential decay causes the changing baseline from 15ms to 40ms. The first peak seen at 19ms with an amplitude of 80μV is believed to be the first EP response, seen around 12ms post TMS, given the present coil positioning at F3. This agrees with Ilmoniemi (1997) and Krings (1997) who found that single pulse TMS elicited an immediate EP EEG response at the stimulated site which spreads within 5-10ms to adjacent areas and, within 20-22ms to homologous areas of the opposite hemisphere.

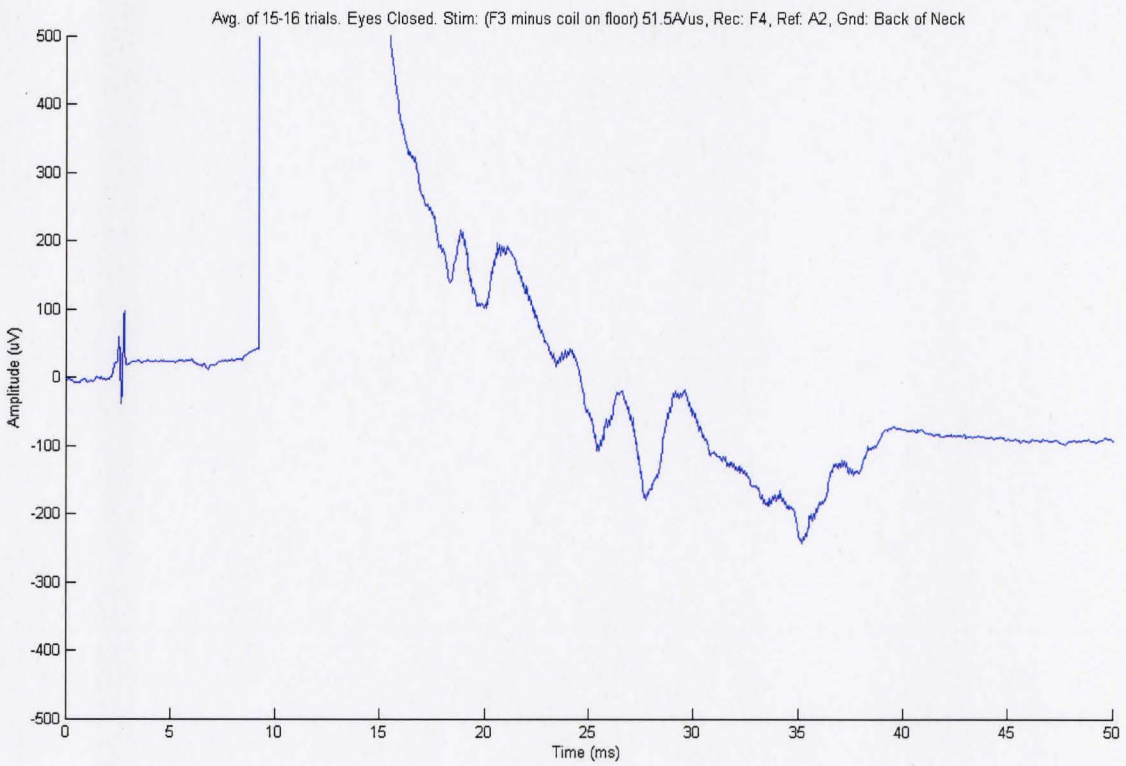

Figure 5.12: Synchronous average plot of TMS EP from 16 control trials and 15 F3 stimulation trials, using subtraction of control average from F3 average, 50ms time axis.

Next, let's look at the later observed peaks, some of which may still be coupled switching noise due to the low number of trials used in the synchronous average. Kahkonen et al (2005) observed EEG deflections at 27ms, 39ms, 52ms, 105ms and 193ms. Due to coil positioning and electrode positioning, there is expected to be significant differences between tests and between subjects. Possible EEG deflections are observed at 12ms, 15ms, 17ms, 20ms, 22ms, 27ms, and 30ms, during the first 50ms post-TMS. The reason Kahkonen et al (2005) observed longer latency responses may be due to the low-slew rate and low-bandwidth amplifier used in their experiments, as compared to the high-slew rate and high-bandwidth amplifier used to collect these results.

Figure 5.13 shows the same plot, but with a 1000ms time scale to show the longer latency responses. As can be seen in the figure, there appears to be an underlying alpha frequency waveform that is heavily masked by 60Hz noise.

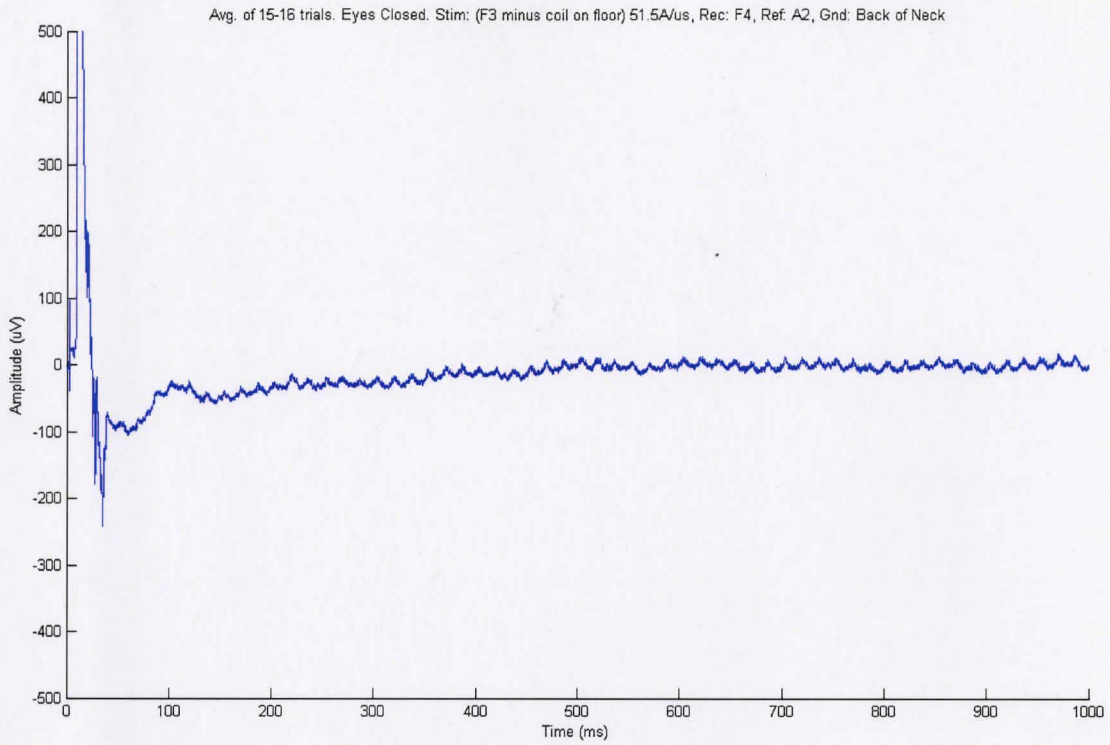

Figure 5.13: Synchronous average plot of TMS EP from 16 control trials and 15 F3 stimulation trials, using subtraction of control average from F3 average, 1000ms time axis.

Figure 5.14 shows the first 50ms of the subtraction of the control average from the F3 average to be used for artifact templating. Figures 5.15, 5.16, and 5.17 show the artifact broken into three regions (rise, plateau, decay, respectively) and curve fit separately.

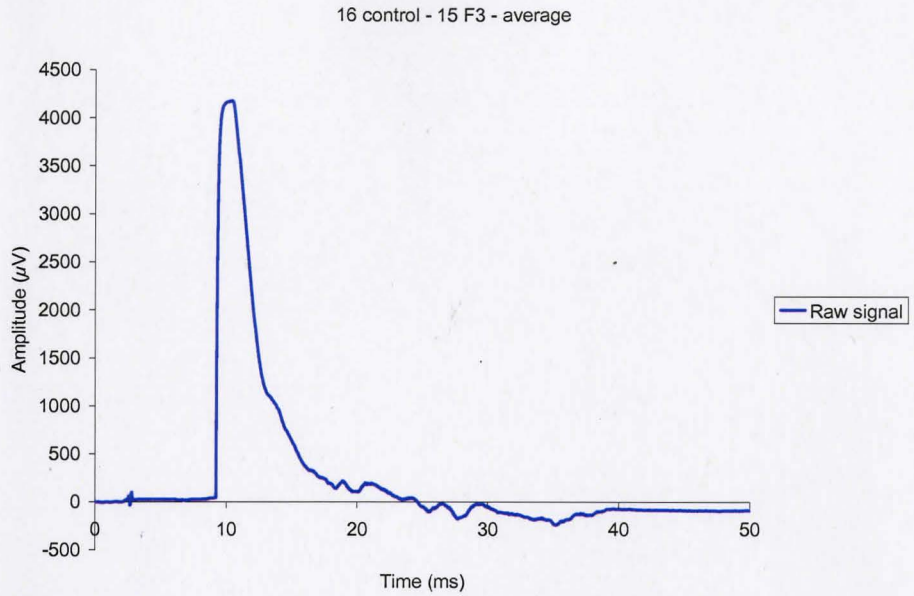

Figure 5.14: First 50ms of subtraction of control average from F3 average to be used for artifact templating.

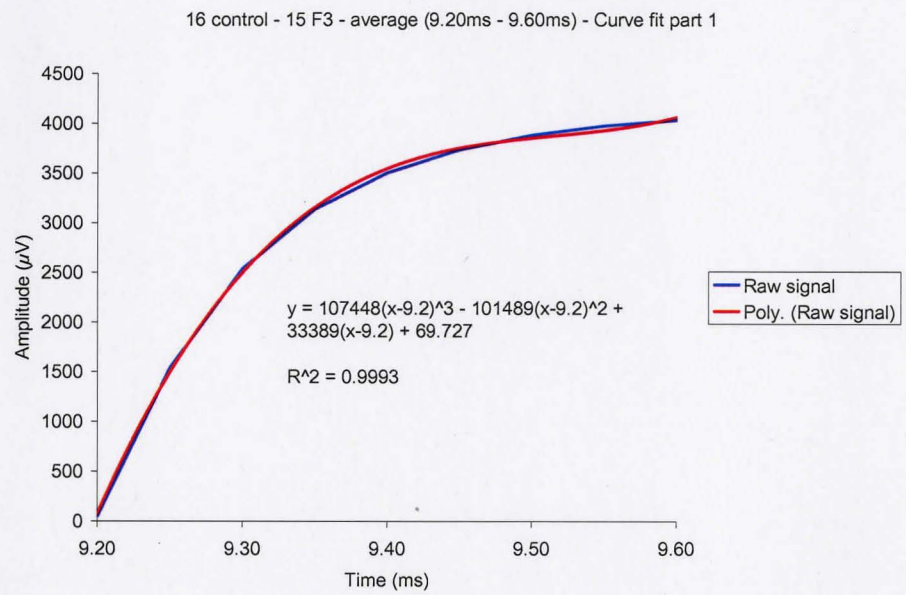

Figure 5.15: Rise portion of the artifact, fitted with a third order polynomial.

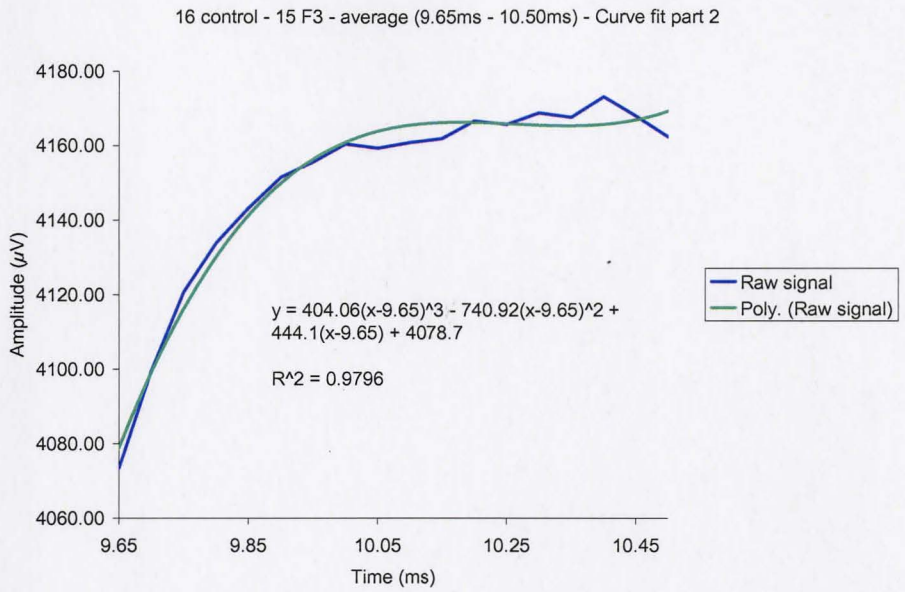

Figure 5.16: Plateau portion of the artifact, fitted with a third order polynomial.

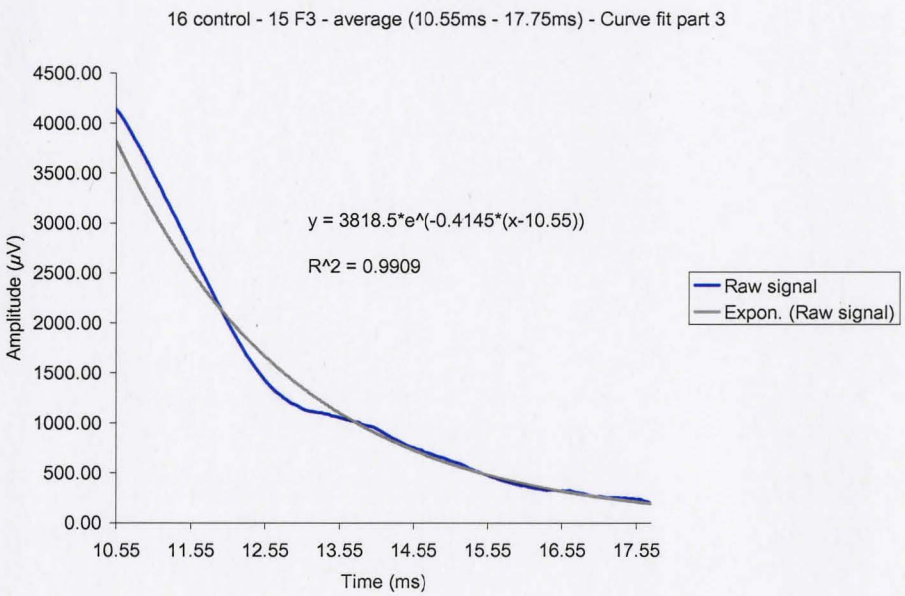

Figure 5.17: Decay portion of the artifact, fitted with an exponential.

Figure 5.18 shows the artifact template removed from the synchronous average of the 15 F3 stimulation trials minus the 16 control trials. The discontinuities created by the template subtraction have been left in.

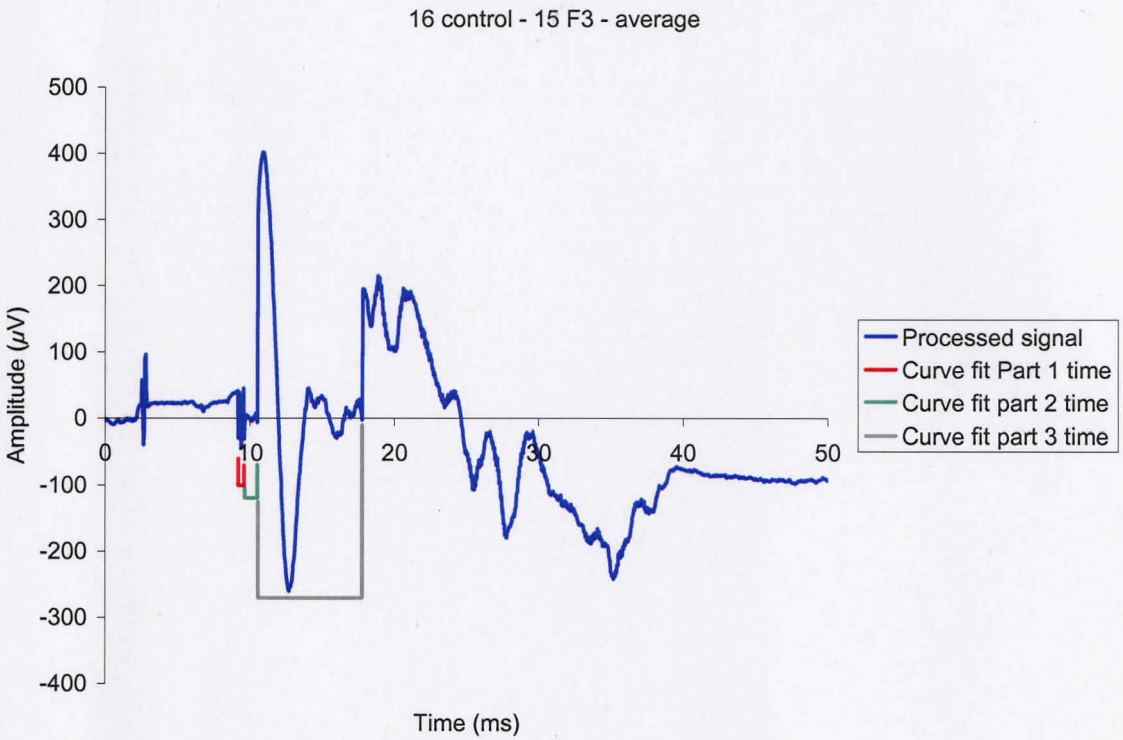

Fig 5.18: Result of subtracting the artifact template from the synchronous average of the F3 average minus the control average. Discontinuities between artifact subtraction functions left in.

Figure 5.19 shows the artifact template removed from the synchronous average of the 15 F3 stimulation trials minus the 16 control trials. The discontinuities created by the template subtraction have been removed.

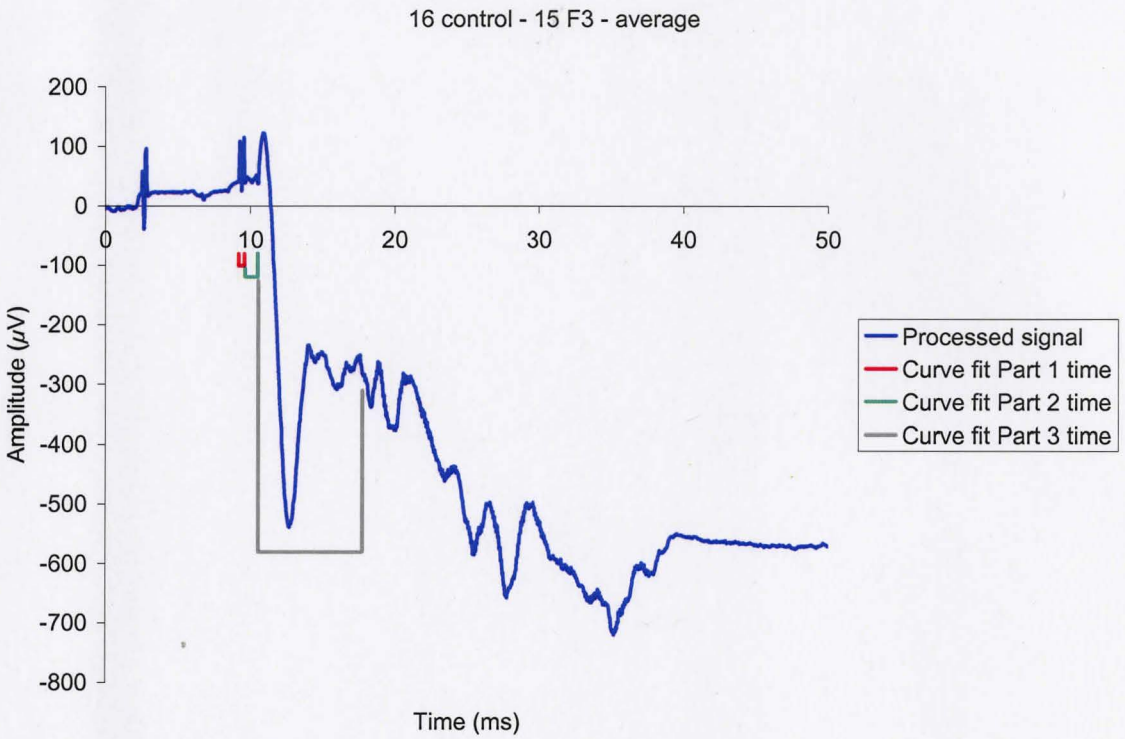

Fig 5.19: Result of subtracting the artifact template from the synchronous average of the F3 average minus the control average. Discontinuities between artifact subtraction functions removed.

5.4 Approach 4 Results - 64 trials

The same series of experiments conducted for 16 trials was redone for 64 trials to see the difference a larger synchronous average would make. The 64 control case trials are shown in figure 5.20.

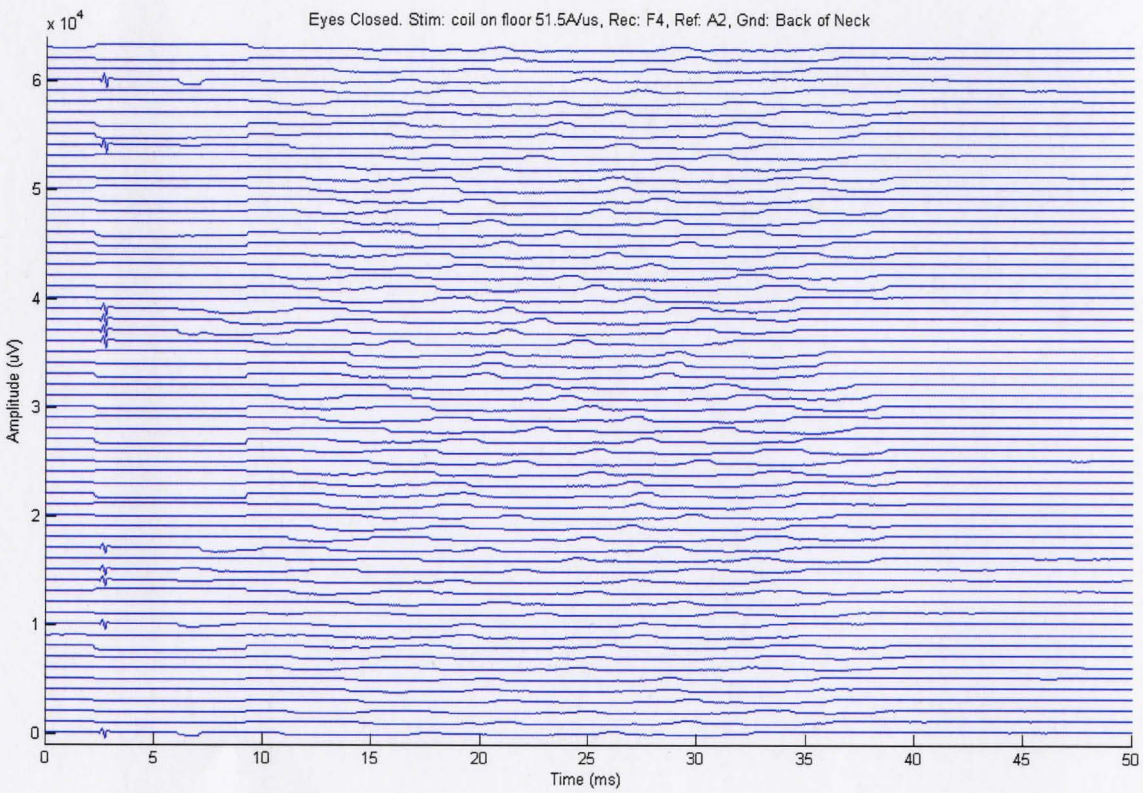

Figure 5.20: 64 control case trials, 51.5A/μs.

The average of the 64 control trials is shown in figure 5.21 and 5.22, with a 50ms and 1000ms time base respectively.

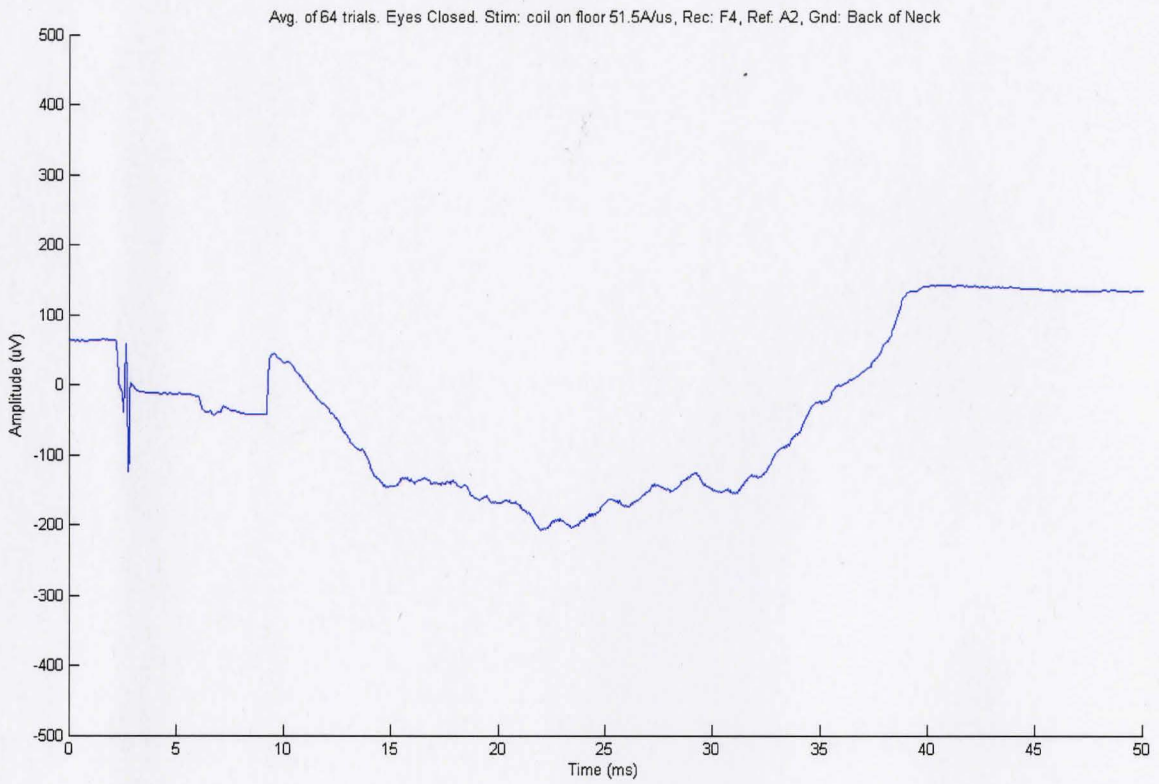

Figure 5.21: Average of 64 control trials, 51.5A/μs, 50ms time axis.

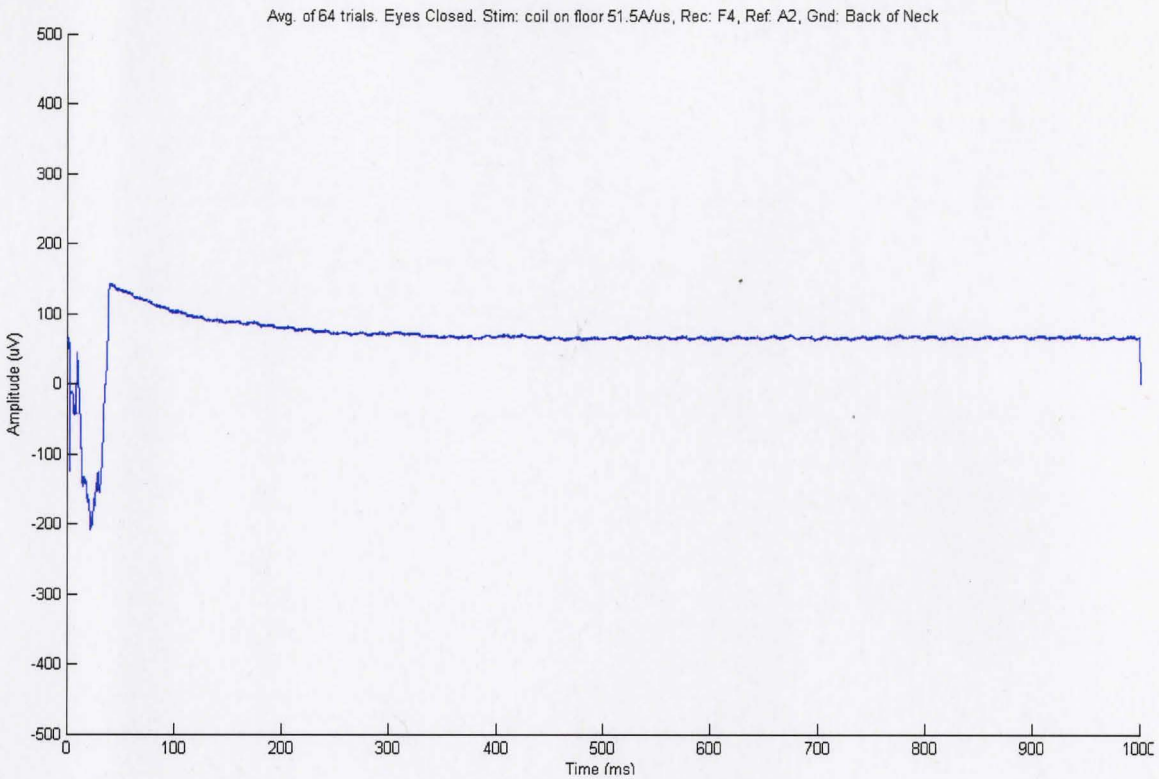

Figure 5.22: Average of 64 control trials, 51.5A/μs, 1000ms time axis.

Next, the coil was moved to F3 and 64 trials repeated. The 64 individual trials are shown in figure 5.23. Once again, a large amount of time jitter is seen in the coupled switching TMS power supply signal, which should allow averaging to remove this source of noise.

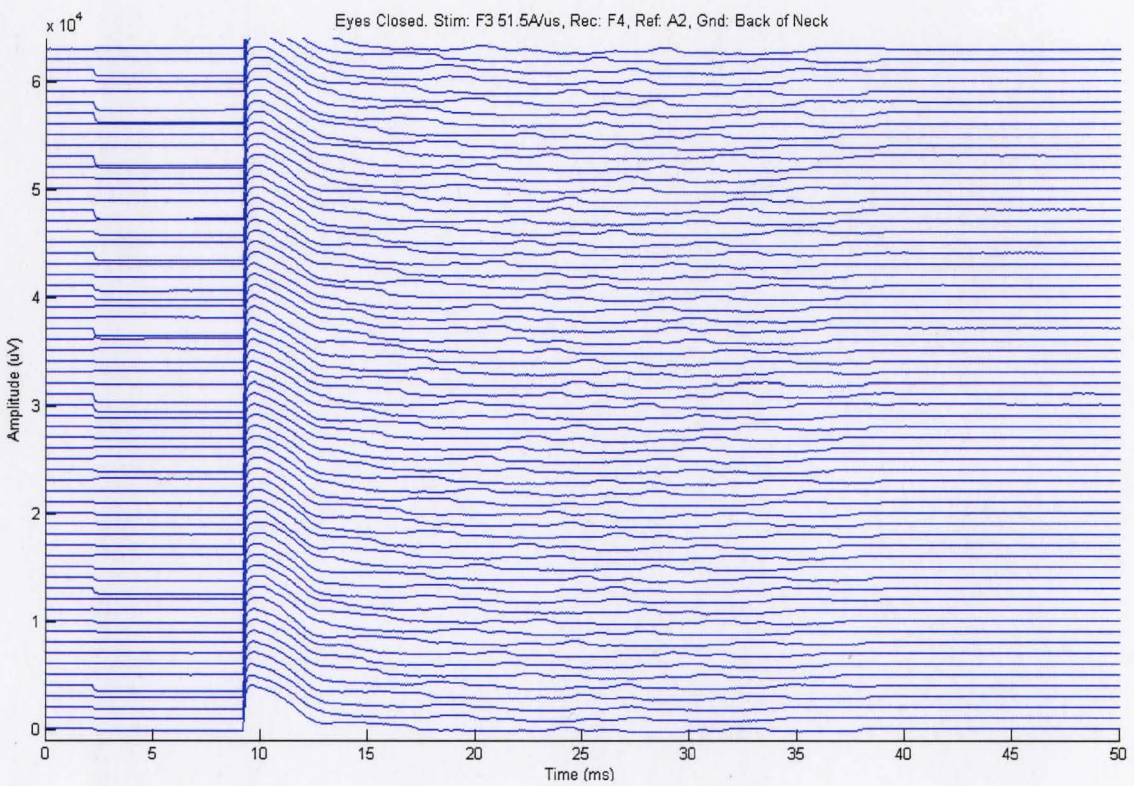

Figure 5.23: 64 trials of F3 stimulation, 51.5A/μs.

The synchronous average of the 64 trials of F3 stimulation was then computed and is shown in figures 5.24 and 5.25, for 50ms and 1000ms time axes, respectively.

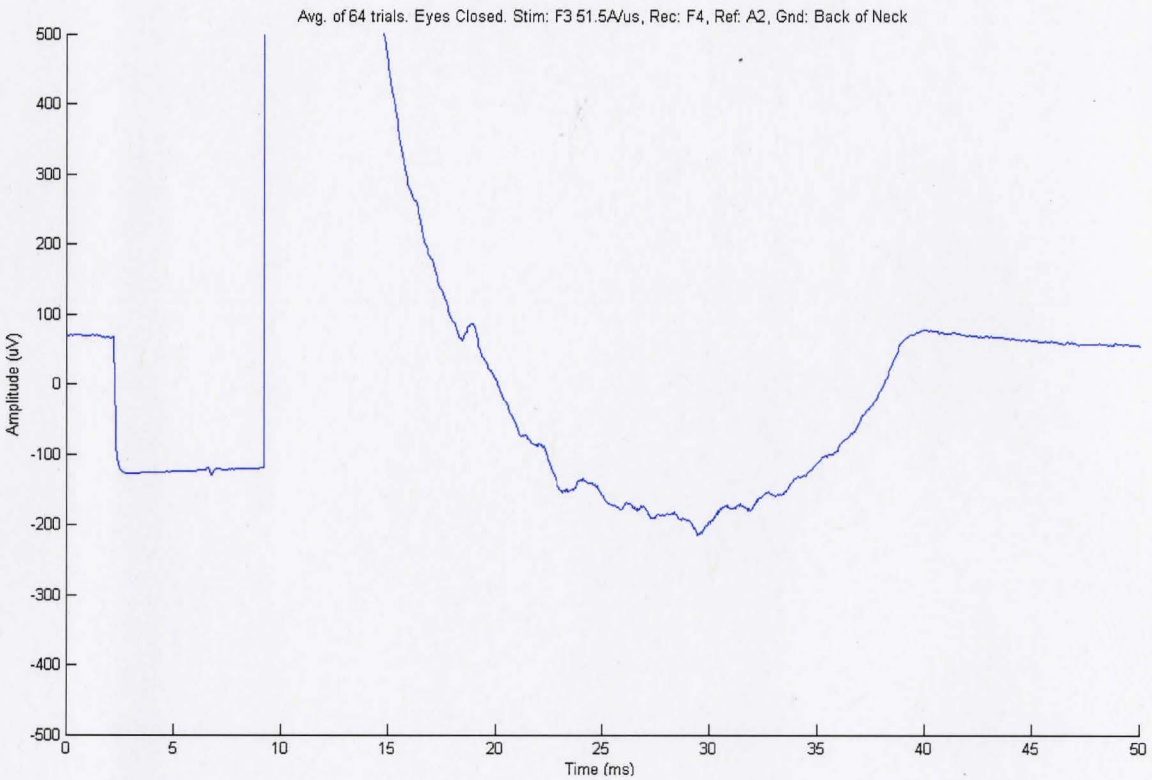

Figure 5.24: Averaged signal from 64 trials of F3 stimulation, 51.5A/μs, 50ms time axis.

The 1000 ms plot of the synchronous average from the 64 trials of F3 stimulation is shown in figure 5.25. As seen in the 1000ms plot from the 16 trials of F3 stimulation, the average created from the 64 trials also has a long latency alpha frequency response, observed between 50ms and 350ms post-TMS.

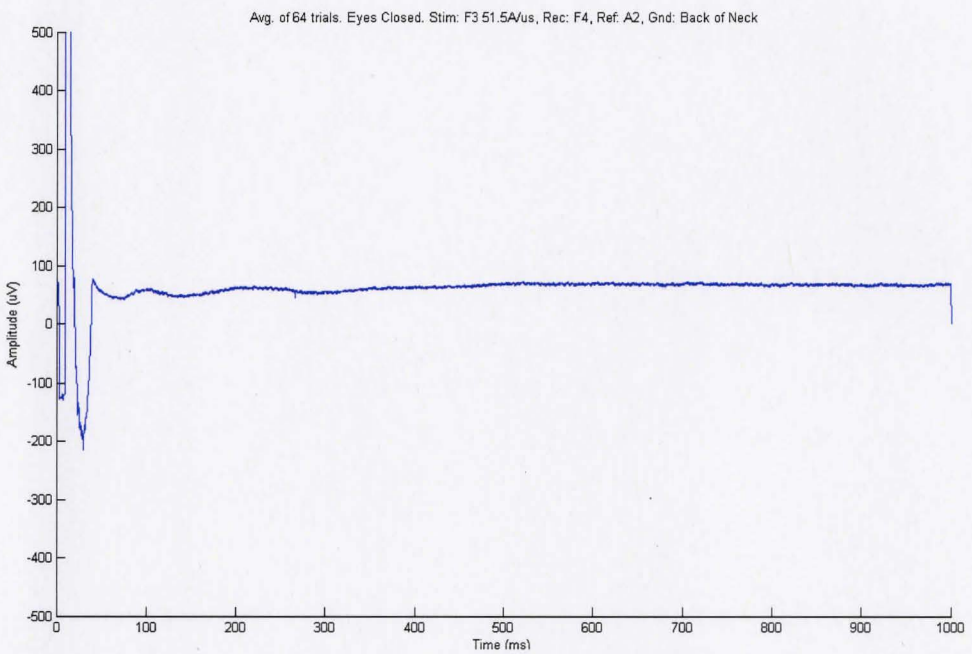

Figure 5.25: Averaged signal from 64 trials of F3 stimulation, 51.5A/μs, 1000ms time axis.

Next, the average of the 64 control trials was subtracted from the average of the 64 F3 trials. Once again, this allowed removal of the ground-coupled switching noise and the valley created by averaging it out, leaving the TMS artifact from the magnetic field (the large off-scale peak followed by exponential decay) and allowed observation of the TMS EP's underlying the noise. The plots of this average are shown in figures 5.26 and 5.27, for 50ms and 1000ms time axes, respectively.

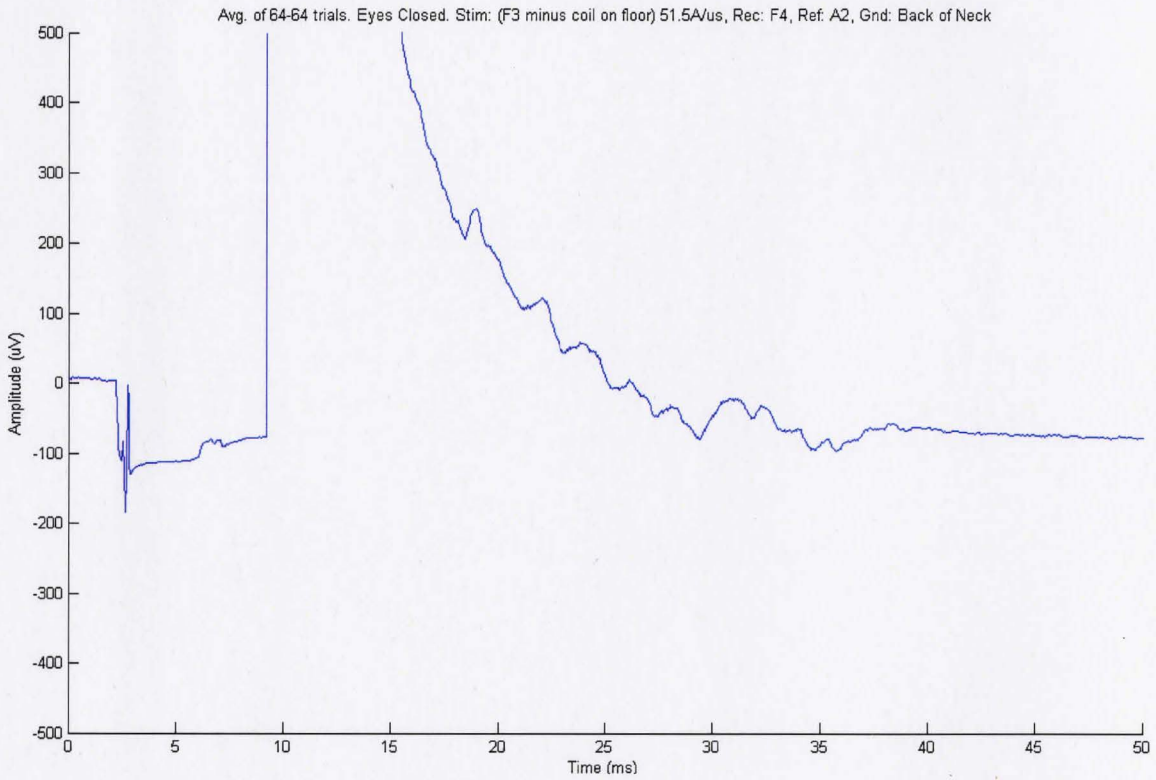

Figure 5.26: Synchronous average plot of TMS EP from 64 control trials and 64 F3 stimulation trials, using subtraction of control average from F3 average, 50ms time axis.

In these figure, peaks are observed at 12ms, 15ms, 17ms, 19ms, 21ms, 24ms, and 26ms, during the first 50ms post TMS. Some of these peaks may, however, be due to residual artifact. The alpha frequency is observed during the first 50ms to 350ms post TMS.

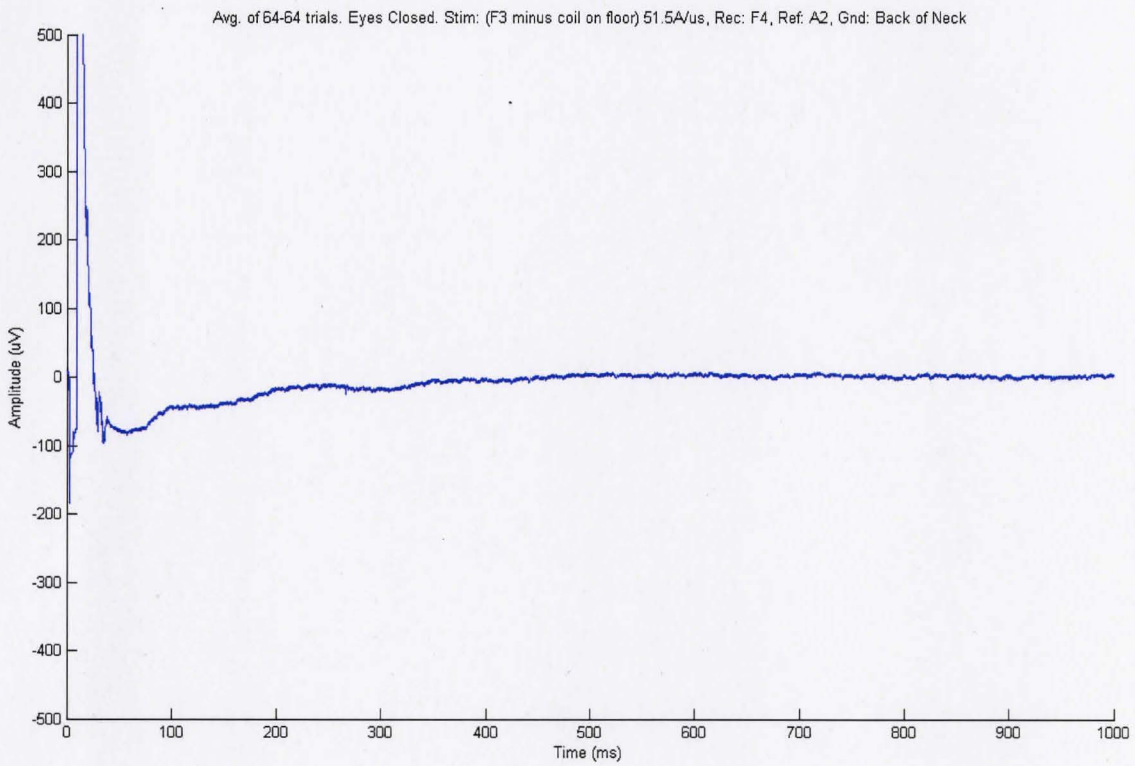

Figure 5.27: Synchronous average plot of TMS EP from 64 control trials and 64 F3 stimulation trials, using subtraction of control average from F3 average, 1000ms time axis.

Figure 5.28 shows the first 50ms of the subtraction of the control average from the F3 average to be used for artifact templating. Figures 5.29, 5.30, and 5.31 show the artifact broken into three regions (rise, plateau, decay, respectively) and curve fit separately.

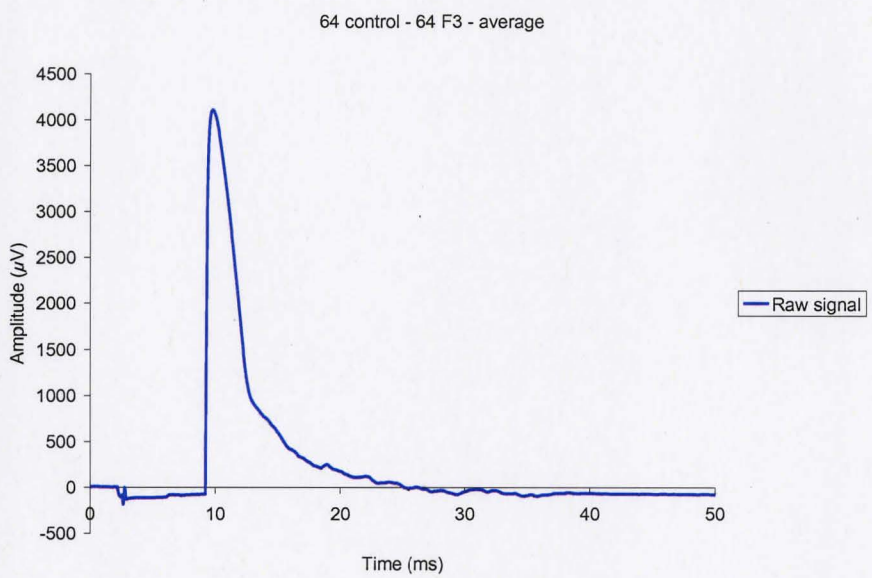

Figure 5.28: First 50ms of subtraction of control average from F3 average to be used for artifact templating.

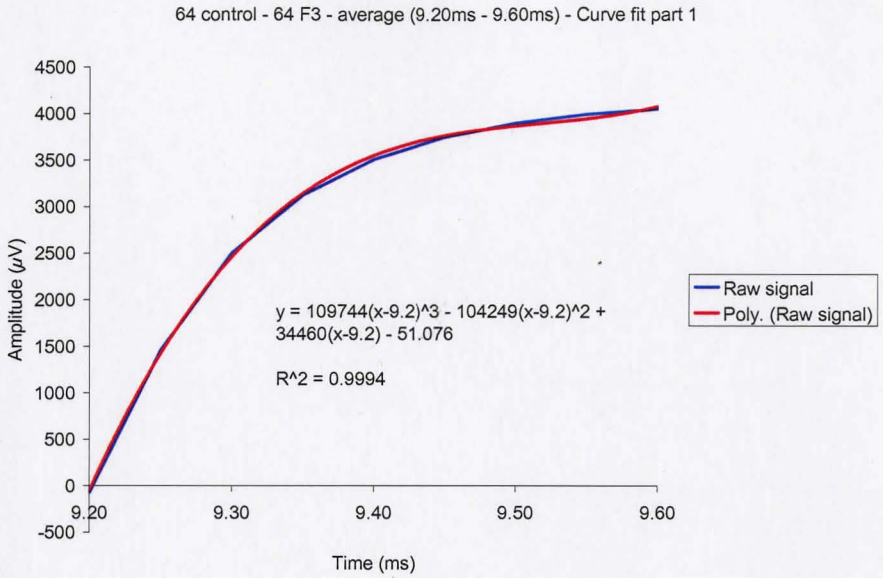

Figure 5.29: Rise portion of the artifact, fitted with a third order polynomial.

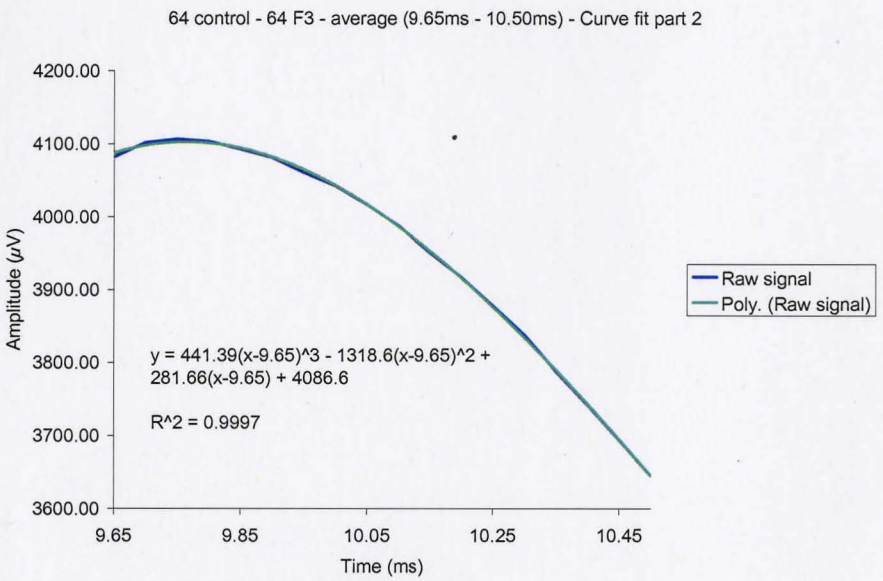

Figure 5.30: Plateau portion of the artifact, fitted with a third order polynomial.

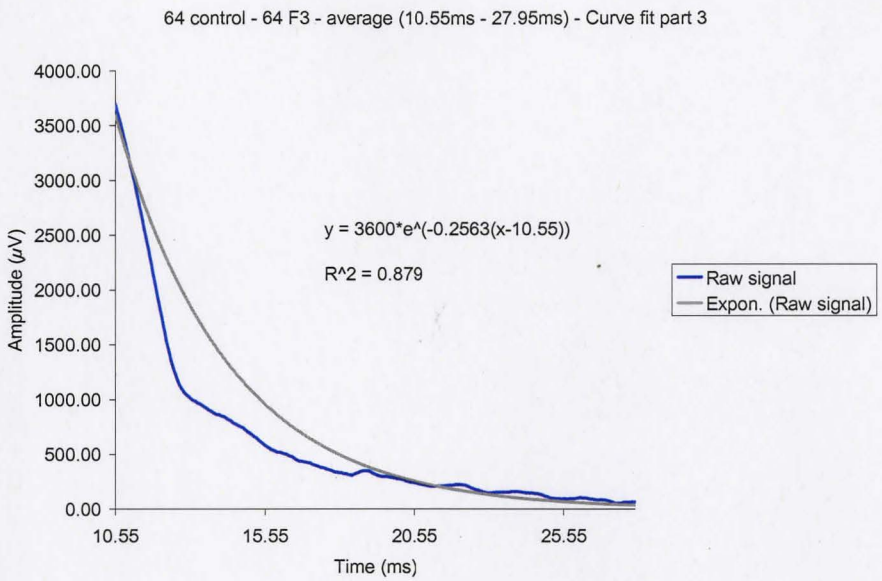

Figure 5.31: Decay portion of the artifact, fitted with an exponential.

Figure 5.32 shows the artifact template removed from the synchronous average of the 64 F3 stimulation trials minus the 64 control trials. The discontinuities created by the template subtraction have been left in.

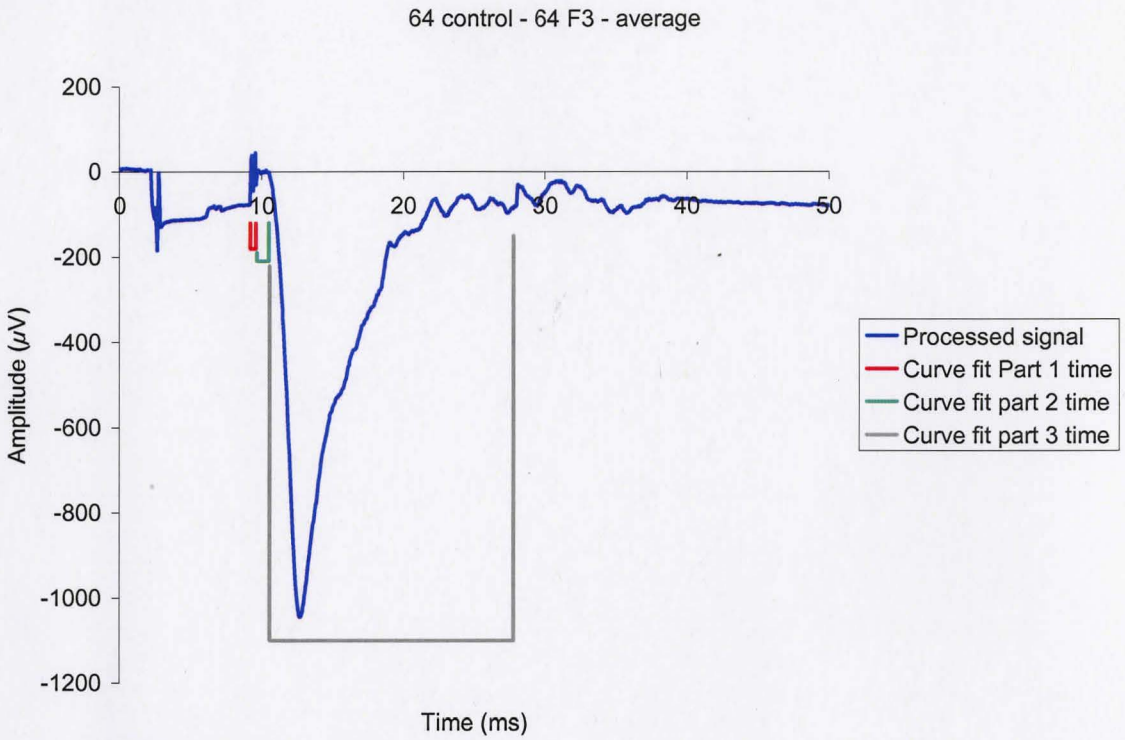

Fig 5.32: Result of subtracting the artifact template from the synchronous average of the F3 average minus the control average. Discontinuities between artifact subtraction functions left in.

As seen in the figure, without a tight fit on the exponential decay from the artifact, a large spike is introduced into the signal by the template.

Figure 5.33 shows the artifact template removed from the synchronous average of the 64 F3 stimulation trials minus the 64 control trials. The discontinuities created by the template subtraction have been removed.

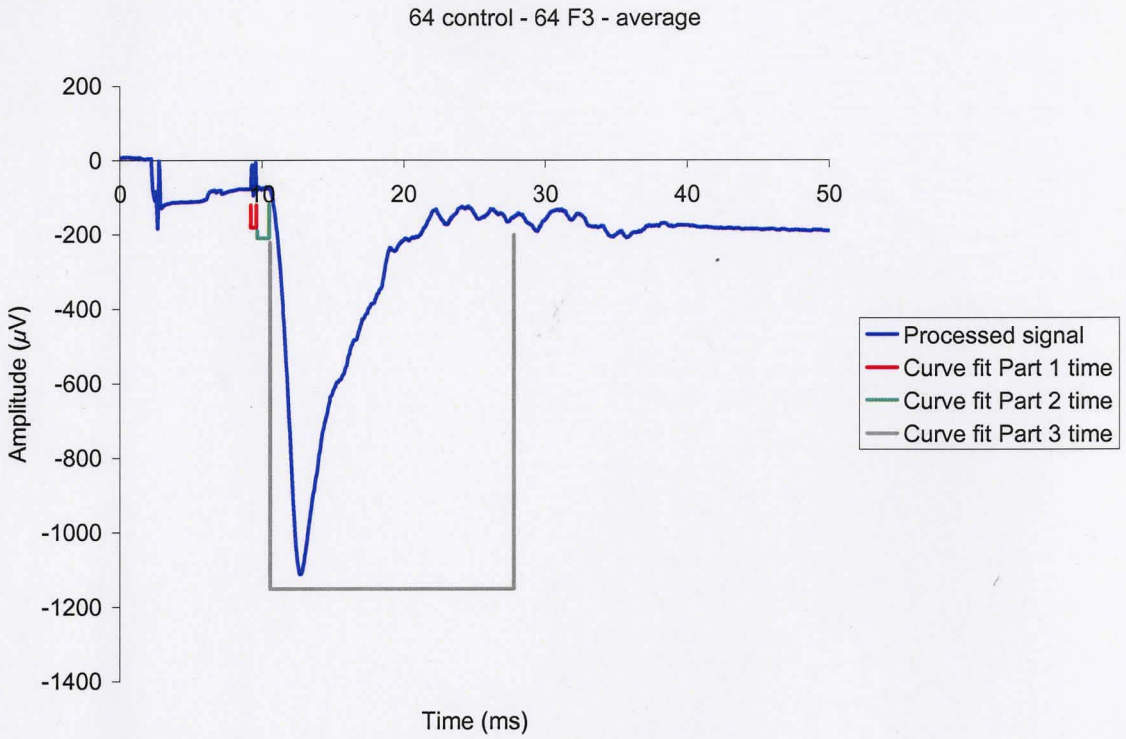

Fig 5.33: Result of subtracting the artifact template from the synchronous average of the F3 average minus the control average. Discontinuities between artifact subtraction functions removed.

Figure 5.34 shows the close up view of the artifact template removed from the synchronous average of the 64 F3 stimulation trials minus the 64 control trials. The discontinuities created by the template subtraction have been removed.

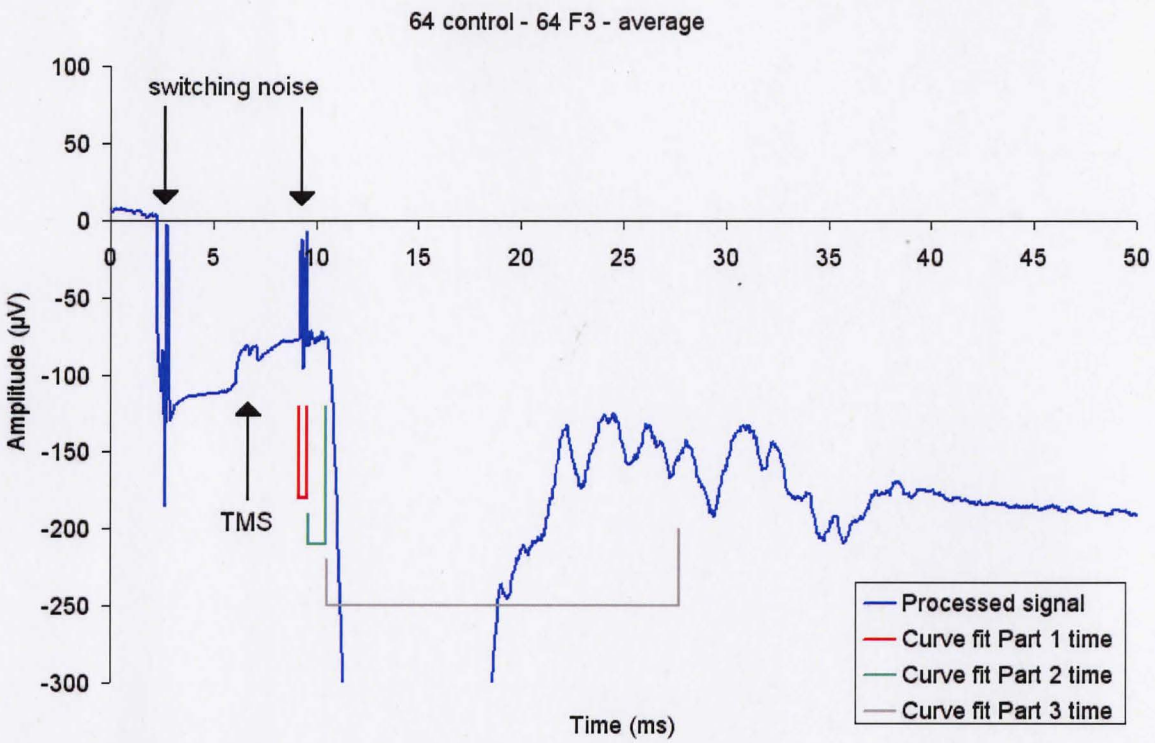

Fig 5.34: Result of subtracting the artifact template from the synchronous average of the F3 average minus the control average. Discontinuities between artifact subtraction functions removed. Close up view.

Some of the peaks seen in figure 5.34 are true EP's. Doubt about which peaks are real EP's and which are artifact could be removed by averaging more trials. The F3 averages certainly look different from the control averages. However, other stimulators may not have the same noise characteristics as the one used here.

Chapter 6: Conclusions

6.1 Conclusions

The results of the first portion of this research show that electrode heating is a concern when collecting EEG during rTMS. However, a number of standard electrodes or slightly modified standard electrodes are suitable for recording EEG during rTMS if certain stimulating parameters are adhered to. For example, for the silver electrodes used to collect preliminary results in chapter five, pulse trains should not exceed 30 pulses and electrodes should be allowed 290s to cool between trains.

The results of the second portion of this work show that approach four, utilizing a multistage front end with sample-and-hold circuitry and a wide bandwidth, is a very capable system for the collection of the TMS EP's seen in the first 30 ms post-TMS, that have until now been unpublished.

Data collected using the designed system showed short-latency significant peaks believed to occur as a result of neuron conduction of the evoked potential from 9ms to 30ms post TMS. During the 50ms to 300ms period post TMS, an alpha frequency waveform is seen to develop. As expected, synchronous averaging with artifact templating and subtraction is required to extract the underlying low amplitude EP signal from the raw EEG signal recorded.

6.2 Future Work

The next stage for this work is to build a multi-channel system using approach four to collect from all of the standard 10-20 EEG placement positions simultaneously. Experiments will need to be performed to determine the optimal hold time on each channel of a multi-channel system. 1-2ms was too short for these preliminary results when considering that the first response did not occur until after 10ms. However, responses from the brain under the coil will have shorter latencies so 1-2ms may be the longest allowable for some channels.

With the multi-channel system, the EP data collected in the first 30ms could then be used to determine neural connectivity differences between subjects; for instance depressed versus normal functioning subjects. The first 30ms of data could also be used to help position the TMS coil during TMS treatment for depression, by looking at the different time delays for the EP to reach different electrodes and using that to determine which brain structures were activated.

A modified magnetic stimulator is needed, which is capable of keeping its charging circuit off during the one second following stimulation. This is needed to prevent coupling of the charging waveform through the ground circuit or the TMS coil itself via capacitive coupling through to the recording equipment.

Future work will also be to evaluate the artifact characteristics of different electrodes (those discussed in chapter three) using the single channel, since the duration of the artifact is very dependent on their R-C characteristics.

References

Archambeault[a] M, de Bruin H, Hasey G, MacCrimmon D. Heating of EEG electrodes during rTMS. *30th Canadian Medical and Biological Engineering Conference Proceedings* (June 16-19, 2007) Toronto, ON, 4 pgs.

Archambeault[b] M, de Bruin H. "Development of an Electroencephalography Data Acquisition System for Clinical Research into Transcranial Magnetic Stimulation Evoked Potentials." *20th Canadian Conference on Electrical and Computer Engineering* (Apr. 22-26, 2007) Vancouver, BC, 4 pgs.

Bonato, C., Miniussi, C., Rossini, P.M. "Transcranial magnetic stimulation and cortical evoked potentials: a TMS/EEG co-registration study." *Clinical Neurophysiology* 117(8) (August 2006), 1699-1707.

"Data sheet for LF398 – Monolithic Sample and Hold Circuit." National Semiconductor. Accessed: April 21, 2007. http://www.national.com/pf/LF/LF398.html#Datasheet.

Esser, S.K., Huber, R., Massimini, M., Peterson, M.J., Ferrarelli, F., Tononi, G. "A direct demonstration of cortical LTP in humans: A combined TMS/EEG study." *Brain Research Bulletin* 69(1) (March 15 2006), 86-94.

Fitzgerald, P.B., Brown, T.L., Marston, N.A., Daskalakis, Z.J., De Castella, A., Kulkarni, J. "Transcranial magnetic stimulation in the treatment of depression: a double-blind, placebo-controlled trial." *Arch Gen Psychiatry* 60(10) (2003), 1002-1008.

Fuggetta, G., Fiaschi, A., Manganotti, P. "A direct demonstration of cortical oscillatory activities induced by varying single-pulse transcranial magnetic stimulation intensity over the left primary motor area: a combined EEG and TMS study." *Neuroimage* 27(4) (October 1 2005), 896-908.

Guyton, Arthur C., and Hall, John E. *Textbook of Medical Physiology*. Philadelphia, Pennsylvania: Saunders, 2000.

Herrmann, L.L., Ebmeier, K.P. "Factors Modifying the Efficacy of Transcranial Magnetic Stimulation in the Treatment of Depression: A Review." *Journal of Clinical Psychiatry* 67(12) (December 2006), 1870-1876.

Hoffman, R.E., Gueorguieva, R., Hawkins, K.A., Varanko, M., Boutros, N.N., Wu, Y.T., Carroll, K., Krystal, J.H. "Temporoparietal transcranial magnetic stimulation for auditory hallucinations: safety, efficacy and moderators in a fifty patient sample." *Biol Psychiatry* 58(2) (2005), 97-104.

Hovey, C., Houseman, P., Jalinous, R. "The New Guide to Magnetic Stimulation." The Magstim Company Ltd. 2003.

Ilmoniemi, R.J., Virtanen, J., Ruohonen, J., Karhu, J., Aronen, H.J., Näätänen, R., Katila, T. "Neuronal responses to magnetic stimulation reveal cortical reactivity and connectivity." *Neuroreport* 8 (1997), 3537-3540.

Ives, J.R., Keenan, J.P., Schomer, D.L., Pascual-Leone, A. "EEG recording during repetitive transcranial magnetic stimulation (rTMS)." *Neurology* 50(4) (1998), A167.

Ives, J.R., Rotenberg, A., Poma, R., Thut, G., Pascual-Leone, A. "Electroencephalographic recording during transcranial magnetic stimulation in humans and animals." *Clinical Neurophysiology* 117 (2006), 1870-1875.

Kahkonen, S. "MEG and TMS combined with EEG for mapping alcohol effects." *Alcohol* 37(3) (2005), 129-133.

Komssi, S., Kahkonen, S. "The novelty value of the combined use of electroencephalography and transcranial magnetic stimulation for neuroscience research." *Brain Research Reviews* 52(1) (August 30 2006), 183-192.

Krings, T., Buchbinder, B., Butler, W., Chiappa, K., Jiang, H., Rosen, B., Cosgrove, G. "Stereotactic transcranial magnetic stimulation: correlation with direct electrical cortical stimulation." *Neurosurgery* 41(6) (December 1997), 1319-1326.

Medtronic data sheets. "TMS2 and TMS3: Circular coils and Figure-8 coils statistics." 2004. Received: January 2, 2007.

Merriam-Webster, *The Merriam-Webster Concise School and Office Dictionary* : Springfield, Massachusetts: Merriam-Webster Inc., Publishers, 1991.

Moritz, A.R., Herriques, F.C. Jr. "Studies of thermal injuries: The relative importance of time and surface temperature in the causation of cutaneous burn." *American Journal of Pathology* 23 (1947), 695-720.

Neggers, S.F.W., Langerak, T.R., Schutter, D.J.L.G., Mandl, R.C., Ramsey, N.F., Lemmens, P.J., Postma, A. "A stereotactic method for image-guided transcranial magnetic stimulation validated with fMRI and motor-evoked potentials." *NeuroImage* 21 (2004), 1805-1817.

Nikulin, V.V., Kicic, D., Kahkonen, S., Ilmoniemi, R.J. "Modulation of electroencephalographic responses to transcranial magnetic stimulation: evidence

for changes in cortical excitability related to movement." *European Journal of Neuroscience* 18(5) (September 2003), 1206-1212.

Nunez, Paul L., and Ramesh Srinivasan. *Electric Fields of the Brain.* New York: Oxford University Press, 2006.

Pascual-Leone, A., Dhuna, A., Roth, B.J., Cohen, L., Hallett, M. "Risk of burns during rapid-rate magnetic stimulation in presence of electrodes." *Lancet* 336(8724) (November 10 1990), 1195-1196.

Roth, B.J., Pascual-Leone, A., Cohen, L.G., Hallett, M., "The heating of metal electrodes during rapid-rate magnetic stimulation: a possible safety hazard." *Electroencephalograph and Clinical Neurophysiology* 85 (1992), 116-123.

Ruohonen, J., Ravazzani, P., Grandori, F. "An analytical model to predict the electric field and excitation zones due to magnetic stimulation of peripheral nerves." *IEEE Transactions on Biomedical Engineering* 42(2) (1995), 158-161.

Serway, Raymond A., Beichner, Robert J. *Physics For Scientists and Engineers.* Orlando: Saunders College Publishing, 2000.

Shutter, D.J.L.G., and van Honk, J. "An electrophysiological link between the cerebellum, cognition and emotion: Frontal theta EEG activity to single-pulse cerebellar TMS." *NeuroImage* 33(4) (December 2006) : 1227-1231.

Tallgren, P., Vanhatalo, S., Kaila, K., Voipio, J. "Evaluation of commercially available electrodes and gels for recording of slow EEG potentials." *Clinical Neurophysiology* 116 (2005), 799-806.

Thut, G., Ives, J.R., Kampmann, F., Pastor, M.A., Pascual-Leone, A. "A new device and protocol for combining TMS and online recordings of EEG and evoked potentials." *Journal of Neuroscience Methods* 141(2) (February 15 2005) : 207-217.

Thut, G., Northoff, G., Ives, J.R., Kamitani, Y., Pfennig, A., Kampmann, F., Schomer, D.L., Pascual-Leone, A. "Effects of single-pulse transcranial magnetic stimulation (TMS) on functional brain activity: a combined event-related TMS and evoked potential study." *Clinical Neurophysiology* 114(11) (November 2003), 2071-2080.

Thut, G., Ives, J.R., Kampmann, F., Pastor, M.A., Pascual-Leone, A. "A new device and protocol for combining TMS and online recordings of EEG and evoked potentials." *Journal of Neuroscience Methods* 141 (2005), 207-217.

Virtanen, J., Ruohonen, J., Näätänen, R., Ilmoniemi, R.J. "Instrumentation for the measurement of electric brain responses to transcranial magnetic stimulation." *Med Biol Eng Comput* 37 (1999), 322-326.

Wassermann, EM. Risk and safety of repetitive transcranial magnetic stimulation: report and suggested guidelines from the international Workshop on the Safety of Repetitive Transcranial Magnetic Stimulation, June 5-7, 1996. Electroencephalography and clinical Neurophysiology 108 (1998) 1-16.

Webster, John. *Medical Instrumentation, Application and Design*. New York: John Wiley and Sons, 1998.

Appendix 1 – S&H circuit schematics

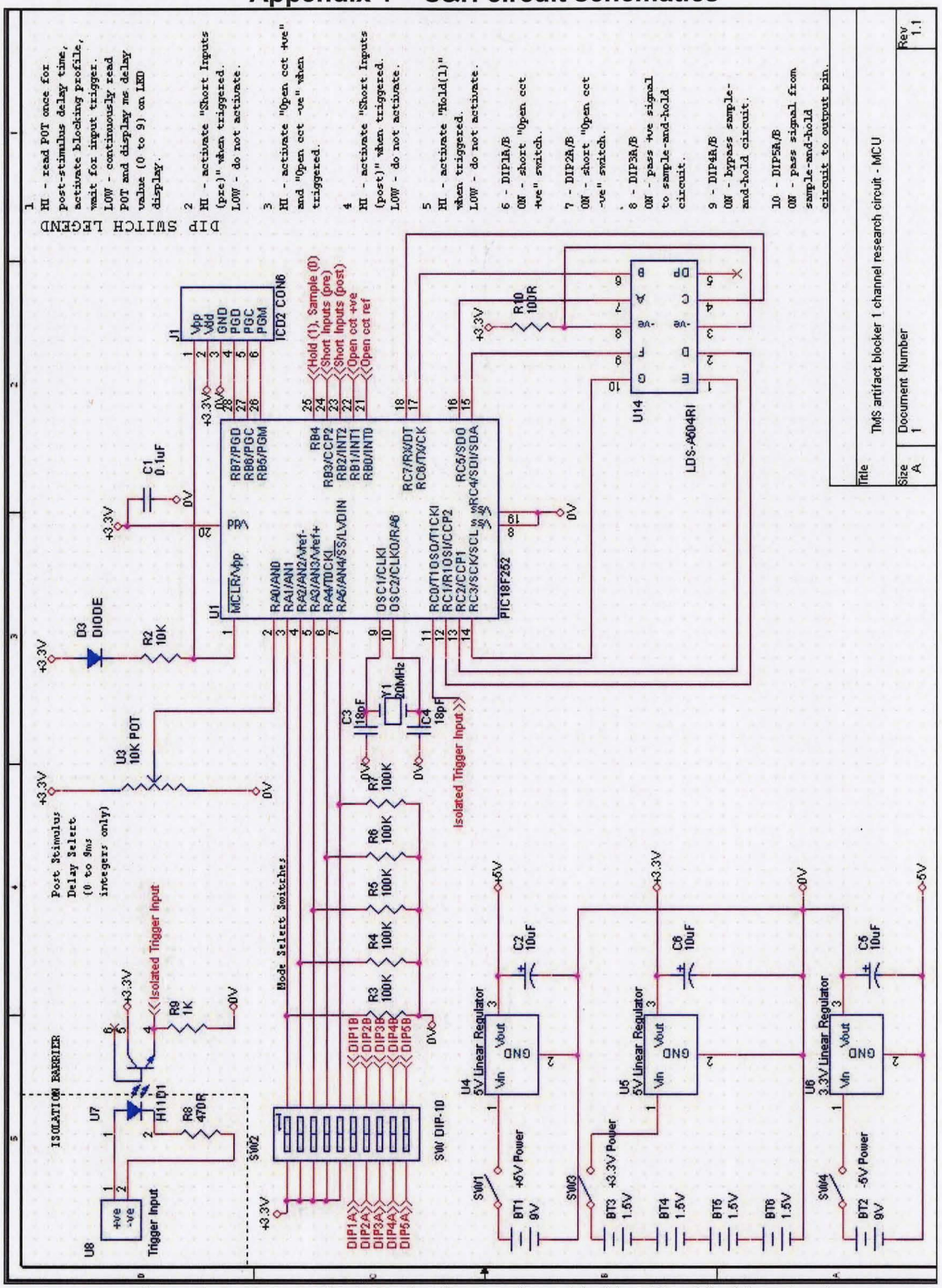

Figure A.1: Page 1 of schematics for sample-and-hold artifact blocking circuit

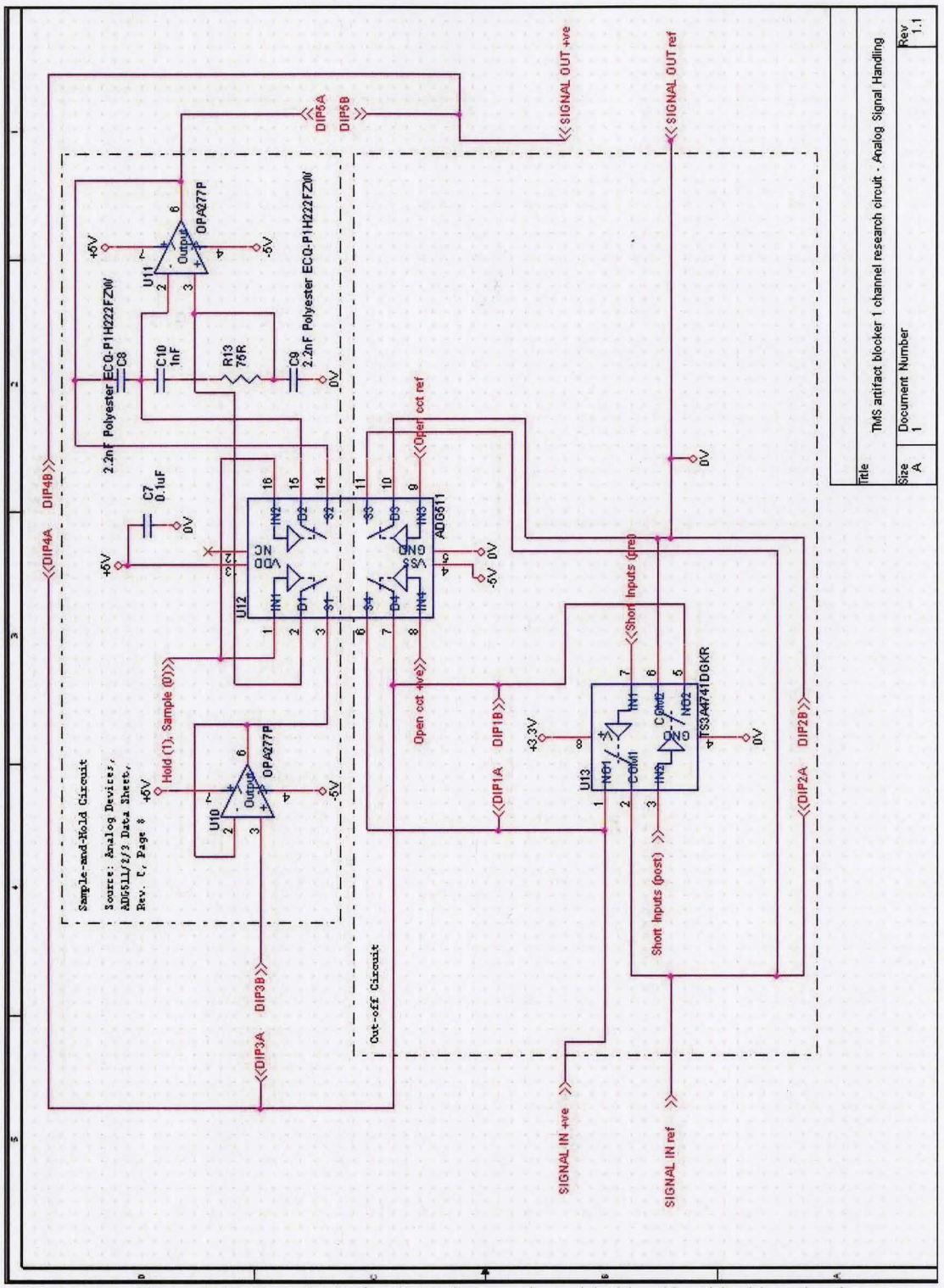

Figure A.2: Page 2 of schematics for sample-and-hold artifact blocking circuit

Appendix 2 – Microcontroller C code

```
/*****************************************************************************
******************** Breadboard Prototype circuit ********************
*****************************************************************************/

// Compiled with Microchip MPLAB IDE v7.20 freeware and Microchip C18 v2.20a demo
// Microcontroller is a legacy PIC18F252 in a 28pin DIP package

#include <p18f252.h>
#include <delays.h>
#include <stdlib.h>
#include <adc.h>
#include <math.h>

/*****************************************************************************
************************** Pin definitions **************************
*****************************************************************************/

#define IN_ISOLATED_TRIGGER PORTAbits.RA4
#define TIME_LOCK_OUT PORTAbits.RA2
#define SHORT_INPUTS PORTAbits.RA1 // Controls switch 1

#define DRIVE_2 PORTBbits.RB5 // Controls switch 2
#define DRIVE_3 PORTBbits.RB6 // Controls switch 3
#define DRIVE_4 PORTBbits.RB7 // Controls switch 4

#define IN_DELAY_TIME PORTAbits.RA0 //AN0 analog input

#define IN_DIP_FACE_READ_POT_HOLD_VALUE PORTCbits.RC0
#define IN_DIP1_TRIG_IN_IS_RISING_EDGE PORTAbits.RA3
#define IN_DIP3_PRE_TRIGGER_BLOCKING PORTAbits.RA5

#define RED_LED PORTBbits.RB0
#define GREEN_LED PORTBbits.RB1

// LED display segment definitions
//  --A--
// |  |
// F  B
// |  |
//  --G--
// |  |
// E  C
// |  |
//  --D--

#define SEGMENT_A PORTCbits.RC1
#define SEGMENT_B PORTCbits.RC2
#define SEGMENT_C PORTCbits.RC3
#define SEGMENT_D PORTCbits.RC4
#define SEGMENT_E PORTCbits.RC5
#define SEGMENT_F PORTCbits.RC6
#define SEGMENT_G PORTCbits.RC7

#define SEGMENT_DP PORTBbits.RB2
#define SEGMENT_DIG1_ON PORTBbits.RB4
#define SEGMENT_DIG2_ON PORTBbits.RB3

// unused pins: RC0, RA5

/*****************************************************************************
********************** Subroutine Prototypes **********************
*****************************************************************************/
void setup_ports(void);
void setup_adc(void);
void cycle_led_display(void);
```

```
void test_led_display(void);
//void test_dip_switches(void);
void post_number_to_display(unsigned short int number_to_display);

/*********************************************************************
***************************** Main routine ****************************
*********************************************************************/

/*
Delay time calculations:
20MHz High Speed oscillator
= 5 MIPS (5x10^6 instructions (cycles) per second)
therefore each cycle is 1/(5x10^6)s = 2x10^-7s = 200ns

to get a delay time of 200us, need 1000 cycles
to get a delay time of 400us, need 2000 cycles
to get a delay time of 1000us (1ms), need 5000 cycles
*/

void main(void) {
        //int last_state_switch_1;
        unsigned short int delay_time_input;
        unsigned short int ms_delay;
        unsigned short int trigger_level;

        setup_ports();

        RED_LED = 1; // Power on LED
        SHORT_INPUTS = 0; // Stop blocking the stimulus artifact

        //cycle_led_display();
        //test_led_display();
        //test_dip_switches();

        do {
                /*************************************************************
                ***** Allow user to select the post-trigger blocking time *****
                *************************************************************/
                SEGMENT_DIG2_ON = 1;
                SEGMENT_DP = 1;
                do {
                        ConvertADC();
                        while(BusyADC());
                        delay_time_input = ReadADC();

                        ms_delay = delay_time_input/64;
                        if (ms_delay > 9) ms_delay = 9; // max delay is 9.0ms

                        post_number_to_display(ms_delay);
                } while (IN_DIP_FACE_READ_POT_HOLD_VALUE != 1);
                SEGMENT_DIG2_ON = 0;
                SEGMENT_DP = 0;

                /*****************************************************
                ***** Set the trigger level to either HIGH or LOW *****
                *****************************************************/
                if (IN_DIP1_TRIG_IN_IS_RISING_EDGE == 1) {
                        // Tigger on a high level
                        trigger_level = 1; // high level trigger
                }
                else { // (IN_DIP1_TRIG_IN_IS_RISING_EDGE == 0)
                        // Trigger on a low level
                        trigger_level = 0; // low level trigger
                }

                /*****************************************
```

```
                ***** Pre-trigger blocking in-effect? *****
                ******************************************/
                if (IN_DIP3_PRE_TRIGGER_BLOCKING == 1) {
                        SHORT_INPUTS = 1; // Pre-trigger block the stimulus artifact
                }

                /*****************************************************
                ***** LOOP WAITING FOR TRIGGER (level triggering) *****
                *****************************************************/
                do {
                        if (IN_ISOLATED_TRIGGER == trigger_level) {
                                SHORT_INPUTS = 1; // Block the stimulus artifact
                                DRIVE_2 = 1;
                                DRIVE_3 = 1;
                                DRIVE_4 = 1;
                                TIME_LOCK_OUT = 1;
                                GREEN_LED = 1;
                                // BLOCK ARTIFACT POST TRIGGER FOR USER SELECTED DELAY TIME (0.1-
0.9ms)
                                if (ms_delay > 0) {
                                        //Delay1KTCYx(5*ms_delay); // Delay exactly 5,000*ms_delay instruction
cycles = 1ms*ms_delay (0 to 9 ms)
                                        Delay100TCYx(5*ms_delay); // Delay .1ms to .9ms
                                }
                                else {
                                        // no delay time. Can't call Delay1KTCYx with 0, since 0 gives a delay of
256,000 cycles (max delay)
                                        Delay1KTCYx(50); // Delay 10ms if zero selected (For testing only)
                                }
                                TIME_LOCK_OUT = 0;
                                GREEN_LED = 0;
                                SHORT_INPUTS = 0; // Stop blocking the stimulus artifact
                                DRIVE_2 = 0;
                                DRIVE_3 = 0;
                                DRIVE_4 = 0;

                                /*****************************************
                                ***** Pre-trigger blocking in-effect? *****
                                *****************************************/
                                if (IN_DIP3_PRE_TRIGGER_BLOCKING == 1) {
                                        // allow the signal to be passed through for 1 second before pre-trigger
blocking again
                                        Delay10KTCYx(250); // Delay 1s (1000ms), 5,000,000 cycles
                                        Delay10KTCYx(250);
                                        SHORT_INPUTS = 1; // Pre-trigger block the stimulus artifact
                                }
                                else { // (IN_DIP3_PRE_TRIGGER_BLOCKING == 0)
                                        // let the signal pass 100ms
                                        Delay10KTCYx(50); // Delay 100ms, 500,000 cycles
                                }
                        }
                } while (IN_DIP_FACE_READ_POT_HOLD_VALUE == 1);
                SHORT_INPUTS = 0; // Stop blocking the stimulus artifact
        } while(1);
}

/*********************************************************************
************************** Subroutines ******************************
*********************************************************************/

void setup_ports(void) {
        // Bits in MSB(left) to LSB(right) order
        //zero all output pins
        LATA = 0b00000000;
        LATB = 0b00000000;
        LATC = 0b00000000;
```

```
	//open all output pins, tristate all input pins
	TRISA = 0b11111001;
	TRISB = 0b00000000;
	TRISC = 0b00000001;

	//configure analog pins

	ADCON0 = 0b10000001; // select AN0 as the analog input to read
	//adcon1 = xxxx1110 (see page 182 in PIC18F252 data sheet)
	ADCON1 = 0b10001110; // make all pins on PORTA digital, except AN0 (make it analog)

}

void test_led_display(void) {
	/*Cycle through 0,1,2,3,4,5,6,7,8,9 to ensure led display is working properly*/
	// Delay 500ms between numbers (5 second cycle time total)
	unsigned short int i;

	do {
		for (i=0;i<=9;i++) {
			post_number_to_display (i);
			Delay10KTCYx(250); // Delay exactly 250,000 instruction cycles = 500ms (at 20MHz clock)
			Delay10KTCYx(250);
		}
	} while (1);
}

void cycle_led_display(void) {

	// cycle first digit and first decimal point

	SEGMENT_DIG1_ON = 1;

	SEGMENT_G = 1;
	Delay10KTCYx(50); // 100ms delay
	SEGMENT_G = 0;

	SEGMENT_C = 1;
	Delay10KTCYx(50); // 100ms delay
	SEGMENT_C = 0;

	SEGMENT_D = 1;
	Delay10KTCYx(50); // 100ms delay
	SEGMENT_D = 0;

	SEGMENT_E = 1;
	Delay10KTCYx(50); // 100ms delay
	SEGMENT_E = 0;

	SEGMENT_F = 1;
	Delay10KTCYx(50); // 100ms delay
	SEGMENT_F = 0;

	SEGMENT_A = 1;
	Delay10KTCYx(50); // 100ms delay
	SEGMENT_A = 0;

	SEGMENT_B = 1;
	Delay10KTCYx(50); // 100ms delay
	SEGMENT_B = 0;

	SEGMENT_DP = 1;
	Delay10KTCYx(50); // 100ms delay
	SEGMENT_DP = 0;
```

```
        SEGMENT_DIG1_ON = 0;

        // cycle second digit and second decimal point

        SEGMENT_DIG2_ON = 1;

        SEGMENT_G = 1;
        Delay10KTCYx(50); // 100ms delay
        SEGMENT_G = 0;

        SEGMENT_C = 1;
        Delay10KTCYx(50); // 100ms delay
        SEGMENT_C = 0;

        SEGMENT_D = 1;
        Delay10KTCYx(50); // 100ms delay
        SEGMENT_D = 0;

        SEGMENT_E = 1;
        Delay10KTCYx(50); // 100ms delay
        SEGMENT_E = 0;

        SEGMENT_F = 1;
        Delay10KTCYx(50); // 100ms delay
        SEGMENT_F = 0;

        SEGMENT_A = 1;
        Delay10KTCYx(50); // 100ms delay
        SEGMENT_A = 0;

        SEGMENT_B = 1;
        Delay10KTCYx(50); // 100ms delay
        SEGMENT_B = 0;

        SEGMENT_DP = 1;
        Delay10KTCYx(50); // 100ms delay
        SEGMENT_DP = 0;

        SEGMENT_DIG2_ON = 0;
}

void post_number_to_display(unsigned short int number_to_display) {
        switch (number_to_display) {
                case 0:
                        LATC = 0b01111110;
                        break;
                case 1:
                        LATC = 0b00001100;
                        break;
                case 2:
                        LATC = 0b10110110;
                        break;
                case 3:
                        LATC = 0b10011110;
                        break;
                case 4:
                        LATC = 0b11001100;
                        break;
                case 5:
                        LATC = 0b11011010;
                        break;
                case 6:
                        LATC = 0b11111010;
                        break;
                case 7:
                        LATC = 0b00001110;
```

```
                    break;
                case 8:
                    LATC = 0b11111110;
                    break;
                case 9:
                    LATC = 0b11001110;
                    break;
        }
}
```

Appendix 3 – LabVIEW wiring diagram

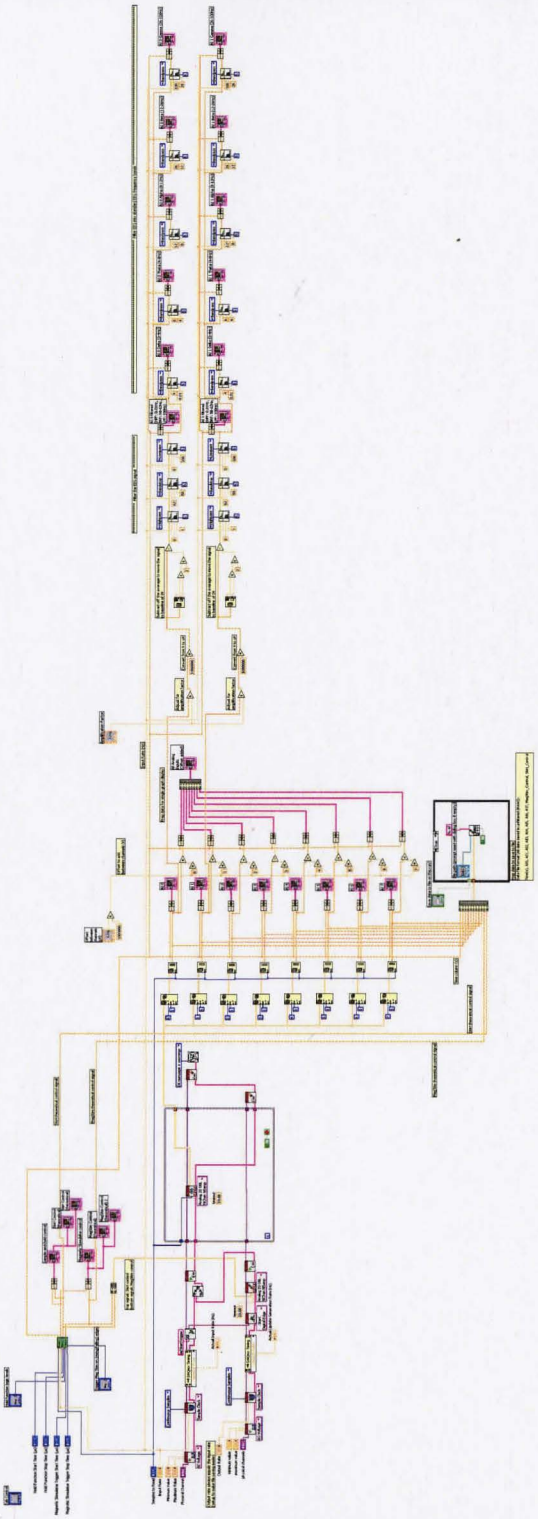

Figure A.3: LabVIEW 8.0 wiring diagram full overview of design

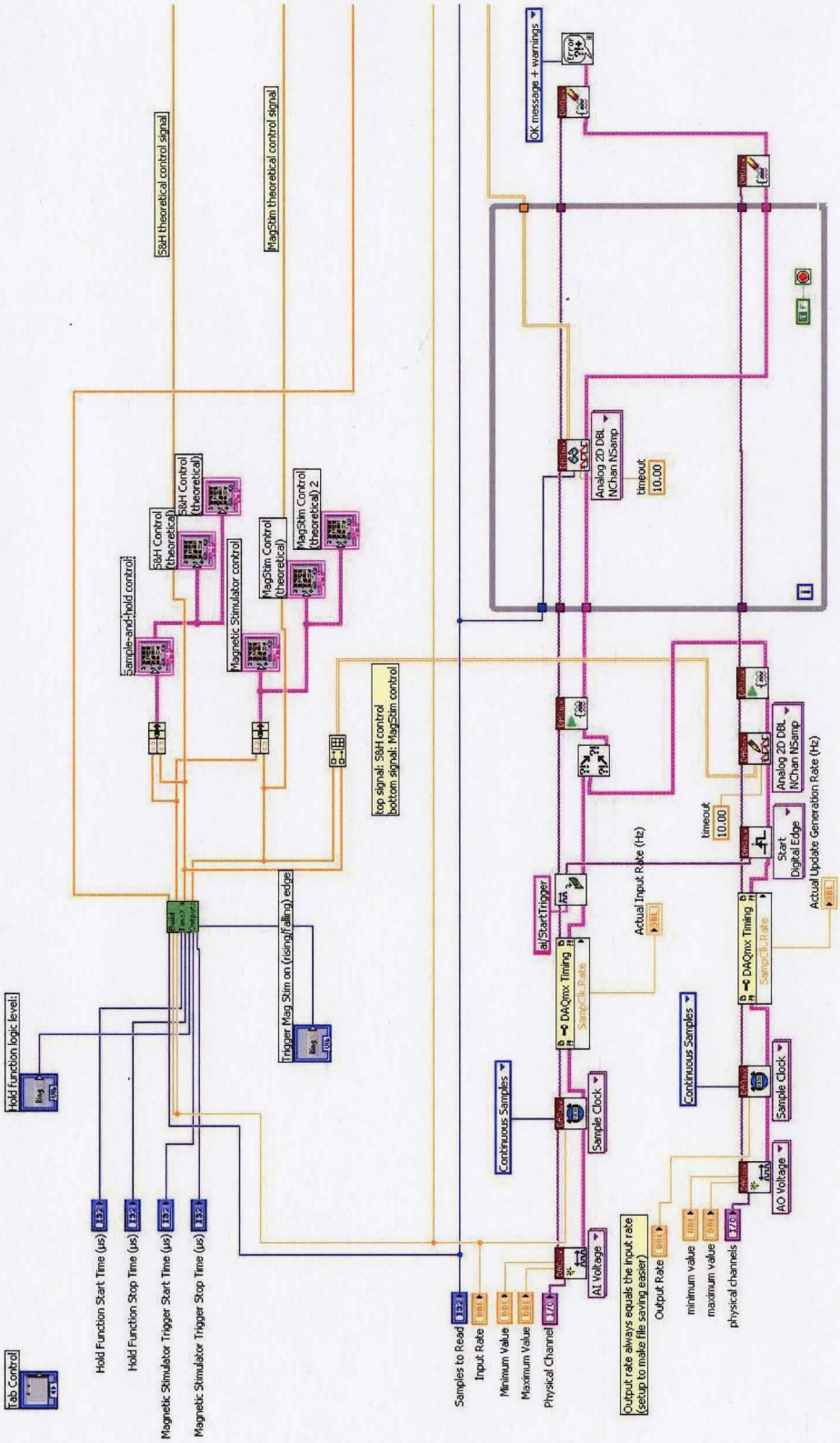

Figure A.4: LabVIEW 8.0 wiring diagram: analog input/output code.

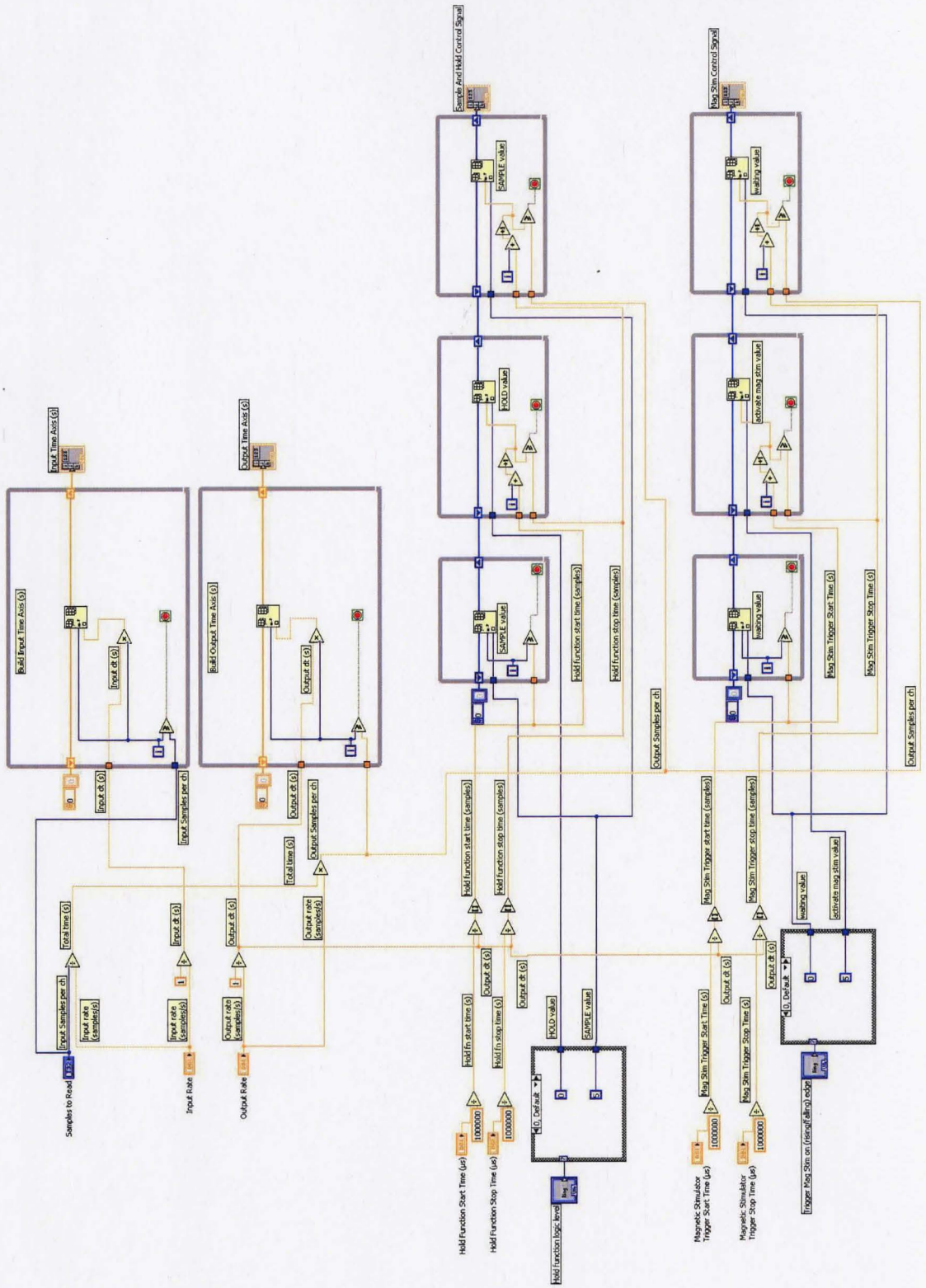

Figure A.5: LabVIEW 8.0 sub VI wiring diagram for "Build Time X & Outputs" sub VI.

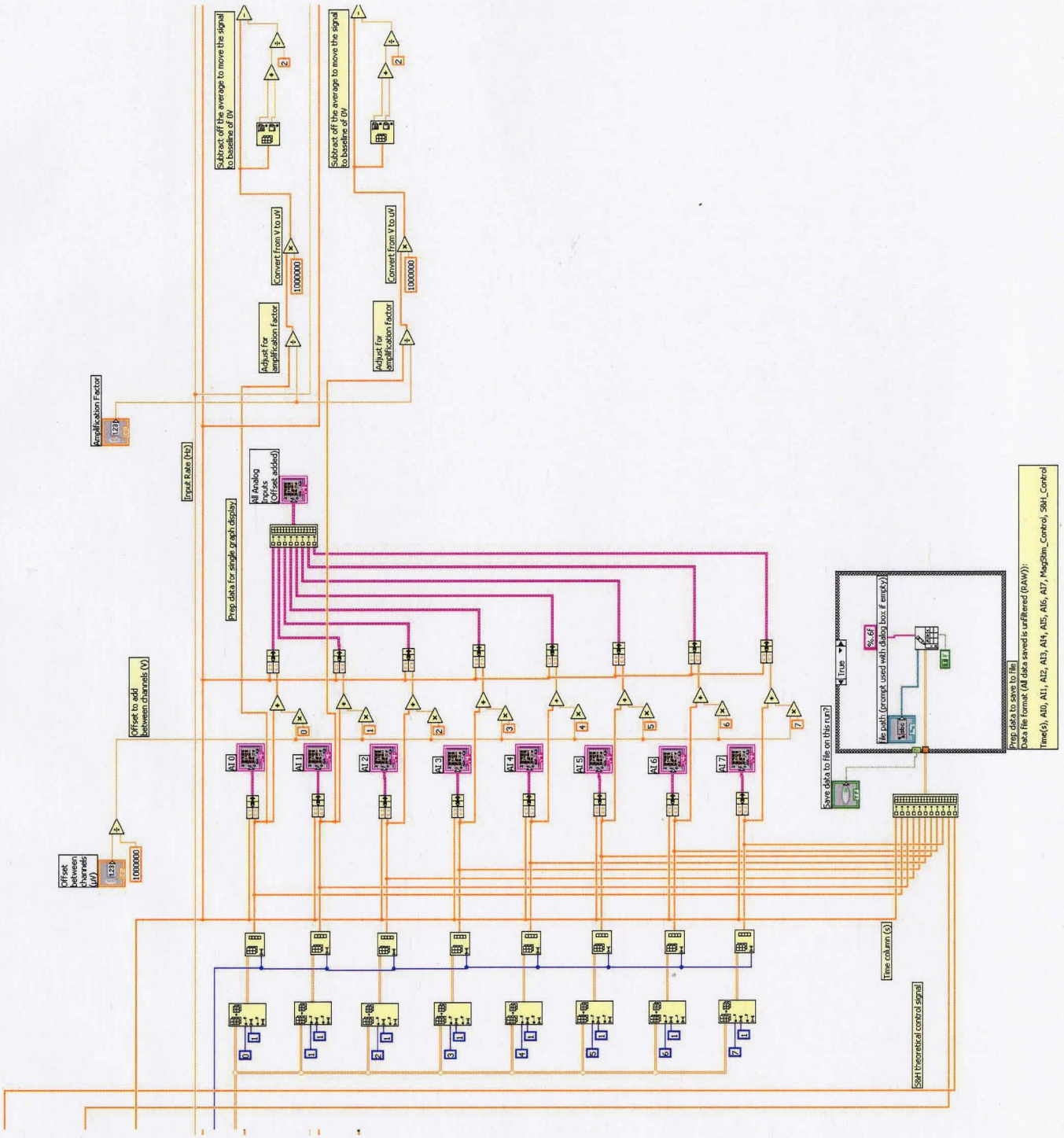

Figure A.6: LabVIEW 8.0 wiring diagram: preliminary signal manipulation.

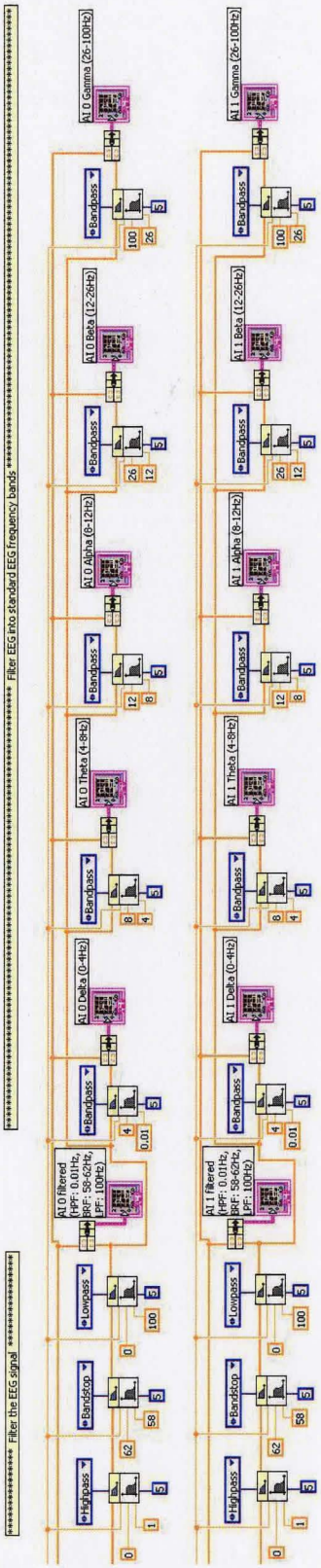

Figure A.7: LabVIEW 8.0 wiring diagram: EEG band analysis.